PERFORMANCE ANALYSIS OF PARABOLIC TROUGH CONCENTRATED SOLAR SYSTEM

MD. KHAIRUL ISLAM

DISSERTATION SUBMITTED IN FULFILLMENT OF THE REQUREMENTS FOR THE DEGREE OF MASTER OF PHILOSOPHY

**INSTITUTE OF GRADUATE STUDIES
UNIVERSITY OF MALAYA
KUALA LUMPUR**

2016

UNIVERSITI MALAYA

ORIGINAL LITERARY WORK DECLARATION

Name of the candidate: **Md. Khairul Islam**

Registration/Matric No: **HGF 120005**

Name of the Degree: **Master of Philosophy**

Title of Thesis: **Performance Analysis of Parabolic Trough Concentrated Solar System**

Field of Study: **Energy Policy**

I do solemnly and sincerely declare that:

(1) I am the sole author/writer of this work;

(2) This work is original;

(3) Any use of my work in which copyright exists was done by way of fair dealing and for permitted purposes and any excerpt or extract from, or reference to or reproduction of any copyright work has been disclosed expressly and sufficiently and the title of the work and its authorship have been acknowledged in this work;

(4) I do not have any actual knowledge nor ought I reasonably to know that the making of this work constitutes an infringement of any copyright work;

(5) I hereby assign all and every rights in the copyright to this work to the University of Malaya ("UM"), who henceforth shall be owner of the copyright in this work and that any reproduction or use in any form or by any means whatsoever is prohibited without the written consent of UM having been first had and obtained;

(6) I am fully aware that if in the course of making these works I have infringe any copyright whether intentionally or otherwise, I may be subject to legal action or any other action as may be determined by UM.

Candidate's Signature Date

Subscribe and solemnly declare before,

Witness Signature Date

Name :

Designation :

ABSTRACT

Concentrating solar system is the latest solar technology. Parabolic trough concentrating collector (PTC) is one of the most matured concentrating technologies. In this research, a PTC is developed with optical and thermal analysis. CO_2, NH_3 and N_2 are utilized for analysis. For the maximum thermal efficiency of the collector, receiver parameters are optimised. Optimum receiver diameter is found 51.80 mm for the maximum efficiency of the collector. During optimisation, mass flow rate and concentration ratio are found to be influencing on the thermal efficiency and heat removal factor. Several nanoparticles (CuO, ZnO, Al_2O_3, TiO_2, Cu, Al, SiC and CNT) in water and Therminol VP1 (ultra high temperature synthetic fluid) are used for investigating the system. Investigation shows improvement in heat transfer for added nanoparticles. Heat transfer rate is better in laminar flow than in turbulent flow. After analytical analysis, an experiment has been done using water and carbon nanotube, and compared with analytical results. In case of mass flow rate changes (1.15-1.25 l/min), experimental results deviate by 4.47% to 5.38% and 3.63% to 4.74% for respectively water and water-CNT. In case of radiation changes (477-640 W/m^2), experimental results deviate by 40.00% to 4.00% and 41.00% to 3.50% respectively for water and water-CNT. Increment of flow rate and irradiation are found to have respective negative and positive influence on thermal efficiency of the collector.

ABSTRAK

Menumpukan sistem solar adalah teknologi solar terkini. palung parabola menumpukan pengumpul (PTC) adalah salah satu teknologi menumpukan paling matang. Dalam kajian ini, satu PTC dibangunkan dengan analisis optik dan terma. CO2, NH3 dan N2 digunakan untuk analisis. Untuk kecekapan haba maksimum pengumpul, parameter penerima yang optimum. diameter penerima Optimum didapati 51.80 mm untuk kecekapan maksimum pemungut. Semasa pengoptimuman, kadar aliran jisim dan nisbah kepekatan yang didapati mempengaruhi kecekapan dan penyingkiran haba faktor haba. Beberapa nanopartikel (CuO, ZnO, Al2O3, TiO2, Cu, Al, SiC dan CNT) di dalam air dan Therminol VP1 (ultra suhu yang tinggi cecair sintetik) digunakan untuk menyiasat sistem. Siasatan menunjukkan peningkatan dalam pemindahan haba untuk nanopartikel ditambah. kadar pemindahan haba adalah lebih baik dalam aliran laminar daripada dalam aliran gelora. Selepas analisis analisis, eksperimen telah dilakukan dengan menggunakan air dan karbon nanotube, dan dibandingkan dengan keputusan analisis. Keputusan eksperimen hanya berbeza 4.47% kepada 5.38% dan 3.63% kepada 4.74% untuk masing-masing air dan air-CNT dalam kes perubahan kadar aliran jisim (1,15-1,25 l / min). Dalam kes perubahan radiasi (477-640 W / m2), keputusan eksperimen menyimpang oleh 40.00% kepada 4.00% dan 41.00% kepada 3.50% masing-masing untuk air dan air-CNT. Kenaikan kadar aliran dan penyinaran didapati mempunyai pengaruh negatif dan positif masing-masing pada kecekapan haba pemungut.

ACKNOWLEDGEMENTS

First of all, I would like to express my utmost gratitude and thanks to the almighty Allah (s.w.t) for the help and guidance that He has given me through all these years. My deepest gratitude goes to my father, mother, and sisters for their blessings and continual supports.

I would like to express my deepest appreciation and gratitude to my supervisors, **Dr. Md. Hasanuzzaman** and **Professor Dr. Nasrudin Abd Rahim** for their brilliant supervision, guidance, encouragement and supports in carrying out this research work. I am deeply indebted to them. Special thanks to the Research Centre for Power Energy Dedicated Advanced Centre (UMPEDAC), University of Malaya for the financial supports.

Finally, thanks to all personnel in Energy Laboratory and UMPEDAC in helping me and for suggestion, ideas, discussions and advice in completing this research work.

TABLE OF CONTENTS

LIST OF FIGURES

LIST OF TABLES

NOMENCLATURES

A_a	:	Trough aperture area
A_{ro}	:	Receiver outer circumferential area
C_p	:	Specific heat capacity of fluid
D_{ro}	:	Receiver outer diameter
D_{ri}	:	Receiver inner diameter
F_R	:	Heat removal factor
F'	:	Collector efficiency factor
Gr	:	Grashof number
H_p	:	Parabola letus rectum
I_b	:	Direct beam irradiation
K_r	:	Receiver thermal conductivity
K_f	:	Fluid thermal conductivity
$K\theta$	:	Incidence angle modifier
L	:	Length of the trough
Nu_f	:	Nusselt number for fluid
Nu	:	Nusselt number for air
Pr_f	:	Prantle number for fluid
Pr	:	Prantle number for air
Q_u	:	Useful heat gain
Re_f	:	Reynolds number for fluid
S	:	Absorbed radiation
T_{CL}	:	Curvature length of the trough
T_a	:	Ambient temperature
Tfi	:	Inlet fluid temperature

T_{fo}	:	Outlet fluid temperature
U_L	:	Heat loss coefficient
W	:	Width of the trough
θ	:	Incidence angle
φ_r	:	Rim angle
θ_z	:	Zenith angle
δ	:	Declination
ω	:	Hour angle
n	:	Day of year
ϕ	:	Latitude
τ	:	Transmittance of the glass cover
ρ_C	:	Reflectance of the mirror or concentrator
α	:	Absorptance of the receiver
$(\tau\alpha)_b$	:	Transmittance-Absorptance product for beam radiation
ρ_d	:	Cover reflectance for diffuse radiation
υ	:	Kinematic viscosity for air
β	:	Temperature coefficient of thermal conductivity
f	:	Focus of the trough
m_f	:	Fluid mass flow rate
v	:	Fluid velocity
h_f	:	Heat transfer coefficient of fluid
η_{th}	:	Collector thermal efficiency

LIST OF ABBREVIATIONS

CNT	:	Carbon nanotube
CR	:	Concentration ratio
CSP	:	Concentrated solar power
IEA	:	International energy agency
PTC	:	Parabolic trough concentrating
PV	:	Photovoltaic
RE	:	Renewable energy
W	:	Water

CHAPTER 1 : INTRODUCTION

1.1 Background

Fossil fuel shortage, uprising fuel prices and global warming are of important concern now. Most of world’s energy is generated from fossil fuel. In Malaysia, 85% of total power generation is primarily from natural gas and coal (EC, 2012). Malaysia could produce natural gas for around twenty nine years continuously (Ahmad et al., 2011). But coal is a totally import dependent fuel which is mainly procured from Indonesia (84%), Australia (11%) and South Africa (5%) (Jaffar, 2009). In future coal may create difficulties to fulfill growing power demand due to fossil fuel depletion. Also fossil fuels cause serious problems like climate change, greenhouse gas emission, global warming, and acid rain (Hasanuzzaman et al., 2012; Reddy et al, 2013). So an urgent need is required to shift power generation to alternative energy resources. Renewable power generation system, which is a low carbon energy technology, is the perfect option to ensure energy security by avoiding environmental problems including greenhouse gas emissions (Ahmed et al, 2013; Devabhaktuni, 2013). This is the only way to change the current path of the world to achieve greenhouse gas emission goals i.e. reduction of greenhouse gas emissions. Every nation of the world must be involved in this paradigm shift.

Nowadays, renewable power generation or hybrid renewable power generation systems are attracting the interest of the whole world due to advanced technologies capable of efficient use of renewable resources including reduction of greenhouse gas emissions (Pepermans, 2005; Xi, 2012). Renewable energy resources are used generally for three main purposes: electricity generation, bio products and heating/cooling systems. Concentrating solar power generation system, geothermal power generation and hydropower generation systems are well-disposed technologies, while solar thermal heating, geothermal district heating and pellet-based heating can provide significant benefits in case of heat supply (Dombi, 2014). In many countries, various schemes like development of technologies, increased economies of scale, and strong policy support have contributed.

However, out of the renewable energy resources, the most ample resource is solar which has immense potentiality (Şen, 2004). Technologies are available to harness solar energy to a useful state. Solar has the potency to meet all residential and industrial energy needs. Already the world is moving toward sustainable technologies especially solar energy technologies. Solar PV system is growing so fast of all renewable technologies with an impressive rate (Hosenuzzaman et al., 2015). Recently solar concentrating system attracts the attention of many countries. Some countries have established such type of system, and in some region of the world, this system is under development.

Today the world stands at an exciting transition moment when renewable energy is competing head to head with fossil fuel and nuclear energy. Due to increased energy consumption, dependence on fossil fuels, solar power generation can be the main and important factor for the world now. Malaysia is a tropical country with an average 1643 kWh/m^2 per year irradiance, which is very suitable for the solar power generation system (Haris, 2008). Solar insolation range is 1400-1900kWh/m^2 and average sun hour is more than 10 hours (Amin, 2009; Ahmad et al., 2011). Solar is the most prospective energy source in Malaysia for present and future situations. It is very much promising to set up large scale solar power generation systems. The Government of Malaysia has taken a lot of initiatives and set policies to expand the solar power generation system so that it can significantly contribute to meet the power demand of the country. Under the Tenth Plan (2011 to 2015), many new strategies and action plan have been undertaken to achieve a smart target of renewable energy production of 985 MW by 2015, sharing

5.5% of total power generation mix in Malaysia. Malaysia has plan to make solar energy as one of the main power source by 2050 (Chen, 2012).

The photovoltaic technology has been developed in Malaysia since 1980 (Amin, 2009). Research and implementation of photovoltaics are ongoing. But there is no notable research on concentrating system for Malaysia. Malaysia has the potential for concentrating solar system due to its geographical position, and weather.

In this research, design, analytical and experimental performance analysis for parabolic trough solar concentrating system have been done. This research also provides an overview about the worldwide promotion of renewable resources utilization including special concern about climate change. Power generations by solar energy resources have been given main focus.

1.2 Renewable energy resources

Since the last 200 years energy demand is fulfilled from non-replenishable sources, viz., oil, natural gas and coal. Recently energy demand is rising, but these resources are continuously depleting. These resources are also responsible for greenhouse gas emissions. A table regarding the sustained life of fossil fuels is given here (Table 1.1) (RE, 2014).

Table 1.1: Estimatedtime remaining for fossil fuels reserve (RE, 2014)

Fossil fuel	**Time left (Years)**
Coal	250
Natural gas	70
Oil	50

Researchers are exploring the potential of renewable sources for the future. This planet has continually replenished some resources such as sunlight, wind, tides and waves, rain, and warmth of earth. The energy is derived from these sources in a sustainable manner. Matured and upgrade technologies are available for exploiting resources. Renewable resources, far cleaner than fossil fuels emits minute level of carbon and help to battle global warming caused by fossil fuels. Renewable energy resources are shown in Figure 1.1 (RE, 2014).

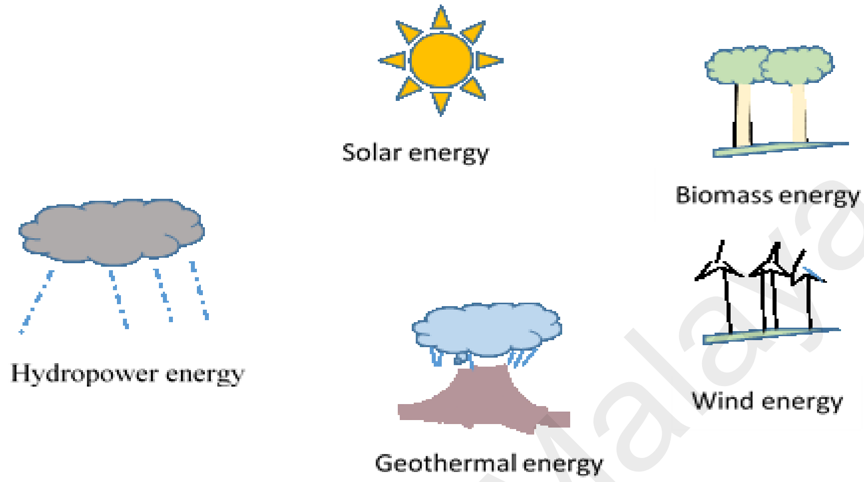

Figure 1.1: Renewable resources (RE, 2014).

Solar radiation has high temperature and high exergy energy source (Fernández-García, 2010). It is the most abundant and limitless resource. Solar energy could serve about 16.67% of global cumulative energy demand for low temperature heating and cooling by 2050 (IEA, 2012). Solar energy source is clean alternative to fossil fuels, which is limited, polluting the environment, threatening public health, and contributing to global climate change. Due to solar energy's copiousness and enormous power, the appeal of this resource is that it plays an eminent role in our energy future.

Biomass, any organic matter—plant materials and animal wastes—is probably the oldest source of renewable energy after the sun. Various types of processes including thermal, biological, mechanical or physical processes are available to efficiently harness biomass and convert it into more valuable energy forms for cooling, heating purposes or for producing electricity (Bridgwater, 2012). Biomass is a sustainable source of energy that diminishes carbon emissions, a prime contributor to climate change. Though biomass after burning emits carbon dioxide gas, it does not emit new carbon into ambiance as the fossil fuel burning does (RE, 2013).

Under the earth crust, a layer of hot molten rock is there. Thermal energy is continuously generated in the layer through the decay of radioactive materials. The energy equivalence of this resource is 5×10^4 times more than that of all known oil and natural gas reserve (UCS, 2014). The total energy of the earth is counted as 12.6×10^{24} MJ and that of the crust is 5.4×10^{21} MJ. This thermal energy can offer temperatures of 200 to 1000^0C at the base of the crust and at the centre temperature ranges from 3500 to 4500^0C (Bertani, 2009). So our earth really possess an immense amount of energy which can be exploited for gaining clean, safe and secured energy. Geothermal resources can be categorized as low, medium and high enthalpy resources (Etemoglu, 2007). Using engineering technologies, these resources can be taped for space heating or cooling, electricity generation.

Wind, which is a resource having energy, blows often fast, and often slow. In some region, wind blows enough, power can be generated by harnessing wind current. Wind turbine generates power at cube power of the wind speed, that is power output increases eight times as the wind speed doubles (Argatov, 2009).

Wind energy is clean and sustainable. Wind energy develops no toxic and heat trapping emissions. So abundance and clean image, i.e. no harmful effect on climate make wind power viable option.

Water, the fuel for hydropower is moving in various states on earth, which are termed as hydrological cycle. Water evaporating from rivers and oceans, convert to clouds, resulting rain and snowfall, and assembling in rivers again and return back to the ocean - all these movements offer a great chance to exploit useful energy.

Hydropower, gained by exploiting movements of water using diversion infrastructure or dams is the sustainable and non-polluting power which can reduce fossil fuels dependency and threat of global warming (Frey & Linke, 2002).

The powerful movement of waves in the sea or river's current rushing are natural forces. The might of moving water can be harnessed to produce clean electricity. There are some options or resources to get hydrokinetic energy such as ocean wave energy resources, tidal energy resources, hydrokinetic energy in streams and rivers, and ocean current energy. Due to water being 832 times denser than air; waves, tides, free flowing ocean or rivers appear as untapped, highly concentrated powerful clean energy resources (Güney & Kaygusuz, 2010; UCS, 2014).

1.3 Role of renewable energy

Renewable energy (RE) utilisation is not new. A little more than 150 years ago, people were capable to create technology to extract energy from biomass. As the use of coal, petroleum and natural gas expanded, people became less reliant on bioenergy. Today, the world again are looking at renewable energy resources to meet growing energy demand. Global energy consumption by fuels over the last 48 years (1965 to 2013) is shown in Figure 1.2 (EC, 2014).

Figure 1.2 shows that still most of the energy consumption is from non-renewable resources. However according to Figure 1.3 (REGS, 2014), in 2012 RE shared 19% of global energy consumption and sustained to grow significantly in 2013. About 9% RE share (traditional or solid biomass) in 2012 was used for household primary energy consumption. The rest 10% of RE (modern renewables: solar/ geothermal/ wind/ hydro/ biomass /biofuels) share was used in four distinct sectors: electricity generation, cooling and heating, fuel transportation and rural off-grid services. Modern renewables' uses increase dramatically due to slow migration away from traditional biomass and increased energy demand.

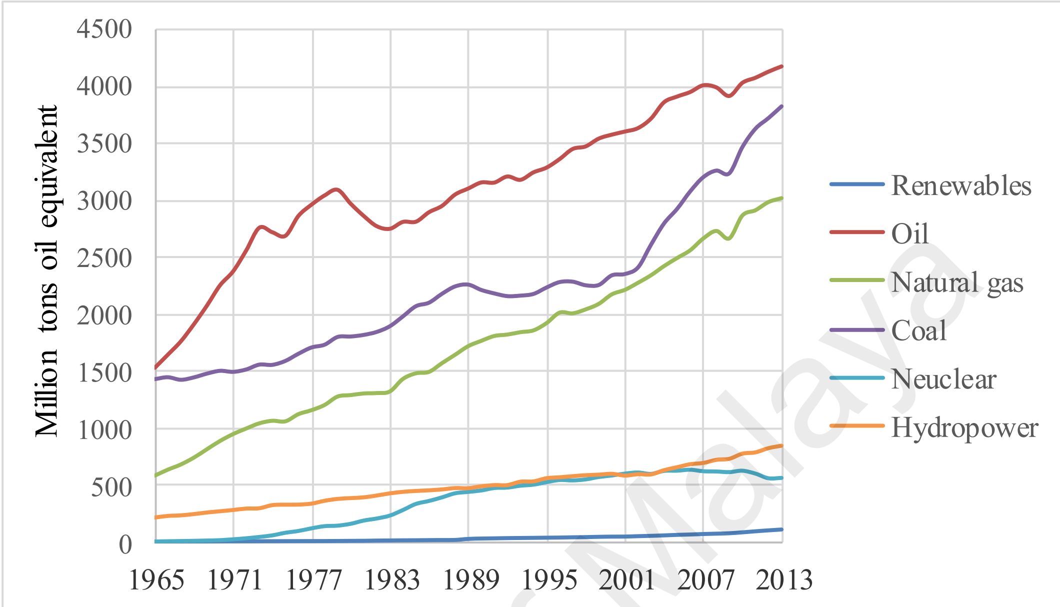

Figure 1.2: Global energy consumption by fuels (EC, 2014).

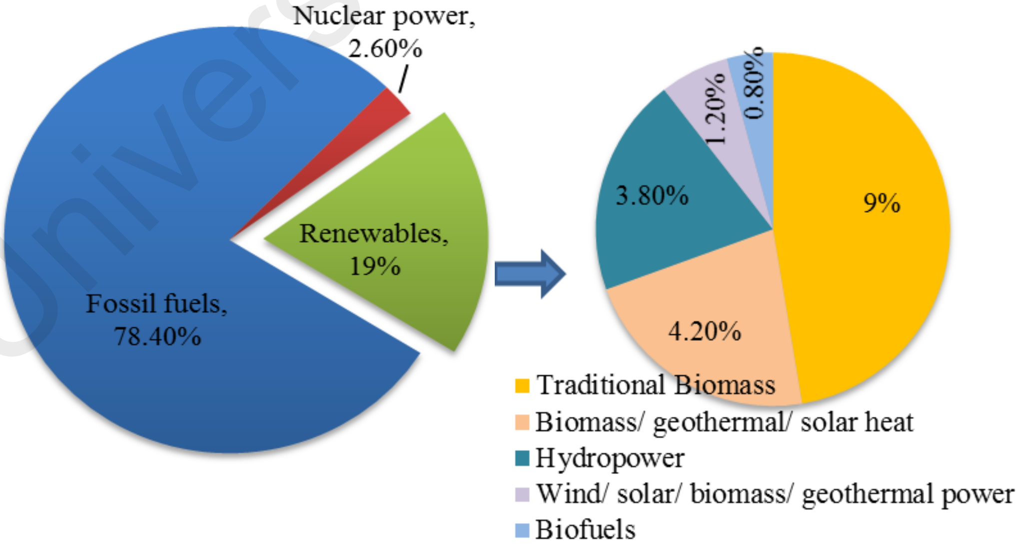

Figure 1.3: Estimated global final renewables share of energy consumption, 2012 (REGS, 2014).

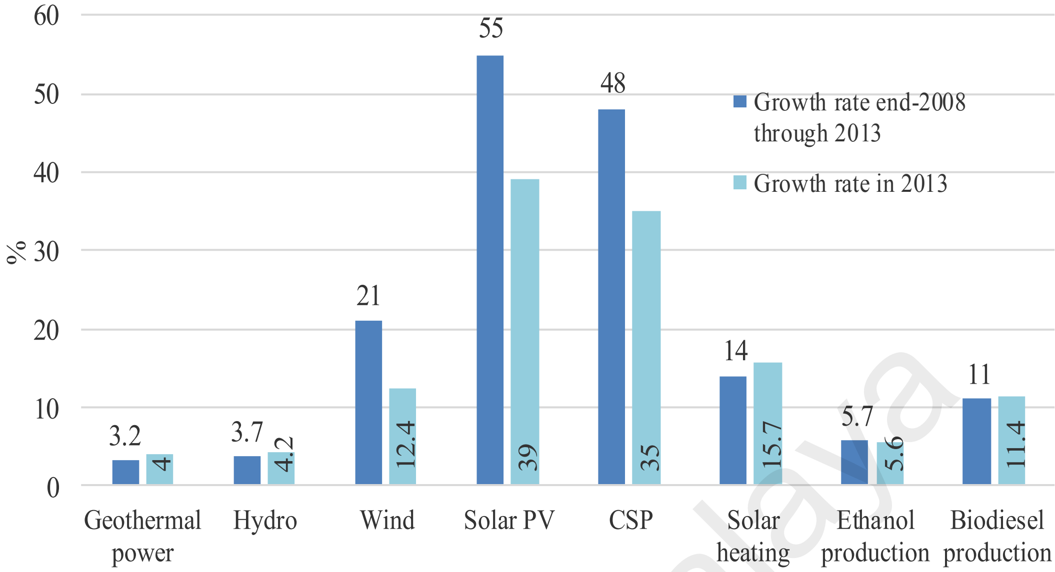

Figure 1.4: Annual Renewable Energy Capacity Growth Rates, End 2008–2013 and in 2013 (REGS, 2014).

Since 2009 through 2013, development of RE technologies grew rapidly, especially in power sector as per Figure 1.4 (REGS, 2014). Although solar PV capacity grew at the fastest rate compared to any energy technology over this period, wind energy provided the major share of the power added to grid. Application of RE in heating and cooling purposes grew gradually. Biofuel production for transport sector slowed down from 2010 to 2012, but picked up again in 2013. Overall, power sector experienced most significant growth with the global capacity of 1560 GW in 2013, an increase of 8.0% over 2012. Hydropower arose by 4.0% to around 1000 GW, whereas other RE increment was around 17.0% to 560 GW. Globally solar PV and hydropower each contributed for around one-third of renewable electrical capacity added in 2013, tracing close by wind energy (29%) (REGS, 2014).

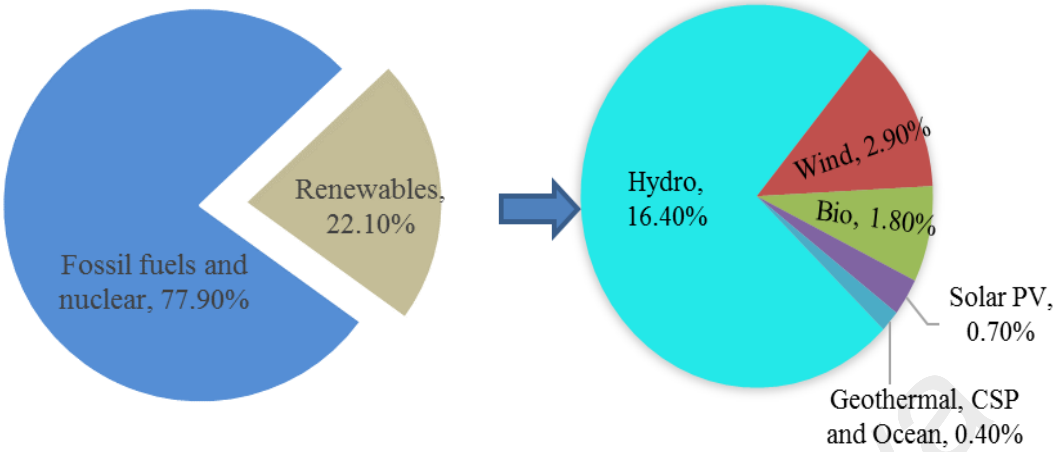

Figure 1.5: Estimated RE share of global electricity generation, end-2013 (REGS, 2014).

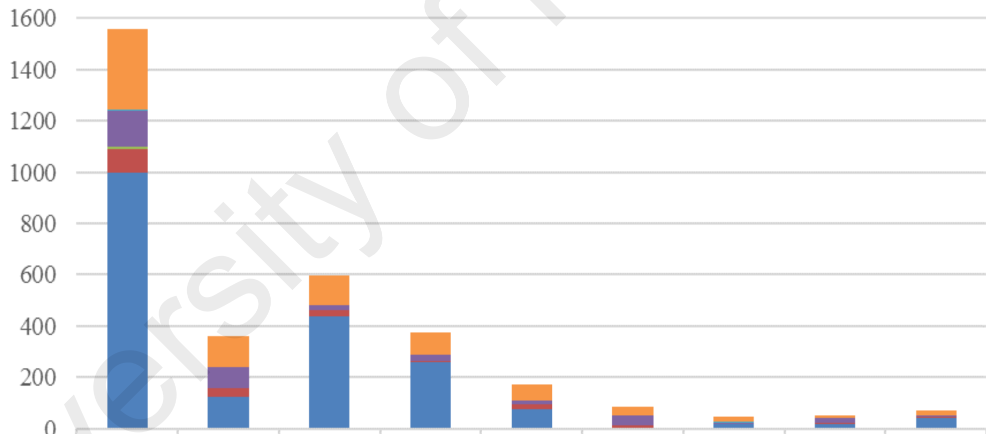

	Global	EU-28	BRICS	China	USA	Germany	Spain	Italy	India
Wind	318	117	115	91	61	34	23	8.6	20
CSP	3.4	2.3	0.1	0	0.9	0	2.3	0	0.1
Solar PV	139	80	21	19.9	12.1	36	5.6	17.6	2.2
Geothermal	12	1	0.1	0	3.4	0	0	0.9	0
Bio	88	35	24	6.2	15.8	8.1	1	4	4.4
Hydro	1000	124	437	260	78	5.6	17.1	18.3	44

Figure 1.6: Global Renewable Power Capacities in 2013 (REGS, 2014).

By the end of 2013, alternative energy contributed 26.40% of global electricity production capacity, which is sufficient to provide an approximate 21% of global electricity as per Figure 1.5 (REGS, 2014). Figure 1.6 (REGS, 2014) illustrates worldwide renewable power capacities of EU zone, BRICS countries, and other top six countries. In terms of total installed renewable electric capacity (non-hydro), China, USA, Germany, Spain, Italy and India remained at the top in 2013. China shared around 24% of the world renewable electricity capacity (an estimated of 270 GW).

The year 2013 experienced expanded installations of grid connected RE systems and also small scale, distributed renewable systems for remote areas. Overall, there was substantial and positive development in renewable energy sector in 2013 (REGS, 2014).

1.4 Solar energy potentiality

Solar, the most copious and clean sustainable resource, could do more than meet the energy demands of the entire global population. Sun power (radiant light and heat) falling onto the earth surface would be two times the quantity of all non-renewable resources (per second solar energy is equivalent to 4 trillion 100-watt light bulbs). So the potency of solar is immense (Solar, 2014). Harnessing technologies could be active or passive, depending on the manner that how they arrest, transform and dispense solar energy. Photovoltaic and solar thermal concentrating systems are active solar techniques. Passive solar system refers to orientation of building with materials of positive thermal mass or light dispersing properties to the sun. These buildings also circulate natural air (Solar, 2014). Solar irradiation in some location has been given in Table 1.2. From Table 1.2, it is shown that solar intensity level is sufficient to generate power. The 2013 and 2014 reports of International Energy Agency (IEA) continuously stressed for developing cost effective and clean solar harnessing technologies with large longer duration and global gains.

Table 1.2: Solar irradiation data for some countries

Country	Irradiance (kWh/m^2/d)	Ref.
China	Average 5.5	(NREL, 2014)
Bangladesh	5	(Shiblee, 2011)
India	4 – 7	(SI, 2014)
Malaysia	4 – 5.3	(Borhanazad, 2013)
Japan	4.3 – 4.8	(Wiki, 2014)
Southern Europe	Avg 5.0	(Wiki, 2014)
North Europe	Avg 3.0	(Wiki, 2014)
Central Europe	Avg 3.9	(Wiki, 2014)
Caribbean	Avg 5.7	(Wiki, 2014)

IEA conceived that solar energy could improve energy defence as this is an endemic, unlimited and import-independent resource. Solar energy will help to build sustainable and secured energy future with reduced pollutions and lower fuel expenditure. So the extra expenses of the incentives for establishment solar technologies must be increased and wisely spent and shared commonly.

1.5 Scopes of the research

The scopes of the research are given below

- Parabolic trough system designing.
- Monitoring solar irradiation and angle of incidence.
- Monitoring the movement of parabolic trough for tracking the sun.
- Monitoring indoor and outdoor ambient temperature.
- Monitoring temperature of heat transfer fluids at outlet and various points of the receiver.
- Monitoring flow rates of thermo fluids.

- Monitoring other thermal parameters such as useful heat gain, heat removal factor, thermal efficiency, heat loss, heat transfer coefficient, etc.
- Analyzing and calculating heat transfer and heat loss in both indoor and outdoor conditions.
- Cost analyzing and comparing with fossil fuel power generation system.
- Field selection for establishing solar thermal power generation.

1.6 Objectives of the research

1. To study the parabolic trough concentrating (PTC) solar system
2. To analyze optical parameter of the PTC solar system.
3. To examine the thermal behavior of PTC solar system.
4. To optimize the performance for different operating fluids of the PTC solar system.

1.7 Structure of the dissertation

This dissertation is written in five chapters. The contents of the each chapter have been are as follows:

Chapter 2 contains a comprehensive literature review available on solar concentrating system, gas, liquid and solid particle solar receiver, effect of nanofluids on solar receiver performance for PTC were discussed in details.

In chapter 3 information on the sources of data and methodologies used to estimate the different parameters is presented. Analytical and experimental model developing, analysis of various parameters regarding the performance of parabolic trough concentrating solar system were carried out in this chapter. Formulations used for analysis is also presented.

The measured parameters such as useful heat gain, thermal efficiency, heat removal factors, etc for PTC, using gas and water, with necessary figures are included in chapter 4. Impact of using nanofluids on PTC performance is also described with figures.

In chapter 5, general conclusions, recommendations for future work has been elaborated.

CHAPTER 2 : LITERATURE REVIEW

2.1 Introduction

This part of the dissertation contains a review of other related studies, its approach development and its significance to this study in order to set up the objectives of this research. Pertinent literatures in the form of Doctoral and Masters' thesis, journal papers, reports, conference papers, internet sources and books collected from different sources are used for this study. It may be mentioned that more than 85% of the journal papers collected from most relevant and prominent peer reviewed worldwide accepted journals such as Applied Energy, Energy, Energy and Buildings, Energy Conversion and Management, Energy Policy, Building and Environment, Applied Thermal Engineering, and International Journal of Energy Research. Moreover, the substantial amount of relevant information has been collected through personal communication with the key researchers around the world in this research area.

2.2 General overview on concentrating solar system

Energy consumption has been steered due to increase in population and wealth. Taking off oil costs, constrained non-renewable assets, expanded ecological consciousness, and plenteous renewable assets drew consideration from all countries to render activities in using alternative energy sources (Schroeder, 2009; Hasanuzzaman et al., 2012; Ahmed et al, 2013; Abdullah et al, 2014). Among all the alternative energies, solar is the most prospective. Sun power can be seized and directed onto little receiving surface by a focusing system. A focusing system or concentrating scheme is gainful for its minimal effort outline, and in addition the accessibility of segments, for example, mirrors, receiver tubes, and perfect mix with fossil fuel advancements to form an amalgam structure. A large amount of electricity along with heat energy can be generated by using a parabolic trough (Lipke, 1996; Kalogirou, 2002). Compared to flat plate collectors parabolic collectors offer higher concentration levels (Arasu, 2007). But the performance of concentrating systems depends on design and material, mirror reflectivity, receiver absorptivity, heat transfer fluid and its flow rate, tracking mechanism and incident angle (Reddy, 2012). A number of studies on parabolic trough concentrator (PTC) system have been carried out. Extensive accomplishments to numerically model and optimize the PTC have been demonstrated through the least squares support vector machine method (Liu, 2012). Similarly modeling of the PTC in 3D numerical simulation is reasonable and consistent (Cheng, 2012). The receivers concentration ratio is notably high in a sphere-shaped receiver, suits parabolic reflectors with pointed focus and 90° edge or rim-angle (Schmidt, 1983). It has been investigated that the semi-cavity and modified cavity receivers in a rim-angle of 65° parabolic dish demonstrate vapor transformation efficiency of 70% to 80% at 450°C (Kaushika, 2000). In a recent analytic model for the optimum length of nanofluid-based volumetric solar receivers the steam power cycle temperatures can reach up to 400°C (Fernández-García, 2010; Veeraragavan, 2012). The performance of the combined-cycle solar power system using PTC is better than the conventional combined-cycle gas turbine power stations (Montes, 2011). A concentrating system can make steam for electricity generation by either water (directly) or intermediary fluids. However, collector performance is significantly affected by the use of intermediate heat transfer fluids (Billah et al., 2011; Cheng, 2012; Islam, 2015). The concentrating mechanism can be accomplished at distinctive concentration levels and can be worked at diverse fluid temperatures. Fluid temperature rises once, concentration ratio is higher and as a result the thermal efficiency enhances (Barlev, 2011). Live steam at 500°C and 12 MPa is capable of reducing the cost of producing power while increasing thermal efficiency (Feldhoff, 2010; Feldhoff, 2012). A PTC can be accommodated according to the application at low temperature or medium temperature or high temperature. Fibreglass-reinforced parabolic trough collector having a smooth rim-angle of 90^0 is designed and developed for warm water supply (Arasu, 2007). A study that is done on the design and construction of five parabolic trough solar collectors with various rim angles in a low-enthalpy process reports that a maximum efficiency of 67% and a temperature of 110°C can be achieved at rim angle of 90^o (Jaramillo, 2013). One more parabolic trough system with an aperture of 0.8 m, length of 1.25 m, and 90^o rim angle is built up through fibreglass as reflector and copper tube for solar ray absorption and results a generation of 75^0C of hot water (Arasu, 2007). In the performance study of a refrigerating machine suitable for remote zones, a parabolic trough having 1.26 m aperture, 0.58 aperture-to-length ratio, and 90^0 rim-angle was used and it produced a maximum of 120^0C (Abu-Hamdeh, 2013). Solnova solar power station with a parabolic collector of 833 m^2-aperture and 150 m long generates 400^0C fluid temperature that is used to yield power steam (SPS, 2013). The 494 m^2 parabolic dish solar concentrator which is the world's largest dish and developed in Australian National University can drive high-temperature applications such as steam power cycle for electricity generation and chemical reaction for fuel production (Pye, 2013). A PTC is potential for widespread use in water heating, cooking, sterilizing, etc., and its efficiency is reasonably high (50%) (Oommen, 2001). For low concentrations it can supply thermal energy at around 90^0C for industrial purposes (Fraidenraich, 2008). In tropical areas, PTC has potential where the higher temperature can be generated due to the higher diffusion of solar irradiation (Pramuang, 2005). The potential application areas of PTC are as in the production of hydrogen, absorption of refrigeration, photovoltaic cells cooling, and generation of electricity (Akbarjadeh, 1996; Hammad, 2000; Lee, 2010; Kaygusuz, 2011).

2.3 Review on gas based solar receiver

2.3.1 Volumetric air receiver

Volumetric air solar receivers are under research and investigation since 1980s. Air flows through the porous structures, can be heated over 800^0C for metals, up to 1500^0C for SiC and 1200^0C for ceramics (Avila-Marin, 2011). This hot air could heat another working fluid or can be used directly in gas turbine (Hennecke, 2008; Zunft, 2011). In 1991, a porous receiver is reported to be installed for a solar electricity station in Spain whose peak outlet temperature was 730^0C. The mean receiver efficiency was 65% at outlet temperature of 550^0C, but at peak temperature 730^0C receiver efficiency reduces to 54% (Chavez, 1991). A two-piece selective volumetric air receiver has been developed, the frontage piece was of clear glass beads or silica honey comb and the second piece was made of silicon carbide. This receiver showed around 90% thermal efficiency at 700^0C outlet gas temperature with minimizing radiative heat losses (Menigault, 1991a; Variot, 1994). A volumetric air receiver with solar tower has been developed for metal processing; it reduces double conversion process: fuel to heat, then to electricity by introducing directly hot air (Sharma, 2015).

2.3.2 Small particle air receiver

In small particle air receiver, air with suspension of submicron or nanoparticles is heated by intense solar radiation in a cavity air-receiver under pressure. The pressurized air in receiver follows high temperature Brayton cycle in transportation of thermal energy (Miller, 1991; Miller, 2000b). This concept of energy transfer by means of solid-gas suspensions was initially proposed in the 1970s (Abdelrahman, 1979a). Large volume of gas particles absorb solar energy in huge amount (Miller, 1991). Some parameters like particle size, particle concentration, particles' optical properties, mass flow rate and temperature have influence on receiver performance; can lead to maximum 90% efficiency (Miller, 1991; Miller, 2000). An experiment carried out with a 25 kW_{th} capacity small particle air receiver provided heated air at around 700^0C (Hunt & Brown, 1983).

2.3.3 Tubular gas receivers

Solar thermal gas receivers are proposed since 1970s, and recently prototypes are developed for high temperature Brayton cycle (Bienert, 1979a; Heller, 2006; Fan, 2007a; Amsbeck et al, 2008; Heller et al, 2009; Hischier, 2009; Uhlig, 2011b). A design regarding the air receiver including air outlet temperature of 815^0C, air inlet temperature of 565^0C, and mass flow rate of air at 0.24 kg /s with a reduction in pressure of 2% has produced thermal efficiency around 85% (Bienert, 1979). Recently tests regarding the central receiver was carried out for a solar-hybrid micro turbine system for applications of 100 kW to 1.0 MW (Amsbeck et al, 2008; Heller et al, 2009). A thermodynamic efficiency above 50% is reported to be attained with a CO_2 Brayton cycle (Anjelino, 1968, 1969; Dostal, 2004; Dostal, 2006; Moisseytsev, 2010; Seidel, 2010). Heat transport fluid CO_2 may be employed in CSP system (Turchi, 2009; Glatzmaier, 2009). But one challenge regarding the use of CO_2 is incorporation with thermal storage; supercritical fluid is feasible for thermal storage system. Intermediate heat transfer media is necessary if CO_2 is used. Analysis of CO_2 receiver for CSP shows promising results (Delussu, 2012).

2.4 Review on Liquid receivers

2.4.1 Tubular liquid receivers

Tubular liquid receivers have been studied since 1970s, though it was first utilized in the 1980s and 1990s in solar power plants named solar one and solar two (Radosevich, 1988; Pacheco, 2002b). Water/steam or molten salt can be used for liquid based receiver. Liquid based tubular receiver, same as recent power tower design approaches, has been experimented at Sandia National Laboratories (Smith & Chavez, 1987; Smith, 1992). Temperature of heat transfer fluid passing the receiver is less than 600^0C. So the re-radiation that may occur at high temperatures of 650-750^0C must be considered. Liquid sodium or fluoride salt or molten nitrate salt are used to attain high temperature and efficiencies. In order to maximize heat transfer and minimize pumping loss, tube diameter and wall thickness may be optimized. Tubular receiver employing a different types of working fluids have shown 84-89% efficiencies (Smith& Chavez, 1987; Singer et al, 2010) reaching above 90% for design point operation (Smith & Chavez, 1987). Fluid characteristic is an important factor for receiver operating temperature that drives receiver efficiency. Fluid type has high influence on designing of receiver. Compared to gaseous heat transfer fluids liquid based receivers possess elevated heat transfer rates and high specific heats. Many heat transfer fluids including sodium (Schiel, 1988) and nitrate salt (Pacheco, 2002) have been investigated to use in solar receiver. Water/steam is used at elevated temperatures in models such as Solar one, PS10 and PS20. But steam above 650^0C possesses huge pressure required for supercritical phase is a concern. An exterior tubular receiver with fused salt that could contain 850 kW/m^2 fluxes has been used in Solar two (Li, 2010). Nitrate salt has also attractive feature; it can also be used as heat transport and storage media at the same time by eliminating in-between heat exchanger linking the receiver and thermal storage. But at higher temperature of above 600-630^0C, the usage of nitrate salt is limited by mass loss. Under this temperature, loss in mass is stable (Freeman, 1956). The drawback of using sodium or liquid metal is that they tend to oxidize. Fluoride salt may be the working fluid for tower receiver. Below 1000^0C liquid fluoride is usually stable that allows low pressure, easy liquid phase handling and carrying (Forsberg, 2007). Although corrosion at higher temperatures is a primary concern, chloride salt has also received consideration (Singer, 2010). Due to material compatibility and affordability, carbonate salt has also been proposed. Carbonate salt can create stable oxide layers which works as protective blockade for the base alloys and has been found noticeably less aggressive with respect to corrosion (Coyle, 1986). But at high temperatures carbonate will degrade, carbonate anion decomposes to carbon dioxide and oxide similar to nitrate salt (Bradshaw, 1990; Stern, 2001). In case of liquid metals and salts, during design and operation, solidification must be considered when melting temperature is above atmospheric temperature. This issue is vital during starting, shutdown and transient running (Pacheco et al, 1994; Pacheco, & Chavez, 1995; Pacheco, 1996). High heat transfer fluid (such as for sodium) conductivity can reduce receiver size by allowing high heat flux. Analytical research on cavity-type as well as external-type receivers are carried out; cavity receiver showed low radiation thermal loss and high convection heat loss than that for external receiver (Falcon, 1986). Tubular receiver performance is examined with slight low thermal efficiency for external-type receiver (Bergan, 1986). Selective receiver coatings may increase thermal efficiency by increasing solar absorption and minimizing thermal emittance. Preferred characteristics regarding the selective receiver coatings ensure constancy at high temperatures in air, resilience to wear, low cost and ease of application. Many coating materials and deposition methods have been investigated for utilization in receiver (Ambrosini, 2011; Hall, 2012).

2.4.2 Falling film receivers

These receivers are distinguished from the others by an approach of gravity controlled fluid velocity. Fluid flows downward an inclined wall and can either be directly or indirectly heated through the wall. Working fluid in such receiver can directly exploit absorbed thermal energy. This approach has been denoted as direct absorption receiving system. Nano molten nitrate salt can be used in liquid film for improving solar absorption (Chavez & Couch, 1987). Addition of oxide dopants to molten salt can improve volumetric absorption (Drotning, 1977a, 1977b, 1978; Jorgensen, 1986). Cobalt oxide can increase receiver efficiency by 4.4% (Bohn, 1989). A recent investigation on suspended nanoparticles has been done with developing an analytic model to determine the effect of thermal loss, particle load, and solar concentration on receiver efficiency (Veeraragavan, 2012). The study on film constancy is conducted with various direct absorption receiver designs. Analytical works have been reported for heat and mass transport in undulating liquid films (Faghri, 1985) and turbulent films (Faghri, 1988, 1989). Correlation regarding the prediction of heat flux that breaks falling liquid film, has also been reported (Bohn, 1993).

2.5 Solid particle receivers

Falling solid particle receivers have been proposed in 1980s (Falcone et al, 1985). This approach can give receiver outlet temperature of over 1000^0C including heat storage capabilities of solid particle. Hot particles can heat up a secondary working fluid for power cycle. Particles are fed into cavity receiver and are directly heated by intense irradiation. Many analytical and lab researches have been done on falling particle receiver (Falcone, 1985; Chen et al, 2007; Chen et al, 2007; Kolb, 2007; Khalsa, 2011) but a single set of on sun test of falling particle receiver was performed by Siegel (Siegel, 2010). Table 2.1 provides a summary of the receivers including the merits and challenges.

Table 2.1: Summary of receivers

Type of receiver	Outlet temperature / thermal efficiency	Benefits	Challenges	References
Gas receivers				
Volumetric air receiver	>700°C / 50-60%	Simple and flexible construction, could achieve high temperature	Radiation heat loss, low thermal efficiency, long term storage, instable flow, material durability.	(Chavez, 1991; Menigault, 1991; Variot, 1994; PitzPaal, 1997; Marcos, 2004; Avila-Marin, 2011;)
Small particle air receiver	>700°C / 80-90% (theoritical)	Capability to achieve high temperature, volumetric gas absorption of energy	Maintain required particle concentration and temperature for solid-gas suspension system, long term storage.	(Abdelrahman, 1979; Miller, 1991; Miller, 2000)
Tubular gas receiver	>800°C / 80-85% (theoritical) &40% (prototype)	Capability to achieve high temperature and gas pressure,	Low thermal efficiency, high radiative and convective heat losses, material durability, long term storage.	(Bienert, 1979; Inc, 1981; Fan, 2007; Uhlig et al, 2009; Amsbeck et al, 2010; Kolb, 2011; Heller et al, 2011)
Liquid receivers				
Tubular liquid receiver	>600°C / 80-90%	Proven performance, could accommodate potentially high pressures	Compatibility of material, tube solidification and plugging, thermal expansion, required high pressure due to pressure drop across the receiver panel.	(Siebers, 1984; Bergan, 1986; Falcon, 1986; Smith, 1987; Schiel, 1988; Epstein, 1991; Smith, 1992; Pacheco, 2002; Singer, 2010;)

Table 2.1: Summary of receivers (continued)

Type of receiver	Outlet temperature / thermal efficiency	Benefits	Challenges	References
Falling film receiver (direct exposer)	>600^{o}C / 80-90%	High receiver outlet temperatures, reduced thermal resistance and startup time due to direct absorption, low pumping losses	Complexity of rotating body, fluid impurities & integrity and film stability in exposed environments, thermal expansion, absorber wall flatness.	(Yih, 1978; Webb, 1985; Faghri, 1985, 1988; Chavez, & Couch, 1987; Bohn, 1987; Wu, 1988;)
Falling film receiver (indirect exposer)	>600^{o}C / >80% (theoritical)	Capable of operating at low insolation, simplicity of fabrication, no need for fluid doping, faster response time, reduced pumping losses	Film stability, absorber wall flatness or shape integrity, distributing flow across the illuminated surfaces for matching the incident flux, thermal loss reduction, efficiency improvement.	(Tracey, 1992; Leon, 1999)
Solid particle receivers				
Falling particle receivers	>800^{o}C/ 80-90% (simulation), 50% (prototype)	Capability to achieve high temperatures, store capability of particles at high temperatures, cost of particles can be cheaper than molten salt.	Essential to reduce radiative and convective heat losses, raise concentration ratios, lower particle attrition, increase solar absorptance, lower thermal emittance, more efficient heat exchangers.	(Falcone, 1985; Kolb, 2007; Chen et al, 2007; Ho, 2009)

2.6 Review regarding the impact of nanofluids on heat transfer for PTC Solar System

Parabolic-trough concentrating (PTC) solar system is one of the potential solar-energy harvesting systems in which the heating of the fluid is an important consideration. Generally, heat-transfer enhancement techniques are related to structure variation; e.g., injection or suction of the fluid, implementation of an electric or magnetic field, addition of a heating surface area, and vibration of the heated surface (Bergles, 1973; Heris, 2007). Improvement of the thermal characteristics of the heat-transfer fluid is important to augmenting the heat transfer. Compared with metals and metal oxides, conventional energy transmission fluids (i.e., water, oil, therminol VP1, ethylene glycol, etc.) have inherently lower thermal conductivity. Fluids with suspended solid nanoparticles of metals or metal oxides are thus expected to possess comparatively better thermo-physical properties (Prasher et al, 2006; Prasher et al, 2006; Sani, 2010; Saidur et al, 2012; Abdin, 2013), which are the key factors to enhancing overall system performance (Kwak, 2010; Javadi, 2013). Compared to conventional fluid, nanofluid is beneficial due to 1) reduced particle blockage, thus improving system contraction, 2) reduced pumping power, 3) adaptable features with thermal conductivity and surface wettability by changing particle concentrations for diverse applications, 4) more heat transfer coverage area between particle and fluid, 5) high scattering constancy with major Brownian motion of particles. By enhancing heat transfer, nanofluids provide the benefit of reducing area of heat transfer of the tubes or heat exchanger (Sokhansefat, 2014). An investigation on the temperature dependence of thermal conductivity showed that over a temperature range of 21^{o}C to 51^{o}C, thermal conductivity of a nanofluid can improve 2-fold to 4-fold (Das, 2003). A study of 35 nm Cu/deionized-water nanofluid flowing in a pipe at steady heat flux is demonstrated that increasing the volume concentrations of nanoparticles in water by 0.5% to 1.2% improves the Nusselt number at the same flow rate from 1.05 to 1.14 (Xuan, 2000). The use of 0.02 and 0.04 volume fractions of Al_2O_3 in water in a horizontal tube with uniform heat flux improves convective heat transfer coefficient by 9% and 15% respectively (Tsai, 2004; Akbari, 2006). An investigation on SiC/water nanofluid in a circular tube has been reported for Reynolds number between 3000 and 13000. Heat transfer could be enhanced up to 60% for a volume fraction of 3.7% (Yu et al, 2009). A series of experiments regarding the effect of solid volume fraction of TiO_2 /water nanofluid under turbulent regime in a double tube heat exchanger has been done. Using different thermal-physical models, it is found that for volume fraction between 0.2% and 2%, heat transfer is the maximum when the optimal particle load is 1% (Duangthongsuk & Wongwises, 2008, 2009, 2010). Duangthongsuk (Duangthongsuk, 2009) has found that 0.2% of TiO_2 in water improves heat transfer coefficient by 6-11%. An investigation on turbulent flow of γ-Al_2O_3/water and TiO_2/water nanofluids in a binary tube heat exchanger has been done. For the Peclet number between 20000 and 60000, Farajollahi et al. has reported optimum fluid concentration which enhanced heat transfer to the maxima (Farajollahi et al., 2010). Improved heat conductivity or arbitrary dispersion of nanoparticles in a fluid enhances the fluid's convective heat transfer (Xuan, 2003). Numerical analysis also showed improved heat transfer in the laminar flow of Al_2O_3/ethylene glycol and Al_2O_3/water nanofluids in a radial-flow system (Roy, 2004; Palm, 2004). Carbon nanohorn-based nanofluids have the prospect to increase the efficiency and compactness of solar thermal systems by enhancing sunlight absorption (Sani, 2011). Lenert (Lenert, 2012) investigated a 28 nm carbon-coated cobalt-therminol VP1 nanofluid-based volumetric solar receiver in high solar flux and high temperature; the receiver's efficiency was found to increase when both the nanofluid column height and the incident solar flux increased. Amrollahi et al. (Amrollahi at al, 2010) tested heat transfer rate of multi wall CNT/water nanofluid under laminar and turbulent flow system in a horizontal circular tube. They found that heat transfer rate rises between 33% and 40% for the solid weight portion of 0.25% CNT in water against pure water. Suresh et al. (Suresh et al, 2011) examined heat transfer characteristic of CuO/water nanofluid for the Reynolds number between 2500 and 6000 in plain and helically dimple tubes. They showed that CuO/water nanofluid with 0.3% concentration in a dimpled tube enhanced heat transfer 39% compared to clean water flows in a plain tube.

Lu (Lu, 2011) experimented with water and water-CuO nanofluid in a high-temperature evacuated tubular solar collector, and found 30% improvement of the evaporating heat transfer coefficient due to water-CuO. A study on heat transfer trend of CuO/water nanofluid with particle size of 23, 51, 76 nm in turbulent flow showed that higher particle size resulted higher heat transfer (Zhang et al, 2010).

A report by Suresh et al. (Suresh et al, 2012) on Al_2O_3/water nanofluid with 0.5% volume fraction flowing in a circular tube having spiral rods showed that nanofluid enhanced heat transfer rate up to 48%. Godson et al (Godson et al, 2012) investigated heat transfer and pressure drop for silver/water nanofluid in a counter flow heat exchanger under laminar and turbulent flow conditions. For 0.9% concentration of nanoparticles they got 70% improvement in heat transfer rate. An investigation on TiO_2/water nanofluid flowing in a horizontal, dual tube, counter flow heat exchanger for a broad series of Reynolds number (8,000 to 51,000) has been done. The investigation showed that nanofluid use is more beneficial at the Reynolds numbers less than 30,000 (Arani & Amani, 2012). An investigation by Azmi et al (Azmi et al, 2013) on SiO_2/water nanofluid in a round tube with maximum solid fraction 4% under constant thermal flux and turbulent flow condition was done. Investigation showed that Reynolds number of 5,000 to 27,000 lead to optimum concentration with maximum heat transfer rate. Hemmat Esfe et al (Esfe et al, 2014) reported on using of MgO nanofluid with solid volume fraction less than 1%. They tested the nanofluid flow in a circular tube in the variety of Reynolds number of 3,000 to 18,000. They noticed a major improvement in heat transfer. An experiment on functionalized MWCNT/water nanofluid in a binary tube heat exchanger under fully developed flow condition was conducted by Hemmat Esfe et al (Esfe et al, 2014). They did an investigation at solid volume fraction of 0.05% to 1% and Reynolds number of 5,000 to 27,000. The investigation showed that for 1% volume concentration, the increment of heat transfer coefficient and Nusselt number have been 78% and 36%, respectively. The investigation showed also that thermal performance factor improved with increasing volume fraction. Kasaeian (Kasaeian, 2012) investigated synthetic oil-Al_2O_3 nanofluid in the receiver tube of a parabolic-trough collector and found that the nanofluid's heat-transfer coefficient augmented with increased concentration of the nanoparticles. Solar absorption improves in nanofluid-containing solar receivers, as shown by the 95% absorption of solar radiation when nanofluids were used in the receivers (Taylor, 2011; Saidur, 2012). Waghole (Waghole, 2014) conducted an experiment on parabolic-trough receiver with/without tape inserts, and with water/silver-nanofluid; the use of tap inserts and of water/silver-nanofluid was found to increase Nusselt number 1.25 to 2.10 times and enhance the efficiency from 135% to 205%.

Existing literatures show that very few researches have utilized nanofluids in PTC system. There is still span to research with fluid flow, and heat transfer improvement using nanofluids. In this research, water and therminol VP1 (synthetic heat transfer fluid composed of biphenyl and diphenyl oxide) were chosen as the base fluids along with eight nanoparticles (CuO, ZnO, Al_2O_3, TiO_2, Cu, Al, SiC, CNT) to examine the effects of nanofluid mass flow rate and volumetric concentration of nanoparticles on the performance of a PTC.

CHAPTER 3 : RESEARCH METHODOLOGY

3.1 Introduction

The design or development of analytical and experimental model for PTC, data collection and various parameters that are used in the research have been described in this chapter. Data has been collected from various sources such as literatures, internet resources, personal communication, etc. Calculations of useful energy, thermal efficiency, concentration ratio, mass flow rate, heat removal factors, etc are discussed here. This chapter also introduced and deduced the related equations that are used in the research.

3.2 Parabolic trough concentrating solar system

Parabolic troughs are solar thermal collectors made by a highly polished metal mirror having a flat dimension in one direction and bended as a parabola in another direction as shown in the Figure 3.1. Solar insolation approaching the mirror is concentrated on the receiver positioned alongside the focused line. By the concentrated solar irradiation, a heat transfer fluid contained in the receiver tube is heated up to an elevated temperature. The hot fluid may be utilized for many industrial and household applications such as space heating, electricity production, heated water supply etc.

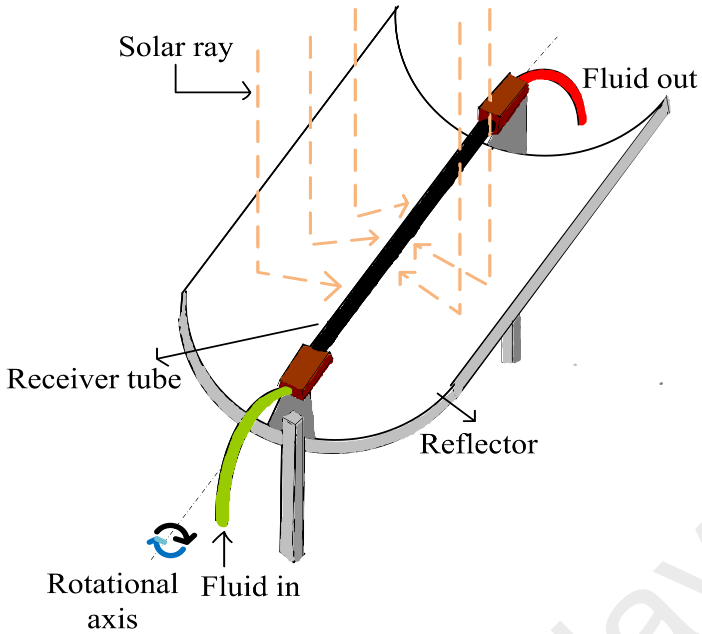

Figure 3.1: Schematic of parabolic trough concentrating solar system.

3.3 Optical modelling

In this study, a PTC is aligned along the north-south horizontal axis in an area of latitude 3.116^0 north of the equator and latitude $101^o39/59//$east of the prime meridian of Kuala Lumpur. It is facilitated to track the sun's traverse from the east to the west. Its angle of incidence θ is computed using the equation below (Duffie, 1991; Kalogirou, 2009).

$$\theta = \cos^{-1}\left[\left(\cos^2\theta_z + \cos^2\delta\sin^2\omega\right)^{\frac{1}{2}}\right] \tag{3.1}$$

where zenith angle,

$$\theta_z = \cos^{-1}\left[\cos\phi\cos\delta\cos\omega + \sin\phi\sin\delta\right] \tag{3.2}$$

and declination,

$$\delta = 23.45\sin\left(360\frac{284+n}{365}\right) \tag{3.3}$$

$(\tau\alpha)_b$ is the product of transmittance-absorptance for the beam radiation which can be found from (Kalogirou, 2009).

$$(\tau\alpha)_b = \frac{\tau\alpha}{1-(1-\alpha)\rho_d} \tag{3.4}$$

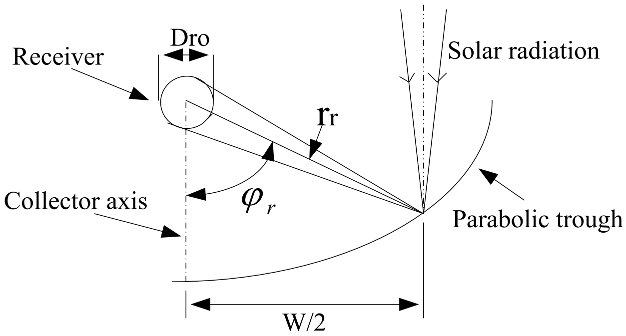

(a)

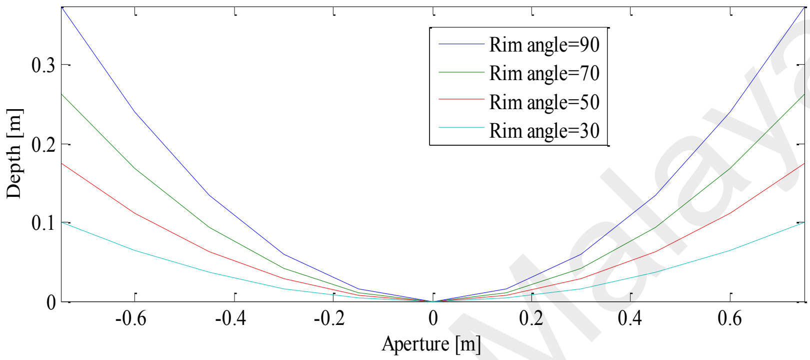

(b)

Figure 3.2: (a) PTC nomenclature, (b) Profile of PTCs at various rim angles.

3.4 Design of parabolic trough system including the gas based solar receiver

The primary design parameters of a PTC are rim angle, trough aperture, and size of the receiver. Rim angle is the angle at which the radiation befalls at the rim of the collector where the mirror radius is the maximum. Rim angle controls the focal distance and focal image or receiver size. In general the incident radiations coming from the sun fall parallel on the trough. The trough directs all the rays to the focal point to make a focal line. The receiver is placed concentric with the focal line. Figure. 3.2(a) is the schematic of a PTC showing different parameters and measurements.

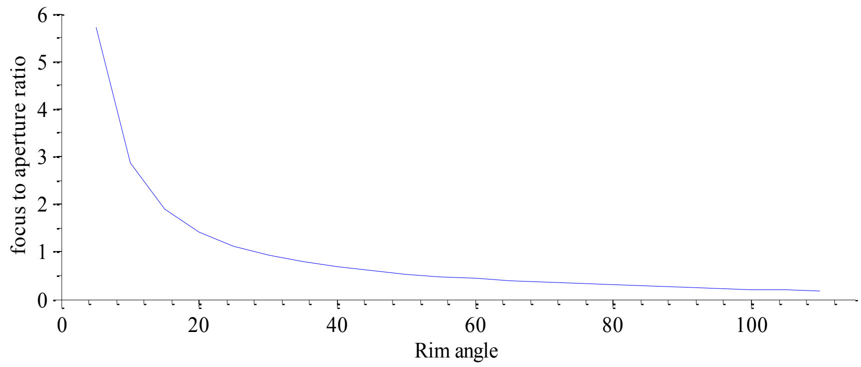

Figure 3.3: Focus-to-aperture ratio as a function of rim angle.

A PTC can be designed on the basis of the equations below:

$$y = ax^2 \tag{3.5}$$

where, $a = \frac{1}{4f}$.

$$\frac{f}{W} = 0.25 \cot \frac{\varphi_r}{2} \tag{3.6}$$

The focal point f can be computed by equation (3.6) (Duffie, 1991). Trough profiles for the same aperture at different rim angles are as shown in Figure. 3.2(b). Figure. 3.3 presents focus-to-aperture ratio as a function of rim angle. It shows that increased rim angle decreases focus-to-aperture ratio. Low focus-to-aperture ratio spread of the reflected beam, resulting lower slope and waned tracking errors. The concentration ratio is maximum at rim-angle 90^0 (Arora, 2012), which also gives optimum intercept factor and a depth that equals the focal length. This study considers a 1.5 m-wide parabolic trough (an aluminium sheet with silver electroplating) and a 90^o rim angle. The trough curvature length is calculated on Equation (3.7) (Duffie, 1991).

$$T_{CL} = \frac{H_p}{2}\left\{ \sec\frac{\varphi_r}{2}\tan\frac{\varphi_r}{2} + \ln\left[\sec\frac{\varphi_r}{2} + \tan\frac{\varphi_r}{2}\right]\right\} \tag{3.7}$$

The receiver size is next calculated on equation (3.8).

$$CR = \frac{W - D_{ro}}{\pi D_{ro}} \tag{3.8}$$

To design an optimum receiver size, a simulation procedure has been followed. Initially a concentration ratio (CR) is taken arbitrarily and then changed to calculate a various receiver diameter D_{ro}. Then thermal analyses have been done on various receiver sizes. By using equation (3.9) (Duffie, 1991; Kalogirou, 2009), the optimum receiver size is calculated in accordance with the maximum thermal efficiency of the collector.

$$\eta_{th} = \frac{Q_u}{I_b A_a} \tag{3.9}$$

The useful heat (Qu) gain is computed as (Duffie, 1991; Kalogirou, 2009):

$$Q_u = F_R\left[SA_a - A_r U_L\left(T_{fi} - T_a\right)\right] \tag{3.10}$$

or

$$Q_u = m_f C_P (T_{fo} - T_{fi})$$

(3.11)

The collector thermal efficiency can thus also be computed by the following equation (Duffie, 1991; Kalogirou, 2009):

$$\eta_{th} = \frac{F_R\left(SA_a - A_r U_L\left[T_{fi} - T_a\right]\right)}{I_b A_a} \tag{3.12}$$

The solar energy absorbed by the receiver has been computed as below (Duffie, 1991; Kalogirou, 2009):

$$S = I_b \rho_C \gamma (\tau\alpha)_b K\theta \tag{3.13}$$

where the incidence-angle modifier can be calculated as:

$$K\theta = 1 - 6.74\times 10^{-5}\theta^2 + 1.64\times 10^{-6}\theta^3 - 2.51\times 10^{-8}\theta^4 \tag{3.14}$$

Collector heat removal factor (F_R) has immense effect on the performance of PTC that can be calculated as (Duffie, 1991; Kalogirou, 2009):

$$F_R = \frac{m_f C_p}{U_L A_{r0}}\left[1 - e^{\left(\frac{-U_L F' A_R}{m_f C_P}\right)}\right] \tag{3.15}$$

where F' is the collector efficiency factor that is related to the convective heat transfer coefficient h_f along with the dimensions of the PTC (Duffie, 1991; Kalogirou, 2009):

$$F' = \frac{1}{U_L\left[\frac{1}{U_L} + \frac{D_{ro}}{D_{ri} h_f} + \left(\frac{D_{ro}}{2K_r}\ln\frac{D_{ro}}{D_{ri}}\right)\right]} \tag{3.16}$$

The heat transfer coefficient h_f for the fluids from the receiver wall surface to the fluids is computed by (Cengel, 2007):

$$h_f = \frac{Nu_f . K_f}{D_{ri}} \tag{3.17}$$

The Nusselt number (Nu_f) can be computed by tube flow equations. For laminar flow Nu_f is given as (Shah, 1978):

$$Nu_f = 4.364 \tag{3.18}$$

where $Re_f \leq 2300$.

For turbulent flow, Nu_f is as follows (Dittus, 1930; Gnielinski, 1976; Cengel, 2007):

$$Nu_f = 0.023 \operatorname{Re}_f^{0.8} \operatorname{Pr}_f^{0.4} \tag{3.19}$$

Where $2300 < Re_f < 1.25\times10^5$ and $0.6 < Pr_f < 100$, or

$$Nu_f = 0.0214 \left(\operatorname{Re}_f^{0.8} - 100\right)\operatorname{Pr}_f^{0.4} \tag{3.20}$$

Where $10^4 < Re_f < 5\times10^6$ and $0.5 < Pr_f < 1.5$.

Natural convection takes place over the glass-cover tube. This natural convection is computed as (Churchill, 1975):

$$Nu^{\frac{1}{2}} = 0.60 + 0.387\left\{\frac{Gr \operatorname{Pr}}{\left[1 + \left(0.559 / \operatorname{Pr}\right)^{9/16}\right]^{16/9}}\right\}^{1/6} \tag{3.21}$$

where $10^{-5} < GrPr < 10^{12}$.

Grashof number Gr is given as:

$$Gr = \frac{\beta \Delta T_g D_g^3}{\nu^2} \tag{3.22}$$

The receiver size has been optimized by a simulation programme written in MATLAB. Three types of fluids: NH_3, N_2, and CO_2 were used in the simulation. The optimization process is as outlined in the flow chart below.

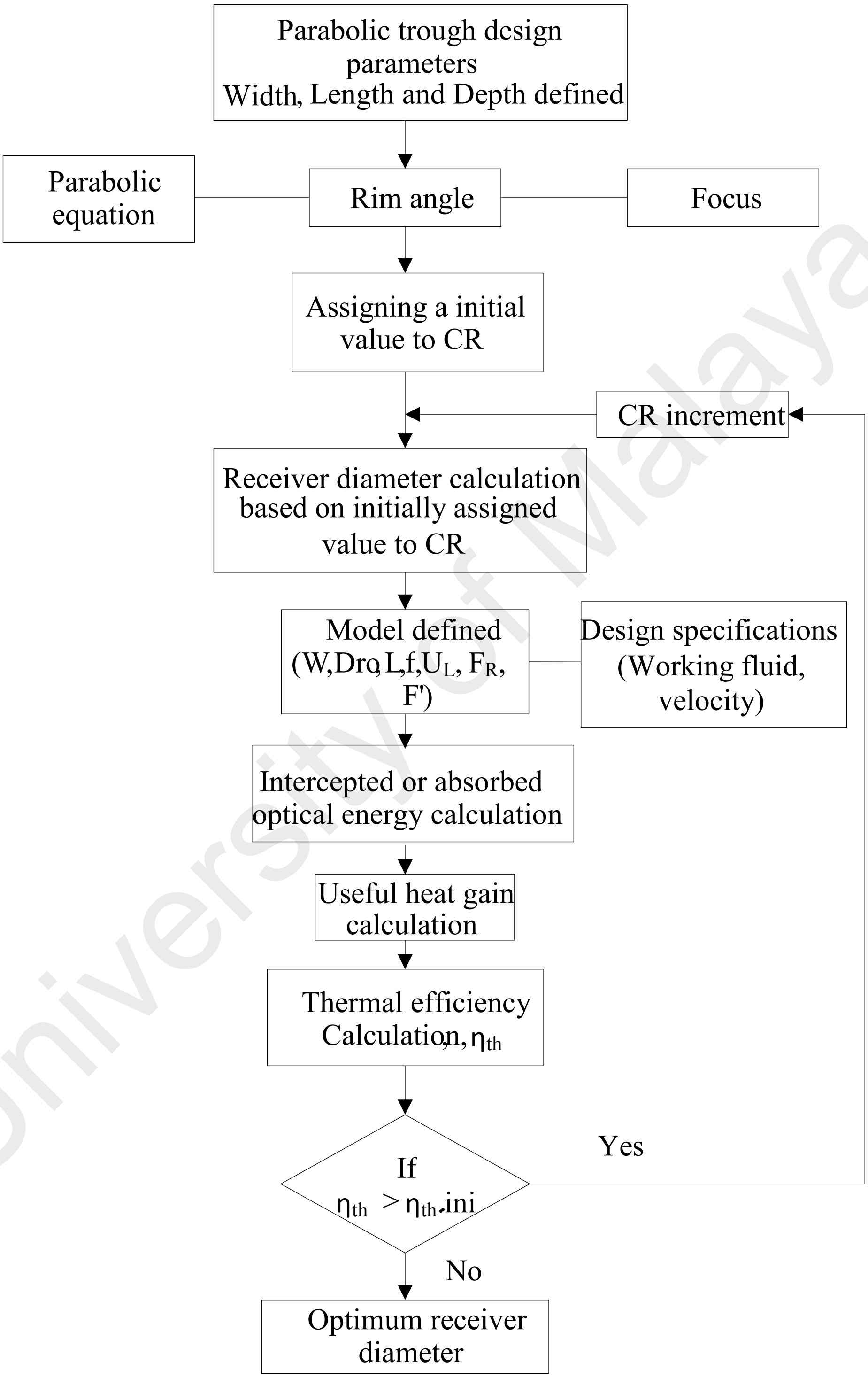

Figure 3.4: Outline of optimizing process for the receiver size.

3.5 Performance of solar receiver for PTC using liquids

The parameters under design consideration and the dimensions of the PTC are as listed in Table 3.1. Water, therminol VP1 and several nanoparticles suspended in water/therminol VP1 have been used. Table 3.2 lists the thermo-physical properties of water, therminol VP1, and selected nanoparticles.

Table 3.1: Dimensions of the system setup and operating conditions

Description	**Specifications**
Parabolic reflector:	
Length	2.0 m
Aperture	1.5 m
Focus	0.375 m
Receiver tube:	
Length	2.0 m
Inner diameter	38 mm
Tube thickness	4 mm
Mass flow rate	0.01 to 1.05 kg/sec
Solid volume concentrations	up to 3%

Table 3.2: Thermal-physical properties of the base fluids and nanoparticles

Material	**K(W/(m.k))**	**Density (kg/m^3)**	**Cp (J/(kg.k))**	**Reference**
Water (34^oC)	0.652	994	4174	(Holman, 1997)
Therminol VP-1 (34^oC)	0.135	1053	1590	(TVP, 2014)
CuO (40 nm)	76	6320	565.11	(Eastman, 1997; Kole, 2012)
TiO_2 (25 nm)	8.4	4157	710	(Eastman, 1997; Kole, 2012)
Al_2O_3 (40 nm)	40	3960	773	(Sarkar, 2011; Kamyar, 2012)
Al (80 nm)	237	2700	904	(Sarkar, 2011; Kamyar, 2012)
Cu (35 nm)	401	890	385	(Sarkar, 2011; Kamyar, 2012)
ZnO (40 nm)	21	5610	523.25	(Eastman, 1997; Kole, 2012)
SiC (16 nm)	150	3370	1340	(Timofeeva, 2010; Sarkar, 2011; Kamyar, 2012)
Multi wall Carbon nanotube (CNT)	3000	1600	796	(Kamyar, 2012)

3.5.1 Formulation of the heat transfer mechanism

The coefficient of heat transfer of base fluid or nanofluid of the parabolic-trough receiver tube was calculated as follows (Cengel, 2007):

$$h_l = \frac{Nu_l K_l}{D_i} \tag{3.23}$$

The Nusselt number Nu_l was calculated for laminar and turbulent flows as follows (Cengel, 2007):

$$Nu_l = 4.364 \tag{3.24}$$

with the constant heat flux considered and $\mathrm{Re}_l <= 2300$.

$$Nu_l = 0.023 \ \mathrm{Re}_l^{0.8} \ \mathrm{Pr}_l^{0.4} \tag{3.25}$$

where 2300 $< Re_l <$ 1.25×10^5 and 0.6 $< Pr_l <$ 100.

In Equation (3.24), Re_l *and* Pr_l are the Reynolds and Prandtl numbers respectively; those were calculated as follows (Cengel, 2007):

$$\mathrm{Re}_l = \frac{4 m_l}{\pi D_i \mu_l} \tag{3.26}$$

$$\mathrm{Pr}_l = \frac{Cp_l \mu_l}{K_l} \tag{3.27}$$

The thermal-physical properties, viz., density, viscosity, specific heat, and thermal conductivity of the nanofluids were calculated with the following correlations (Brinkman, 1952; Cho, 1998; Yu, 2003; Shahrul, 2014):

$$\rho_l = \phi \rho_p + (1 - \phi) \rho_{bf}$$

(3.28)

$$\mu_l = \mu_{bf}(1-\phi)^{-2.5} \tag{3.29}$$

$$Cp_l = \frac{\phi\rho_p Cp_p + (1-\phi)\rho_{bf} Cp_{bf}}{\rho_l} \tag{3.30}$$

The nanofluids' effective thermal conductivity was calculated as follows (Leong, 2006):

$$Keff = \frac{(K_p - K_l)(2\beta_1^3 - \beta^3 - 1)\phi K_l + (K_p + 2K_l)[(K_l - K_f)\phi\beta^3 + K_f]\beta_1^3}{(K_p + 2K_l)\beta_1^3 - (K_p - K_l)(\beta_1^3 + \beta^3 - 1)\phi} \tag{3.31}$$

$$Uncerta\ \mathrm{int}\ y\ /\ deviation = \left|\frac{Theoritica\ lvalue - Experiment\ alvalue}{Theoritica\ lvalue}\right| \times 100\ \% \tag{3.31}$$

The influence of particle size, interfacial layer, and $\beta_1 = 1 + \frac{h}{d}, \beta = 1 + \frac{h}{r}$ is considered in equation (3.30). Calculation for rheological and physical properties were done at the inlet temperature. Constant and various mass-flow rates and also various volumetric concentrations (0.025%-3%) were considered for calculating Nusselt number and convection heat transfer coefficient.

3.6 Experimental setup

A model of PTC has been developed to examine the performance. Experiment is done in Solar Thermal Laboratory, Wisma R&D, University of Malaya, Malaysia. Figure. 3.5 illustrates the test setup or model of PTC that comprises solar simulator, parabolic trough, receiver tube, centrifugal pump, flow meter, variac, data taker and water tanks.

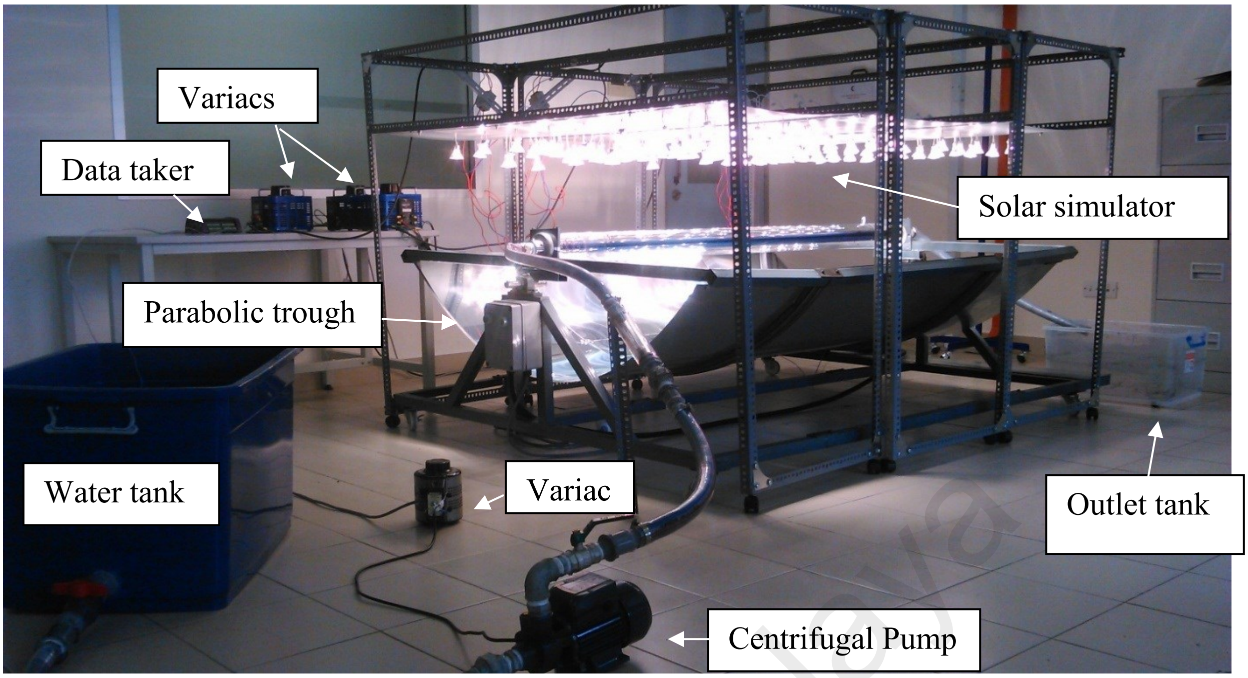

Figure 3.5: Setup of the parabolic trough solar concentrating system.

A mobile iron structure is used to support the parabolic trough and receiver tube is along the focal line of the trough. Trough is silver electroplated aluminum sheet with reflectivity 0.90. Aluminum–nitrogen/aluminum selective absorptive layer is coated on receiver surface to augment the heat absorption. An evacuated glass envelope contains the absorber tube with lessening conduction, convection and radiation losses.

Trough reflects solar radiations and focuses radiations to the absorber or receiver where these radiations are transformed into heat and transported to the heat transmission fluid that is flowing through the receiver. Water and water/CNT nanofluid are used as the heat transmission fluid. Setup comprises three (3) solar simulators. Each simulator contains fourty (40) OSRAM halogen bulbs in two series. This two series are in parallel connection. Each simulator can give maximum 2 KW where every bulb rating is of 50W, 12V and current 7.5A. Simulator is supported by structure made of iron rod angles and iron sheet. Rollers are used to make the simulator portable. Table 3.3 presents the specifications of parabolic trough, receiver tube, solar simulator and other auxiliaries.

Table 3.3: Specifications of parabolic trough, receiver, solar simulator and auxiliaries

Description of items	Specifications
Parabolic trough:	
Material	Silver electroplated aluminum sheet
solar reflectivity	0.90
Length	2.00 m
Aperture	1.50 m
Rim angle	85^0
Receiver tube:	
Material of solar absorptivity	Copper tube with selective coating (0.94)
Thermal emittance	0.08
Length	2.00 m
Inner diameter	48.00 mm
Tube thickness	4.00 mm
Solar simulator:	
Quantity	3
Halogen bulb	12 V, 50 W (overall 120 bulbs)
Pyrenometer	0 to 1280 W/m^2
K-type thermocouple	-75°C to 250°C
Variacs	3.00 KVA
Heat transfer fluid	Water, Water/CNT nanofluid
Pump	Maximum 35.00 l/min
Mass flow rate	0.80 l/min to 1.30 l/min

Three variable control AC power supply transformers (variac) each rating 3kVA power three simulators. Variac can vary bulb irradiation intensity. Concentrator reflects bulb irradiation onto the receiver. Fluid (water or water/CNT nanofluid) is pumped through the absorber tube from a tank by a centrifugal pump (model Pentax CP45). Fluid absorbs heat from the absorber. A variac drive the pump with varying the flow rate. The pump capacity is maximum 35 l/min; with discharge head of maximum 35 m; and operating horse power of 0.50 kW. Two K-type thermocouples have been utilised to gauge temperature at inlet and outlet of the absorber tube. Pyranometer gives irradiance value. Three photographic views have been shown in Figure. 3.6(a) data taker and variacs, 3.6(b) Centrifugal pump and, 3.6(c) parabolic mirror and receiver.

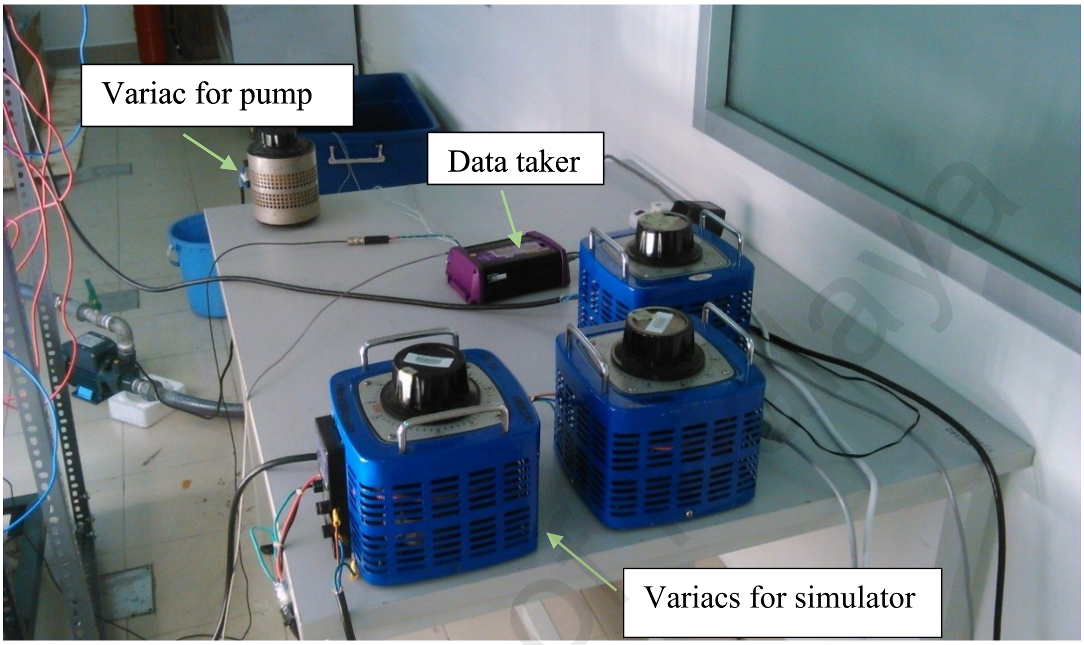

(a)

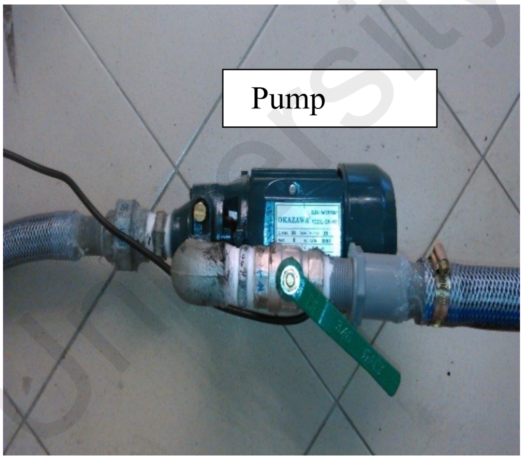

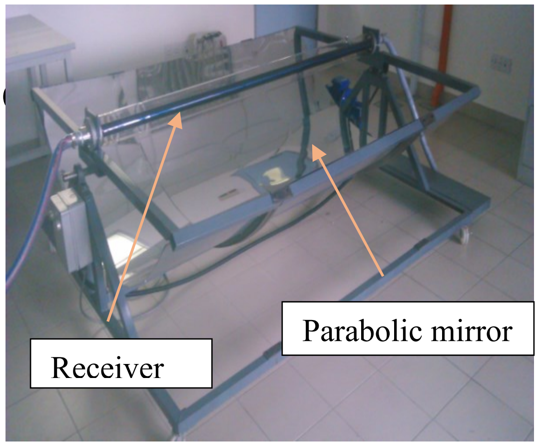

(b) (c)

Figure 3.6: (a) Variac and data taker, (b) Centrifugal pump and (c) Parabolic mirror and receiver.

3.6.1 Instrumentation for investigation

In investigating the PTC performance, various instruments have been used. Pyranometer, thermocouple, flow meter and data taker have been used. Data for temperature and irradiation intensity is recorded by a digital Data Taker (model DT80). A flow meter records the fluid mass flow rate. Fluid temperature at inlet and outlet of the receiver is measured by PTFE exposed welded-tip K-type thermocouple whose temperature measuring range is between -75°C and 250°C. A pyranometer LI-COR PY82186 whose radiation measuring range is from 0 to 1280 W/m^2, spectral range is from 300 nm to 1100 nm and operating temperature ranges from -40^{o}C to 75^{o}C; is used for measuring the radiation intensity of the solar simulator. Before utilization pyranometer is well calibrated.

3.6.2 Experimental test condition and data acquisition

Variation in different parameters has been done for investigating the performance of the PTC. Room temperature is kept within the range 27^{0}C to 30^{0}C. Irradiation intensity and water mass flow rate differ from 340 W/m^2 to 650 W/m^2 and 0.80 l/min to 1.30 l/min respectively. Change of each parameter is independent relating to other. Only one parameter varies, whereas the other remains unchanged. At regular intervals of one minute, data is collected and recorded by Data Taker. The collected data is explored to examine the influence of irradiation intensity, temperature and flow rate on the performance of the PTC. To investigate the impact of nanofluid on thermal performance of PTC, carbon nanotube (CNT) is used in water, based on availability in Malaysia. Using CNT/water nanofluid, experiment is done at 1.15 l/min and 1.25 l/min flow rates. Irradiations are varied between 477 W/m^2 and 640 W/m^2. The collected data is analyzed and compared with water and theoretical results.

CHAPTER 4 : RESULTS AND DISCUSSION

4.1 Introduction

This chapter contains the experimental results and the inferences obtained from their analysis. The estimated variables such as useful heat gain, thermal efficiency, heat removal factors, etc are analyzed using gas and liquid for PTC with necessary figures in this chapter. Impact of using nanofluids on the performance of PTC is also pointed out.

4.2 Gas based solar receiver for PTC

In this section, a receiver size was optimized including thermal analysis for a PTC using gas. Three gases such as NH_3, N_2 and CO_2 are used. Some parameters like heat removal factor, useful heat gain, concentration ratio, thermal efficiency, and mass flow rate of the heat transfer fluid have been examined using these gases at a flow velocity of 18 m/s. The influence of the CR and absorber tube diameter on the collector efficiency have been depicted in Figure 4.1.

Initially the collector efficiency is increased through all the thermo fluids with the increase of CR and reached to a maximum value at CR =8.90 and then decreased. The highest collector efficiency with each fluid is happened at CR = 8.90 as illustrated in Figure 4.1 (a). Similarly the collector efficiency is enhanced with the greater receiver size and reached to a maximum when receiver diameter is 51.80 mm (CR = 8.90) as revealed in the Figure 4.1 (b).The highest efficiencies of NH_3, N_2, and CO_2 were 67.05%, 66.81%, and 67.22%, respectively. After that efficiencies decreased with increasing receiver diameter. Both Figure 4.1 (a) and Figure 4.1 (b) exhibit similar increasing/decreasing behaviors.

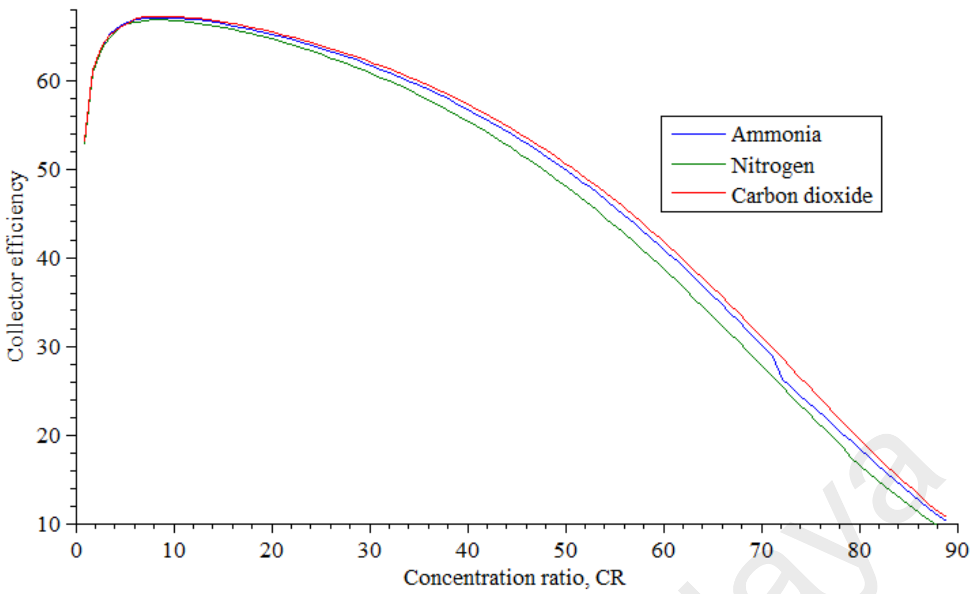

(a)

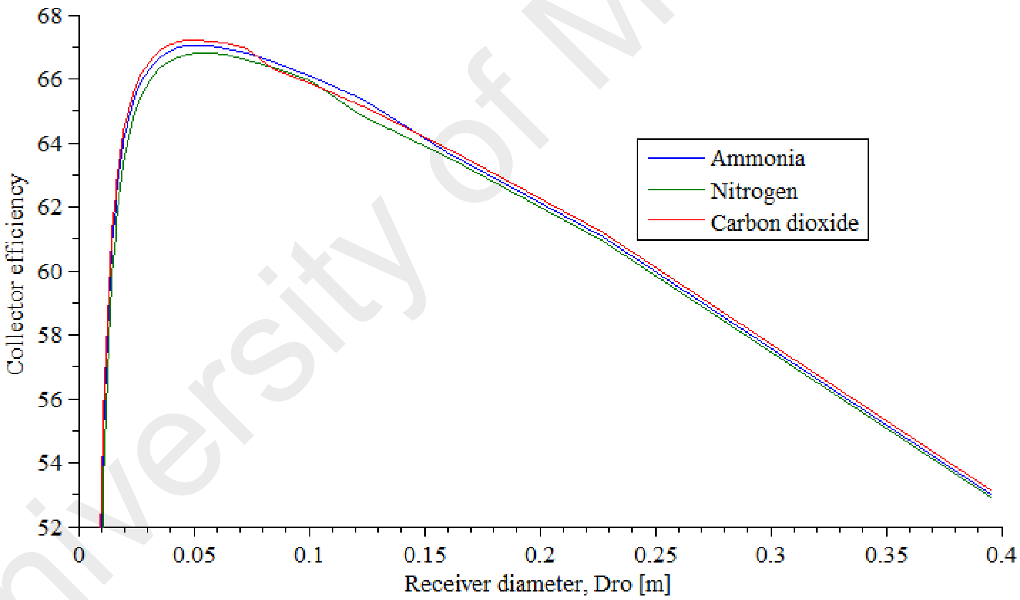

(b)

Figure 4.1: Collector efficiency as a function of (a) concentration ratio and (b) receiver diameter.

Figure 4.2(a) and Figure 4.2(b) exhibit the effects of concentration ratio and receiver diameter on useful heat gain, respectively. As can be seen from the figures heat gain at first increases with CR or receiver size up to reaching a value of CR at 10.8, then the heat gain fell. Both figures also reveal that at CR=10.80, the collector efficiencies are found 64.43%, 64.02%, and 64.67% respectively for ammonia, nitrogen, and carbon dioxide. However, these efficiency values are lower than their respective maximums.

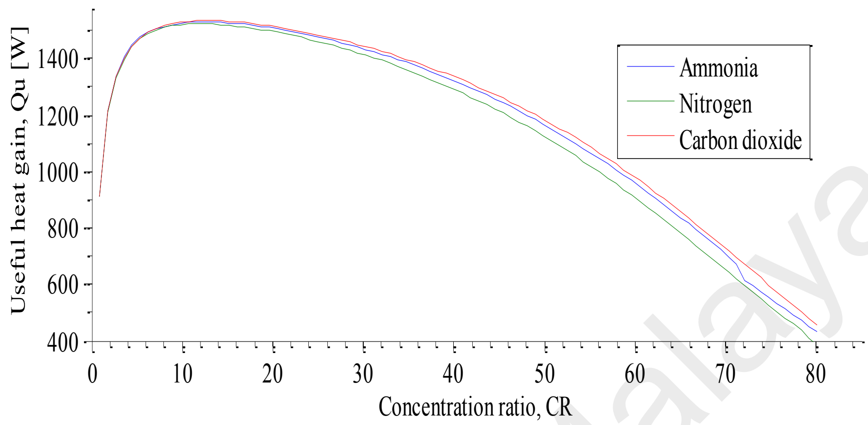

(a)

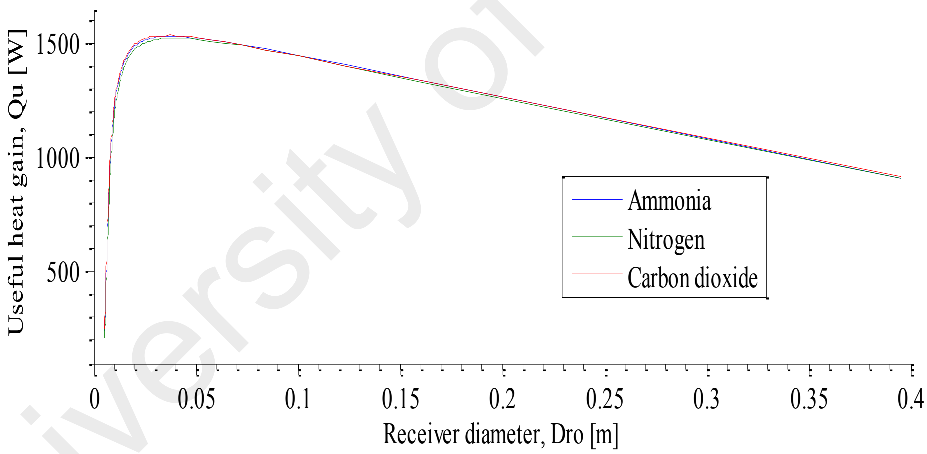

(b)

Figure 4.2: Useful heat gain as a function of (a) concentration ratio and (b) receiver diameter.

Heat removal factor and collector efficiency have mathematical correlation with each other. The thermal energy transfer characteristic of the collector and the influence of convection heat transport on the collector thermal performance is reflected by the dimensionless group heat removal factor.

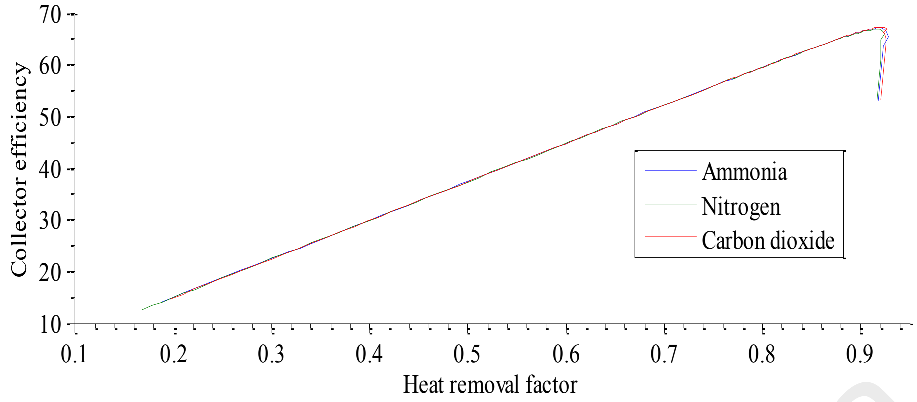

Figure 4.3: Collector efficiency as a function of heat removal factor.

Figure 4.3 illustrates that initially efficiency upsurge linearly with heat removal factor, but then drops at a heat removal factor around 0.9. The maximum collector efficiencies in case of CO_2, NH_3, and N_2 are found 67.22%, 67.05%, and 66.81%, respectively against the above mentioned heat removal factors.

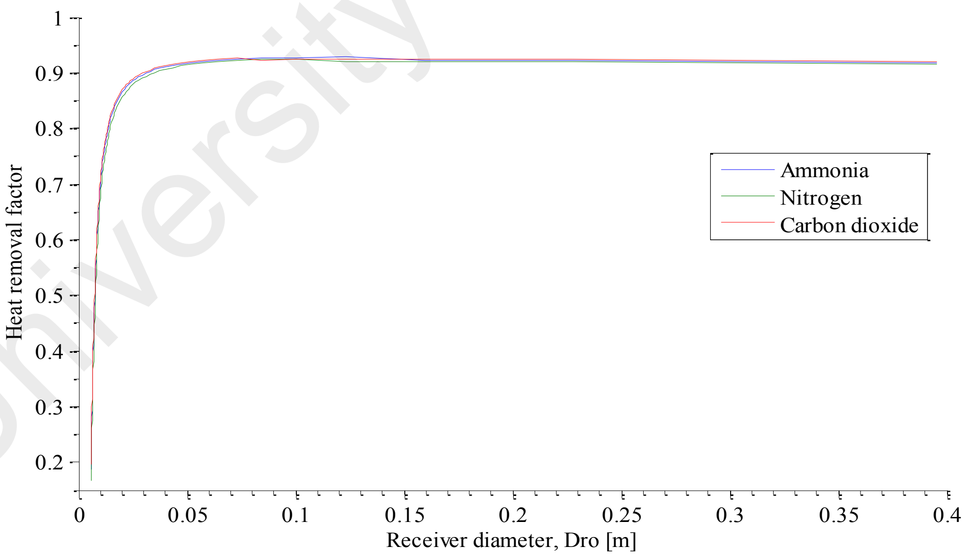

Figure 4.4: Heat removal factor as a function of receiver size.

The influence of receiver size or diameter on heat removal factor is shown in Figure 4.4. It reveals that, the heat removal factor has improved with the receiver size, but after 51.80 mm diameter the heat removal factor is almost constant for all fluids. Heat removal factor is dependent on fluid mass flow rate. Figure 4.5 exhibits the influence of mass flow rate on heat removal factor. When the flow rate is increased the heat removal factor of each fluid is also improved. The increasing rates of all the fluids are similar until a heat removal factor of 0.91. After that a gentle variation in the increase rates have been observed. Subsequently the heat removal factors of each fluid have reached to their highest values (0.928 at 0.119 kg/s for NH_3, 0.927 at 0.102 kg/s for CO_2, and 0.925 at 0.146 kg/s for N_2), then suddenly dropped before stabilized again with a declining tendency. The decline rate for NH_3 has been shown greater compared to the other two fluids. The collector efficiency is mostly dependent on the heat removal factor.

Also notable was that maximum mass flow rates differed among the fluids. Fluid velocity was kept fixed and the density of three gases were different. Solar concentration was changed continuously at an interval. The receiver diameter was calculated at every concentration value. Mass flow rates were calculated using receiver diameter, velocity and gas density. Minimum concentration (0.89) and gas density limit the maximum mass flow rates of the gases (1.28 kg/s, 2.42 kg/s, 3.29 kg/s).

An increasing trend in collector efficiency with fluid mass flow rate can be noticed from Figure 4.6. Maximum efficiencies of 67.22%, 67.05% and 66.81% are obtained at the mass flow rates of 0.0491 kg/s for CO_2, 0.0192 kg/s for NH_3 and 0.0362 kg/s for N_2, respectively. Thus as the mass flow rate is increased collector efficiency falls. This declining trend is prominent with NH_3. Heat removal factor has relation with mass flow rate, specific heat, heat loss coefficient, receiver outer area, and collector efficiency factor.

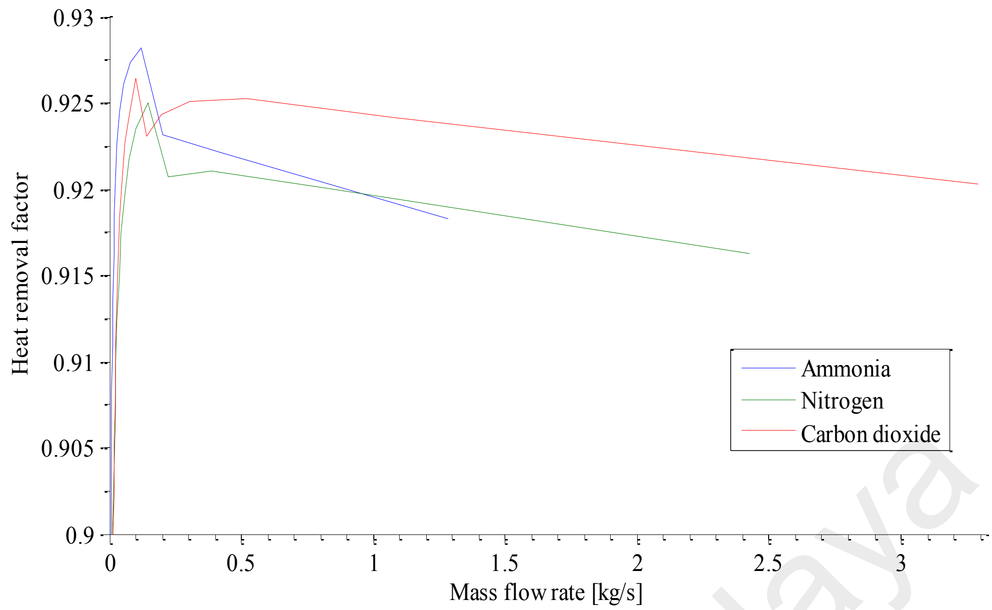

Figure 4.5: Heat removal factor as a function of fluid mass flow rate.

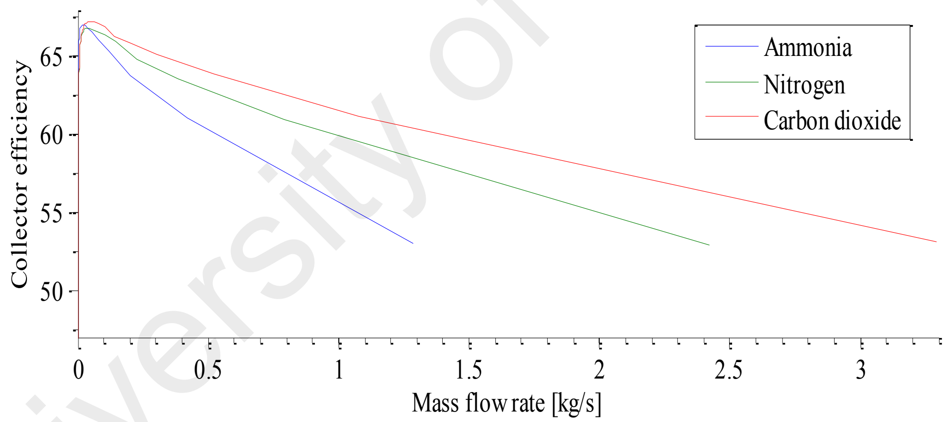

Figure 4.6: Collector efficiency as a function of fluid mass flow rate.

In addition to the inferences mentioned above there are dependencies among heat removal factor, heat gain, collector aperture area, receiver size, and collector efficiency as well. Fluid mass flow rate increases with receiver size increasing whereas an increase in receiver size decreases the heat gain. As the mass flow rate is different for all fluids at the same aperture area of 2.836 m^2; different flow rates, viz., 0.049 kg/s for CO_2, 0.019 kg/s for NH_3 and 0.036 kg/s for N_2, produce highest collector efficiencies of 67.22%, 67.05%, and 66.80%, respectively.

4.3 Liquid based solar receiver for PTC

In this section, thermal analysis using liquids for solar receiver of a PTC is presented. Water, therminol VP1 and several nanoparticles suspended in water and therminol VP1 were used. Nanoparticles addition to fluid can enrich thermal properties of fluid, viz., thermal conductivity, radiative heat transfer, mass diffusivity, etc. Nanoparticle volume fraction affects heat transfer significantly, and can enhance collector efficiency (Javadi et al, 2013). The effects of mass flow rate and nanoparticles volume fraction on heat transfer coefficient have also been explained in this section.

4.3.1 Thermal performance at constant mass-flow rate

To investigate thermal performance, heat transfer coefficients were measured. The performance due to water-based nanofluids and therminol-VP1-based nanofluids including base fluids with 1% nanoparticles at constant flow rate (0.8 kg/s) are presented and discussed in this section.

4.3.1.1 Investigation on heat transfer coefficient

The effects of nanoparticles on heat transfer along the receiver tube are shown in Figure 4.7 and Figure 4.8, respectively for water and therminol-VP1-based nanofluids. Adding 1% several type nanoparticles to water and therminol VP1, heat transfer coefficients were found 3183.8 W/(m^2.K), 3247 W/(m^2.K), 3234.5 W/(m^2.K), 3268 W/(m^2.K), 3225.7 W/(m^2.K), 3313.9 W/(m^2.K), 3294.9W/(m^2.K), 3294.4 W/(m^2.K), 3310.3 W/(m^2.K) for respectively water, W-CuO, W-ZnO, W-Al_2O_3, W-TiO_2, W-Cu, W-Al, W-SiC, W-CNT and 490.24 W/(m^2.K), 503.53 W/(m^2.K), 503.31 W/(m^2.K), 507.01 W/(m^2.K), 504.73 W/(m^2.K), 510.11 W/(m^2.K), 509.05 W/(m^2.K), 510.69 W/(m^2.K), 510.13 W/(m^2.K) for therminol VP1, VP1-CuO, VP1-ZnO, VP1-Al_2O_3, VP1-TiO_2, VP1-Cu, VP1-Al, VP1-SiC, VP1-CNT, respectively. Heat transfer coefficient of base fluids (water and therminol VP1) is lower than that of nanofluids. Adding nanoparticles enhances heat transfer rate. W-Cu and VP1-SiC have the maximum heat transfer coefficients among water and therminol VP1 based nanofluids respectively.

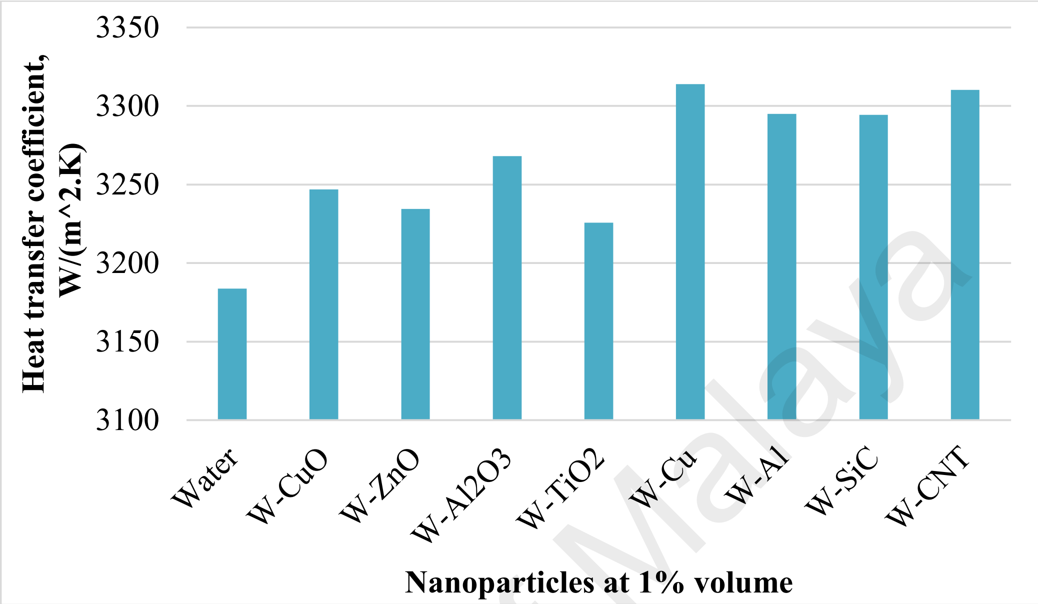

Figure 4.7: Heat transfer coefficients of water and water based nanofluids at constant mass flow rate (0.8 kg/s).

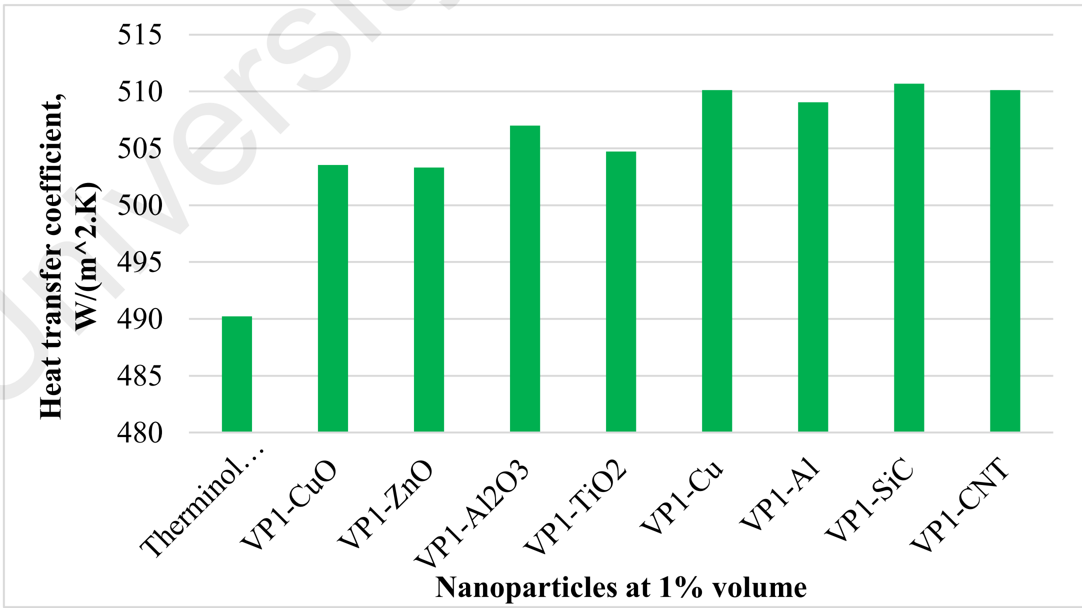

Figure 4.8: Heat transfer coefficients of therminol VP1 and therminol VP1 based nanofluids at constant mass flow rate (0.8 kg/s).

Figure 4.9 and Figure 4.10 exhibit the augmentation in heat transfer coefficient by using nanoparticles in water and therminol VP1 respectively. The enhancement of heat-transfer coefficients at 0.80 kg/s mass flow rate were found to be 1.98%, 1.59%, 2.64%, 1.31%, 4.08%, 3.49%, 3.47% and 3.97%, for respectively W-CuO, W-ZnO, W-Al_2O_3, W-TiO_2, W-Cu, W-Al, W-SiC and W-CNT nanofluids. With therminol-VP1 nanofluids, the enhancement of heat-transfer coefficients at the same mass-flow rate were 2.71%, 2.66%, 3.42%, 2.95%, 4.05%, 3.84%, 4.17%, and 4.06% for respectively VP1-CuO, VP1-ZnO, VP1-Al_2O_3, VP1-TiO_2, VP1-Cu, VP1-Al, VP1-SiC and VP1-CNT. The results prove that W-Cu nanofluid possess the highest coefficient of heat transfer among water-based nanofluids, whereas the maximum heat transfer coefficient in the case of therminol-VP1-based nanofluids is for VP1-SiC. The specific heat of nanofluid is the main reason. Cu and SiC have higher specific heat than other nanoparticles. However, the thermal conductivities of W-Cu and W-SiC are 0.6815 W/(m.K) and 0.6814 W/(m.K) respectively, and nearer to the maximum 0.6825 W/(m.K) of W-CNT among water-based nanofluids. The specific heat of W-Cu nanofluid (4154.9 J/(kg.K)) is 14.46% and 0.49% higher than that of W-SiC and W-CNT nanofluids respectively, although the specific heat of SiC and CNT particles are respectively 32.5%, and 40.5% higher than that of Cu particle. The specific heat of water is also comparatively higher. The density of Cu particle thus dominate, leading to a comparatively lower-density nanofluid W-Cu (992.96 kg/m^3, which is 2.50% and 0.72% lower than the density of W-SiC, W-CNT) and produce a heat transfer coefficient of 3313.9 W/(m^2.K) which is the maximum among water based nanofluids. In case of therminol VP1 based nanofluids, VP1-SiC and VP1-CNT have the same thermal conductivity of 0.1474 W/(m.K). VP1-Cu also has almost same figure of 0.1473 W/(m.K). The density of VP1-SiC (1067.2 kg/m^3) is 0.82% and 1.50% higher than that of VP1-CNT and VP1-Cu respectively. But VP1-SiC is the one with the maximum heat-transfer coefficient. The increased specific heat of the nanofluid is due to the high specific heat (1340 J/KgK for SiC) of the nanoparticle. The specific heat of VP1-SiC nanofluid (1582.2 J/(kg.K)) is higher than that of other therminol-VP1-based nanofluids which produces the highest heat-transfer coefficient 510.69 W/(m^2.K) and thus enhances heat transfer coefficient to the maxima of 4.17%.

Other water-based nanofluids differ in their thermal conductivities, so thermal conductivity is a crucial element here. Nanofluids with higher thermal conductivity produce higher heat transfer coefficients and consequent higher heat transfer enhancement. W-TiO_2 nanofluid was observed to have the lowest improvement of heat transfer coefficient, owing to its low thermal conductivity of 0.6629 W/(m.K) which is the lowest among all of the nanofluids though its specific heat capacity is 4.44% and 3.28% higher than that of W-CuO and W-ZnO nanofluids respectively.

All therminol-VP1-based nanofluids have almost the same thermal conductivities. Specific heat capacity is the main reason for the increased heat-transfer coefficients in therminol-VP1-based nanofluids. Nanofluids with higher specific heat produce higher heat transfer coefficients and thus cause greater enhancement of heat transfer. But the VP1-ZnO causes the lowest improvement of heat transfer although VP1-CuO possesses the lowest specific heat capacity of 1531.4 J/(kg.K). The low improvement is due to the both thermal conductivity 21 W/(m^2.K) and specific heat 523.25 J/(kg.K) of ZnO nanoparticle, respectively 72.4% and 7.4% lower than that of CuO.

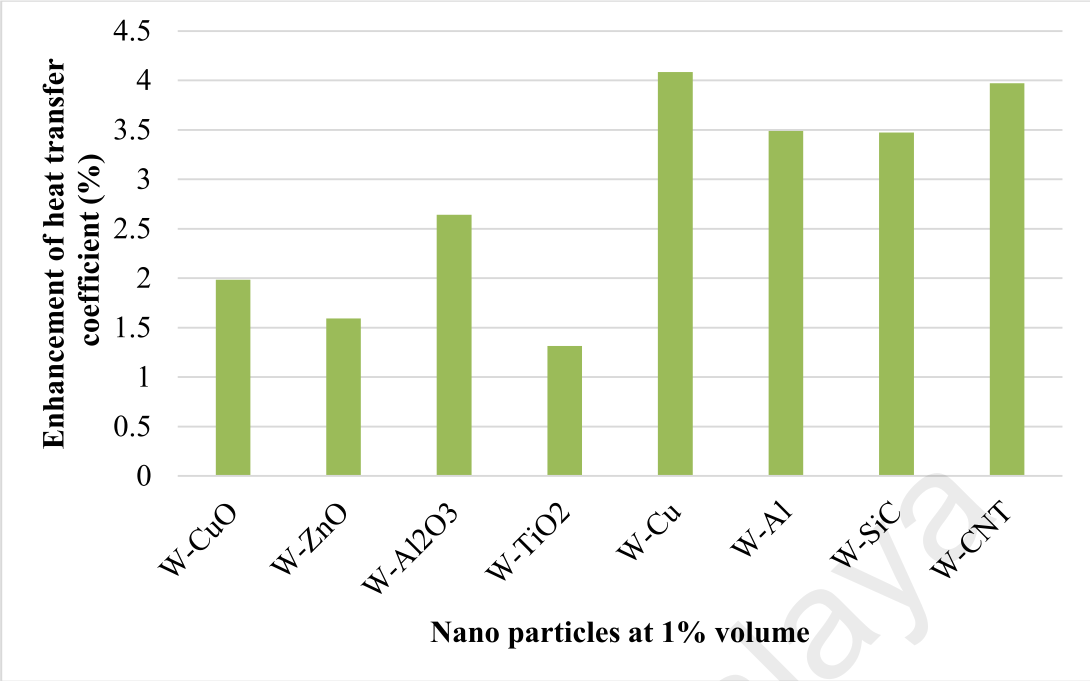

Figure 4.9: Heat transfer coefficient augmentation for water-based nanofluids at a mass flow rate of 0.8 kg/s.

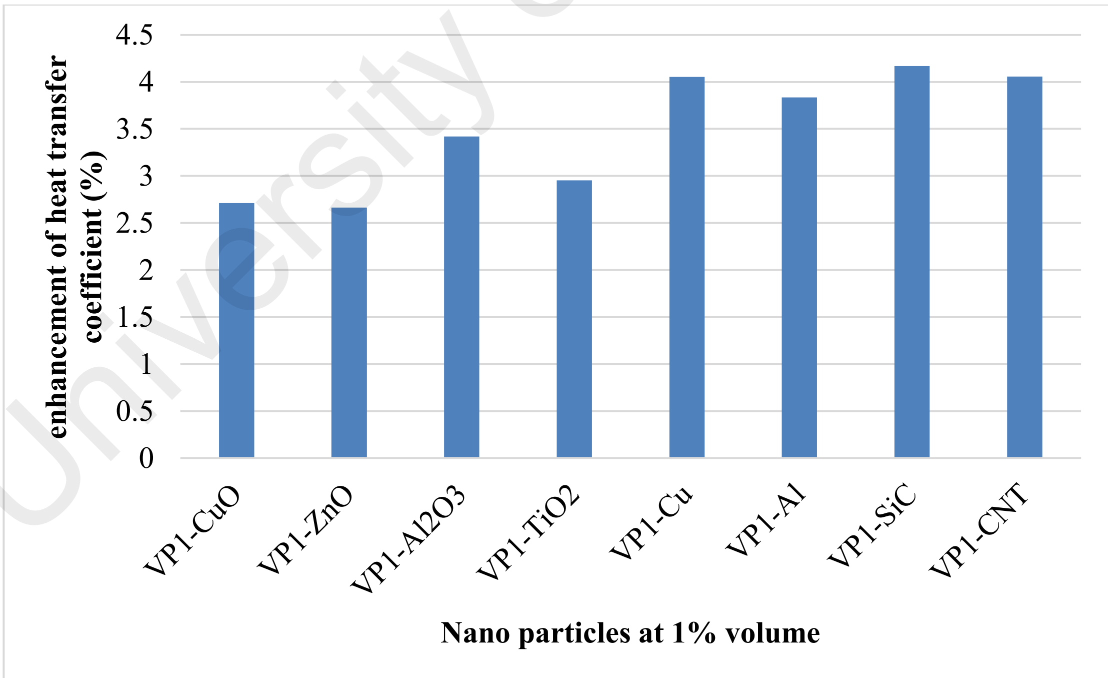

Figure 4.10: Enhanced heat-transfer coefficient of therminol-VP1-based nanofluids at 0.8 kg/s mass flow rate.

4.3.2 Thermal performance at different mass flow rates

In this section, investigation on heat transfer coefficient by using nanoparticles in water and therminol VP1 at different mass flow rates have been discussed. 1% nanoparticles (CuO, ZnO, Al_2O_3, TiO_2, Cu, Al, SiC, CNT) were added for the investigation.

4.3.2.1 Investigation on heat transfer coefficient at different mass flow rates

Four different mass flow rates (0.08 kg/s, 0.39 kg/s, 0.80 kg/s and 1.30 kg/s) were observed. Analysis on heat transfer coefficient for water and water based nanofluids, therminol VP1 and therminol VP1 based nanofluids have been shown in Figure 4.11 and Figure 4.12 respectively. Insertion of nanoparticles in fluid enhances heat transfer. W-Cu and VP1-SiC have given maximum heat transfer coefficient 525.22 W/(m^2.K) to 4886.8 W/(m^2.K) and 16.93 W/(m^2.K) to 753.07 W/(m^2.K) at 0.08 kg/sec to 1.3 kg/sec flow rate.

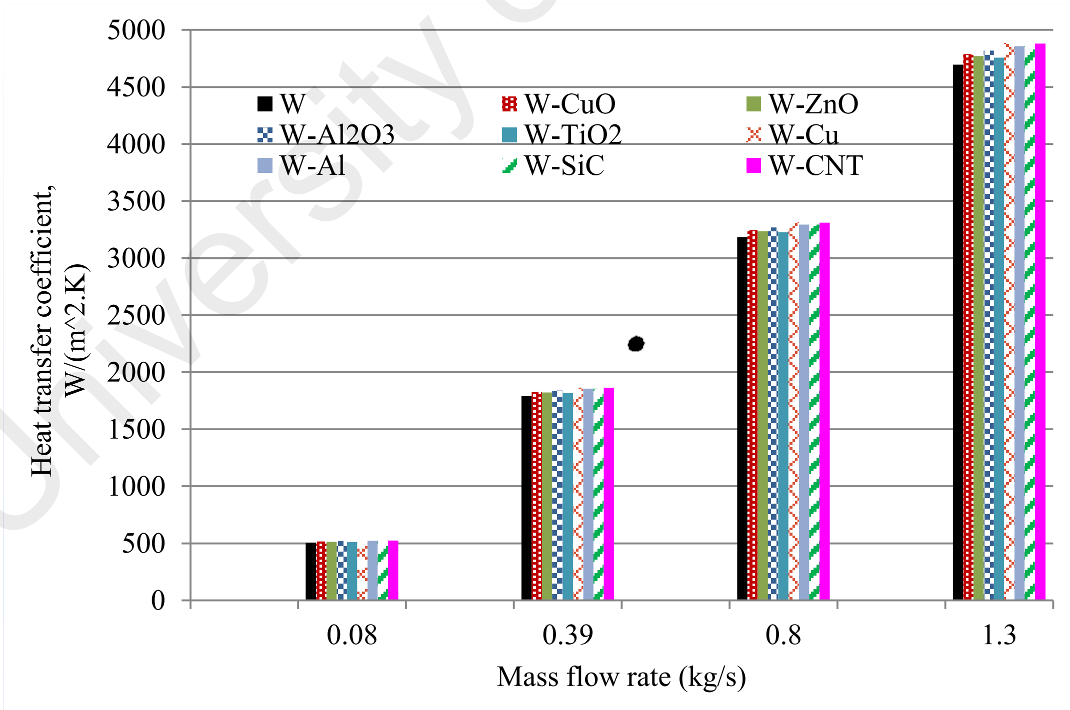

Figure 4.11: Heat transfer coefficients of water and water based nanofluids at different mass flow rates.

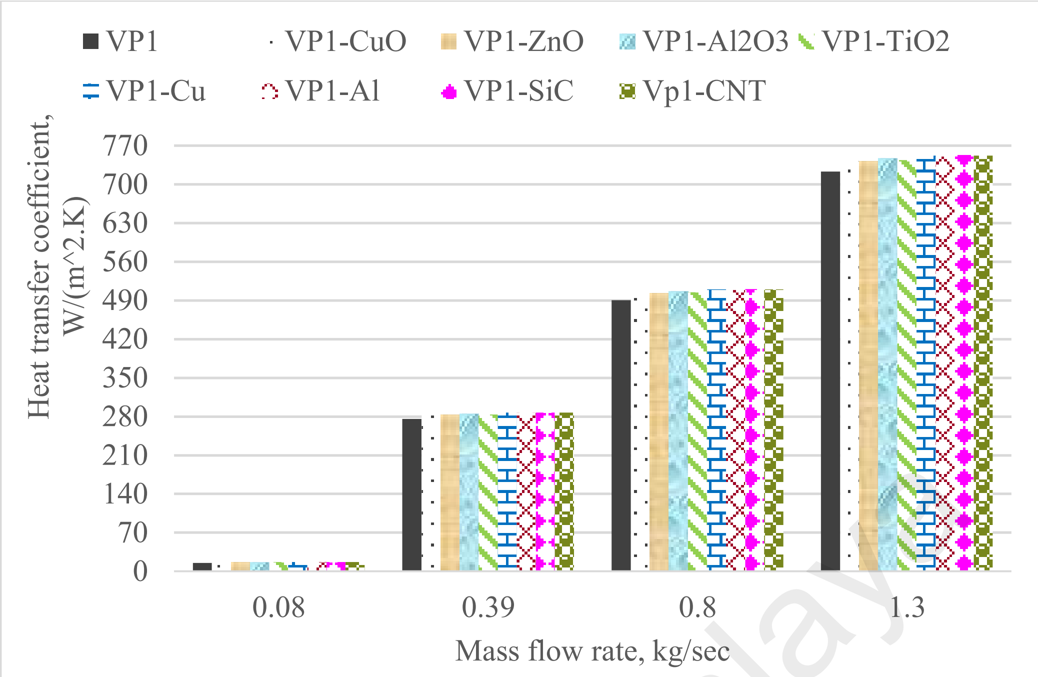

Figure 4.12: Heat transfer coefficients of therminol VP1 and therminol VP1 based nanofluids at different mass flow rates.

Figure 4.13 and Figure 4.14 presented the enhanced coefficients of heat-transfer of water and therminol-VP1-based nanofluid, respectively. The figures show that during laminar flow, enhancement of heat transfer coefficients does not vary with varying mass flow rates. In the transition period, the heat transfer coefficients drop until turbulent flow is reached. During turbulent flow, enhancement of the heat transfer coefficient remains constant while the mass-flow rate is changed. Because during laminar or turbulent flow, heat transfer enhances at the same rate in base fluid and nanofluids. Figure 4.13 shows 8.64%, 7.56%, 8.24%, 6.07%, 9.04%, 8.93%, 9.03%, and 9.19% enhanced heat-transfer coefficients in laminar flow, and 1.98%, 1.59%, 2.64%, 1.31%, 4.08%, 3.49%, 3.47% and 3.97% in turbulent flow, both respectively in W-CuO, W-ZnO, W-Al_2O_3, W-TiO_2, W-Cu, W-Al, W-SiC and W-CNT nanofluids. Figure 4.14 shows 9.02%, 8.74%, 8.92%, 8.28%, 9.12%, 9.07, 9.21%, and 9.20% enhanced heat-transfer coefficients in laminar flow, and 2.71%, 2.66%, 3.42%, 2.95%, 4.05%, 3.84%, 4.17%, and 4.06% in turbulent flow, both respectively for VP1-CuO, VP1-ZnO, VP1-Al_2O_3, VP1-TiO_2, VP1-Cu, VP1-Al, VP1-SiC and VP1-CNT nanofluids. Since Nusselt number is constant in all the nanofluids (refer to equation 3.23) thermal conductivity is the only factor to upgrade the heat transfer coefficient during laminar flow (refer to equation 3.22). The highest enhancement of the heat transfer coefficient is provided by W-CNT and VP1-SiC nanofluids due to their maximum thermal conductivities. The heat transfer coefficients of other nanofluids, too, have been found to depend on their thermal conductivities.

During turbulent flow, the heat transfer coefficient of water-based nanofluids is enhanced. W-Cu and W-TiO_2 have the maximum and the minimum enhancement of heat transfer coefficient, respectively. In therminol VP1-based nanofluids, however, specific heat is the major enhancer of heat transfer, with VP1-SiC and VP1-ZnO respectively having the highest and the lowest heat transfer coefficient.

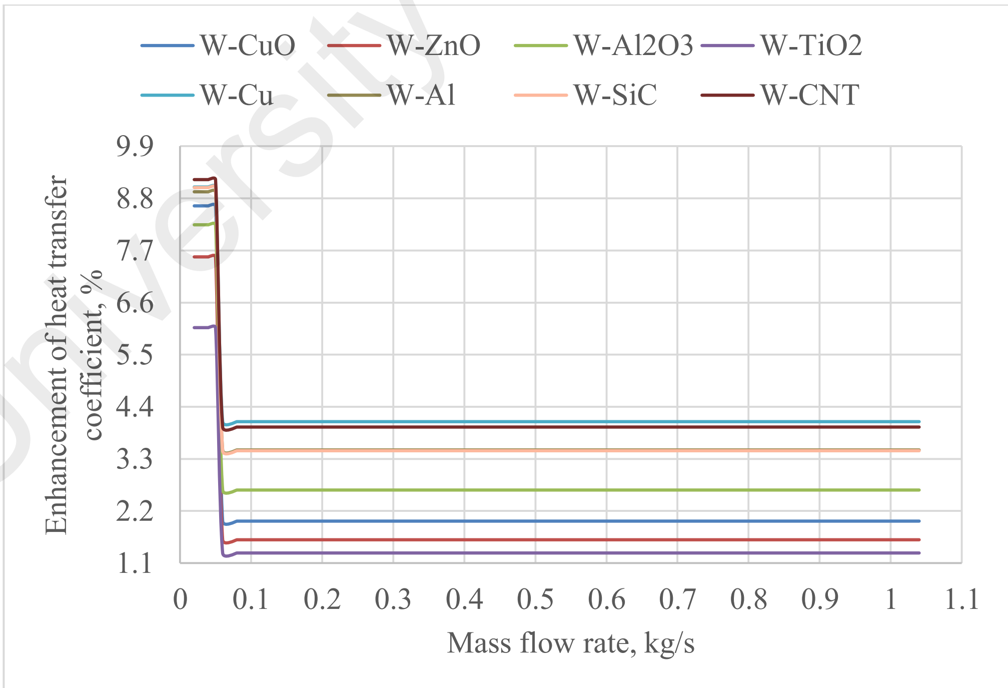

Figure 4.13: Improvement of heat transfer coefficient in water-based nanofluids at various mass-flow rates.

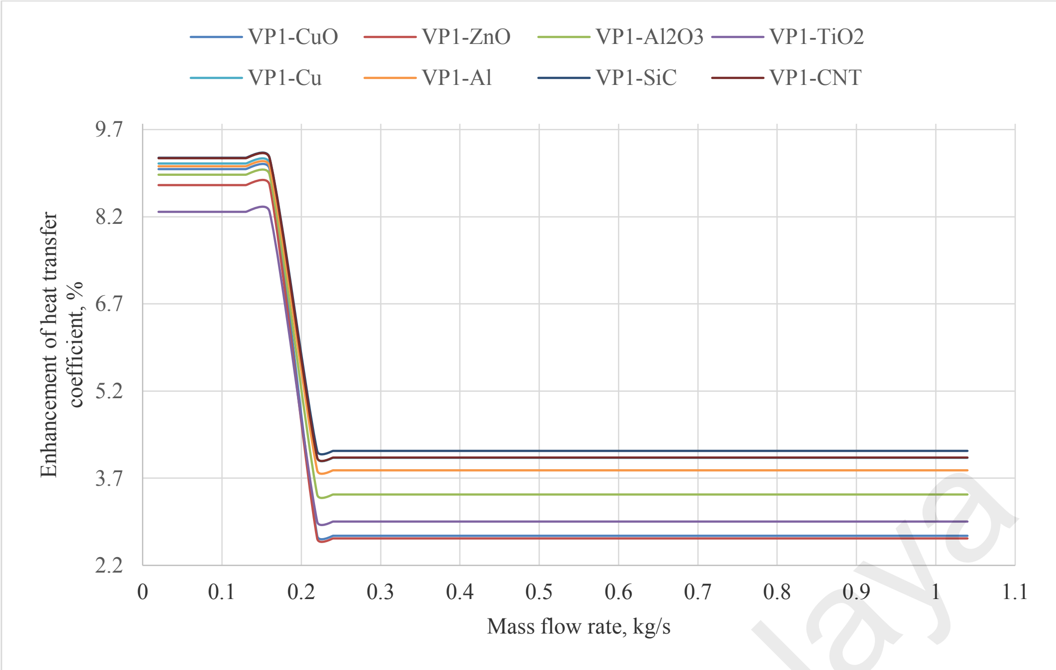

Figure 4.14: Improvement of heat transfer coefficient in therminol-VP1-based nanofluids at various mass-flow rates.

4.3.3 Effect of the volumetric concentrations of the nanoparticles

Figure 4.15 and Figure 4.16 illustrate the influence of the volumetric concentrations of the nanoparticles on coefficient of heat transfer. The figures show that adding low volumetric concentrations (0.025%-3%) of nanoparticles (except below 0.05%) to base fluids significantly enhances the heat transfer coefficient. This indicates that the addition of nanoparticles enhances the heat absorption capacity of the heat-transfer fluid which may be attributed to the high thermal conductivity of nanoparticles. The Brownian motion in nanoparticles with a large surface area for molecular collisions enhances thermal conductivity. High volumetric concentrations of nanoparticles cause high momentum, which carries and transfers heat more effectively and at a longer distance within the base fluid, thus enhancing the rate of heat-transfer of the fluid (Hong, 2005).

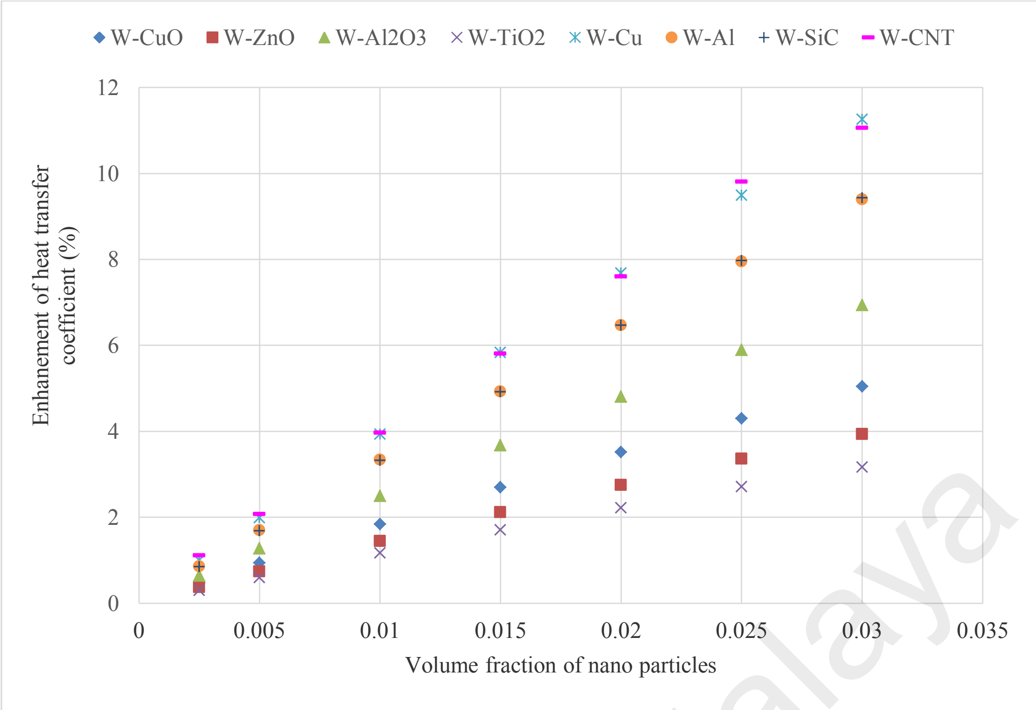

Figure 4.15: Improvement of heat transfer coefficient in water-based nanofluids with various volumetric concentrations of nanoparticles.

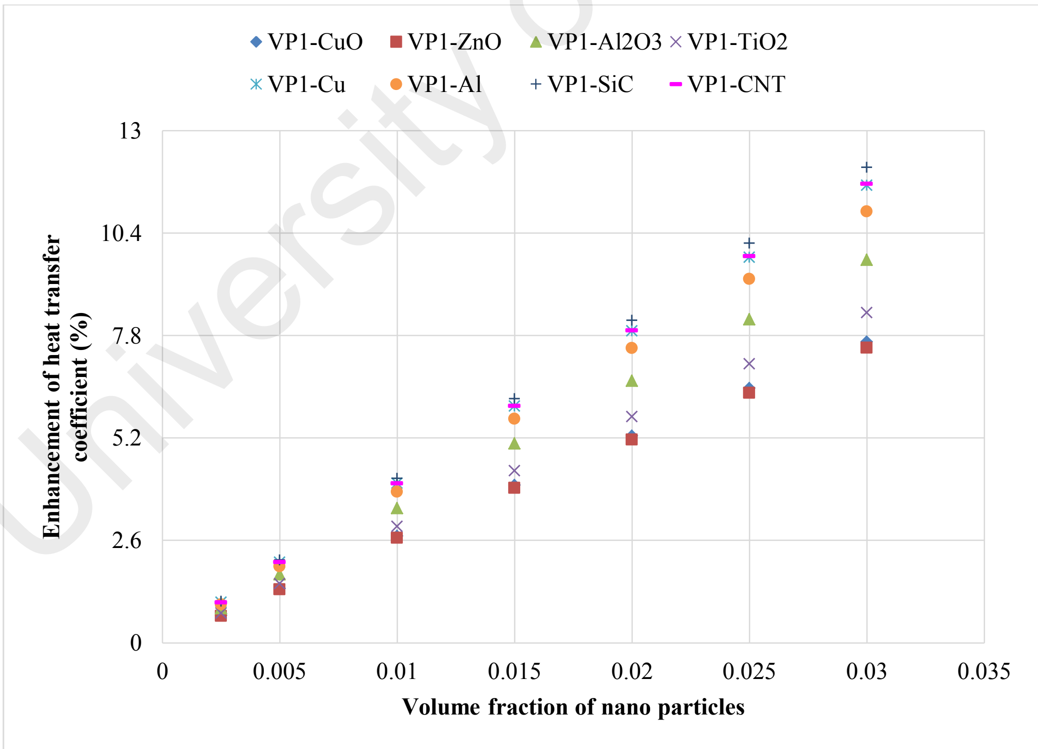

Figure 4.16: Improvement of heat transfer coefficient in therminol-VP1based nanofluids with various volumetric concentrations of nanoparticles.

4.4. Experimental investigation of PTC

A PTC has been investigated experimentally at the condition of constant and variable irradiation using water and water/carbon nanotube (CNT) nanofluid. Investigation in detail has been discussed in this section.

4.4.1 Thermal performance of PTC at constant irradiation

4.4.1.1 Thermal performance of PTC by using water

Irradiation is kept at 640 W/m^2 in investigating thermal performance of the PTC. Water flow rate is varied. Increasing flow rate from 0.80 l/min to 0.90 l/min, 0.90 l/min to 1.10 l/min and 1.10 l/min to 1.22 l/min cause lowering water temperature at outlet by 4.93%, 6.30%, and 4.10% respectively. Figures 4.17 and 4.18 respectively exhibit the effect of flow rate on water temperature at outlet and deviance between outlet and inlet water temperatures.

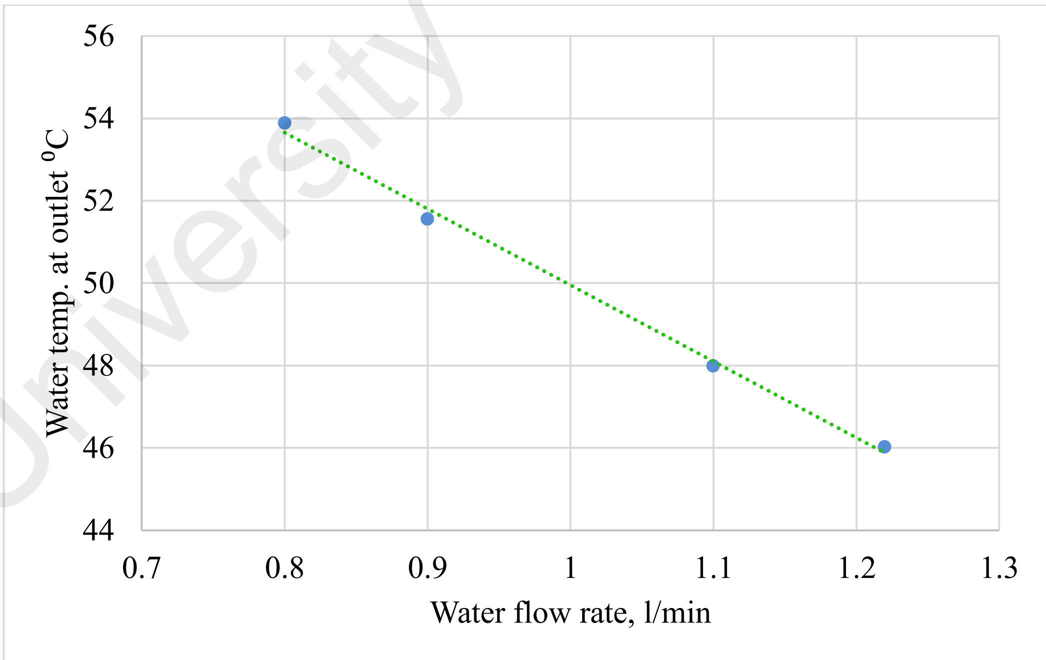

Figure 4.17: Water temperature at outlet in relation to water flow rate.

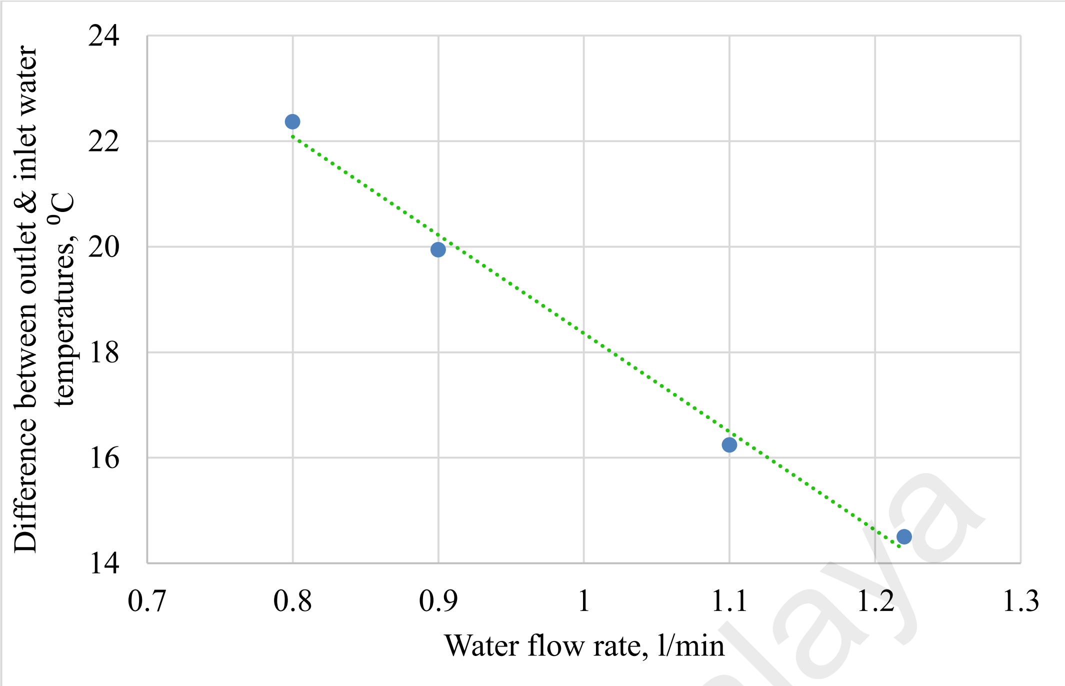

Figure 4.18: Difference of outlet and inlet water temperatures in relation to water flow rate.

Outlet water temperature and the difference of outlet and inlet water temperatures follows linear relation with water flow rate. Because of every 0.10 l/min augment of water flow rate, water temperature at outlet drops by around 2.0^{0}C. Heat gain and thermal efficiency decrease due to the reduction of outlet water temperature. The values for heat gain and thermal efficiency are found to be 1.272 kJ/s, 1.275 kJ/s, 1.269 kJ/s, 1.257 kJ/s and 66.23%, 66.42%, 66.12%, 65.47% respectively at 0.80 l/min, 0.90 l/min, 1.10 l/min and 1.22 l/min which are expressed graphically in Figure. 4.19 and Figure 4.20. Heat gain and thermal efficiency diminish with increasing flow rate. Increment of flow rate decreases contact time of water with receiver and lower heat transfer rate. Heat gain or thermal efficiency decline by 0.46% and 0.97% respectively at 0.90 l/min to 1.10 l/min and 1.10 l/min to 1.22 l/min. At 0.80 l/min, heat gain and thermal efficiency are relatively lower than that of 0.90 l/min. Very low mass flow rate is the reason behind this. Very low mass can carry very low heat. Theoretical analysis shows, heat gain and thermal efficiency have been found 1.297 kJ/s, 1.296 kJ/s, 1.295kJ/s, 1.294kJ/s and 70.82%, 70.77%, 70.69%, 70.62% respectively at 0.80 l/min, 0.90 l/min, 1.10 l/min and 1.22 l/min. From both figures, it is found that heat gain and thermal efficiency in experiment are lower by 6.47%, 6.15%, 6.57% and 7.29% than that of theoretical values.

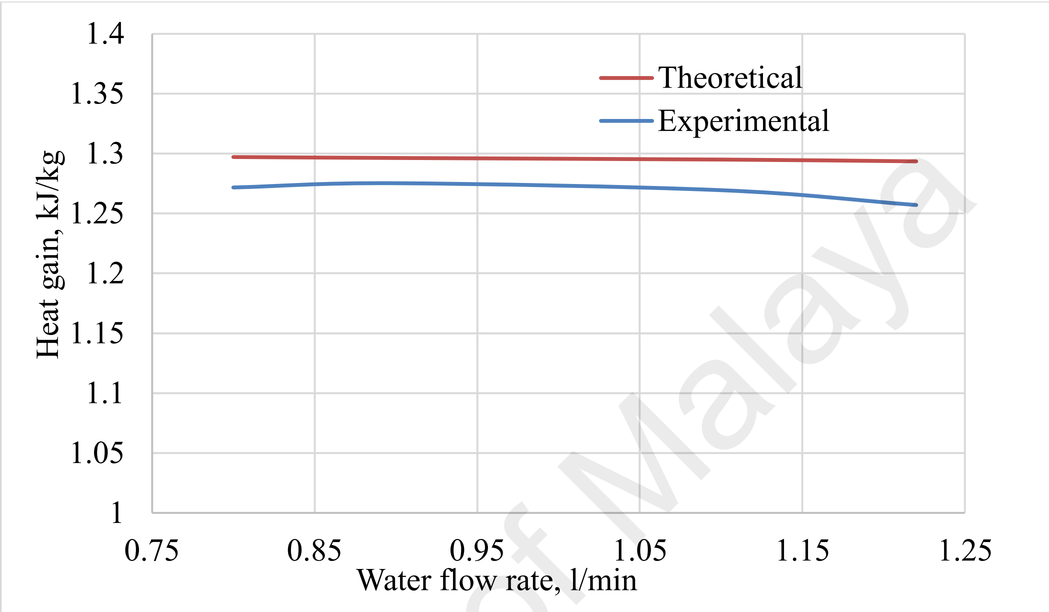

Figure 4.19: Heat gain at different flow rate and 640 W/m^2 irradiation.

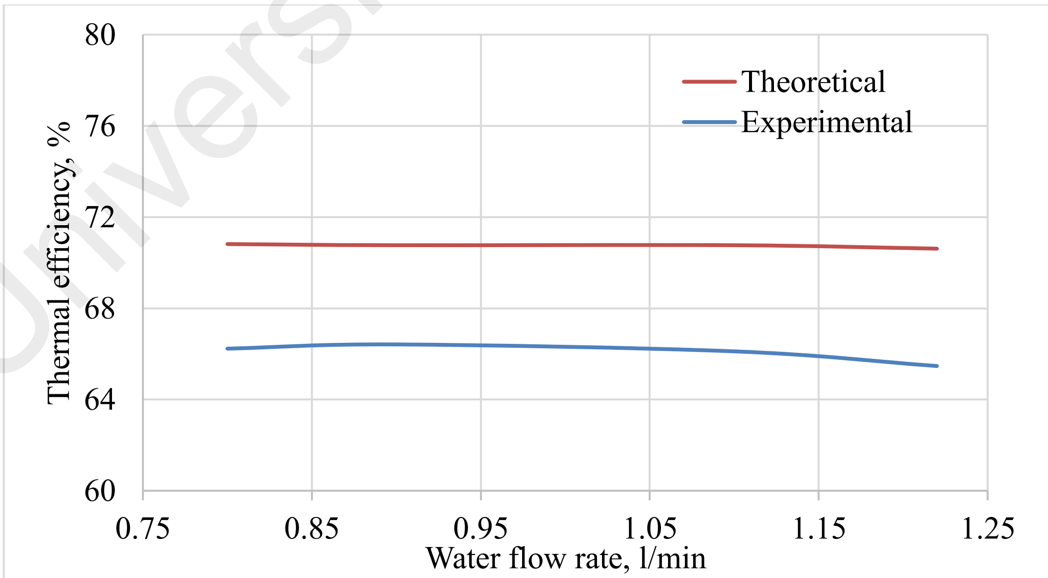

Figure 4.20: Thermal efficiency at different flow rate and 640 W/m^2 irradiation.

4.4.1.2 Thermal performance of PTC by using Water-Carbon nano tube (W-CNT) nanofluid

Figure 4.21 and Figure 4.22 respectively exhibit the effect of flow rate on heat gain and thermal efficiency at 640 W/m^2. Water and Water-Carbon nano tube nanofluid are used in this experimental investigation and experimental results have been compared with theoretical values. At flow rates 1.15 l/min and 1.25 l/min, heat gains and thermal efficiency for W-CNT are found 1.25 kJ/s, 1.24 kJ/s and 68.58%, 67.73% respectively. Compared to water, W-CNT nanofluid augments heat gain by 1.23%, 0.98% at 1.15 l/min and 1.25 l/min; thus improves thermal efficiency. Both figures show, experimental results of heat gains for water and W-CNT nanofluid are lower by 2.60%, 3.49% and 1.85%, 2.99% respectively than theoretical values. Similarly, thermal efficiencies are lower by 4.47%, 5.38% for water and by 3.63%, 4.74% for W-CNT nanofluid than theoretical values. Also it is shown that augmentation in flow rate reduces heat gain and thermal efficiency.

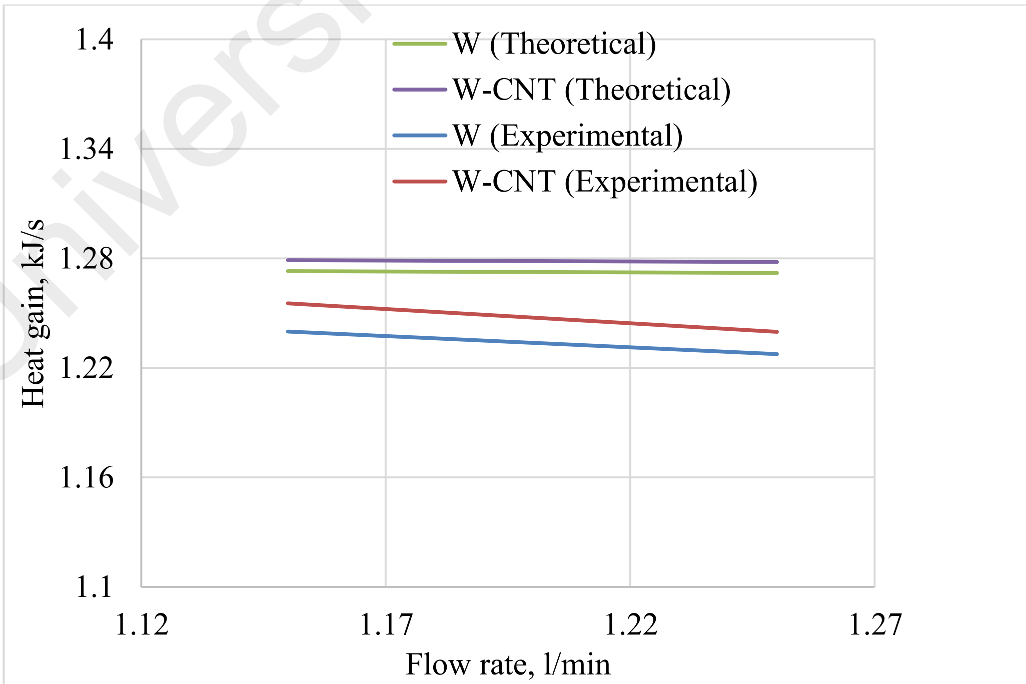

Figure 4.21: Effect of flow rate on heat gain at 640 W/m^2 irradiation.

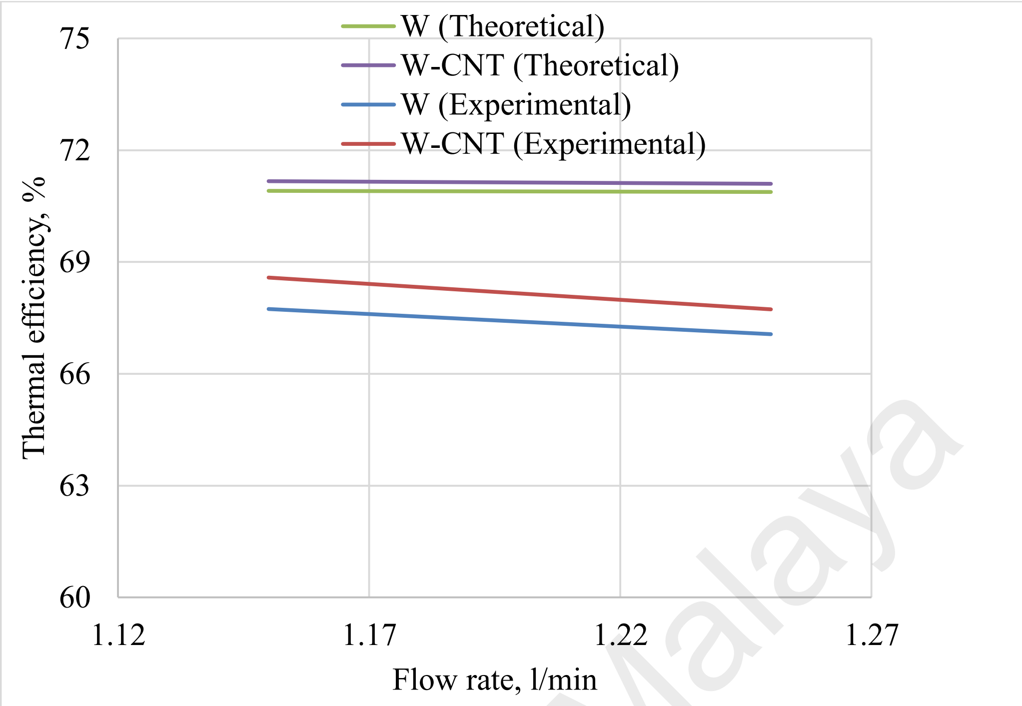

Figure 4.22: Effect of flow rate on thermal efficiency at 640 W/m^2 irradiation.

Figure 4.19 until Figure 4.22 shows some deviation in experimental results in comparison to the theoretical results. Ambient temperature, fluid inlet temperature could not be kept fixed, which affect experimental results and cause deviation.

4.4.2 Thermal performance at variable irradiation

4.4.2.1 Thermal performance of PTC at variable irradiation by using water

Thermal performances are investigated for water at variable solar irradiation while flow rate is kept at 0.90 l/min. Figure 4.23 and Figure 4.24 present the outlet water temperatures and the difference in inlet and outlet water temperature of the receiver, respectively at different irradiation levels. From Figures 4.23 and 4.24, it is shown that outlet water temperature rise by 5.95%, 8.29%, 10.42%, 5.71%, 2.22%, 7.04% and water temperature difference rise by 9.70%, 30.61%, 39.19%, 17.20%, 7.00%, 15.16%

with the augment of radiation (344.00 W/m^2, 405.17 W/m^2, 477.50 W/m^2, 509.47 W/m^2, 555.90 W/m^2, 601.49 W/m^2, and 645.29 W/m^2).

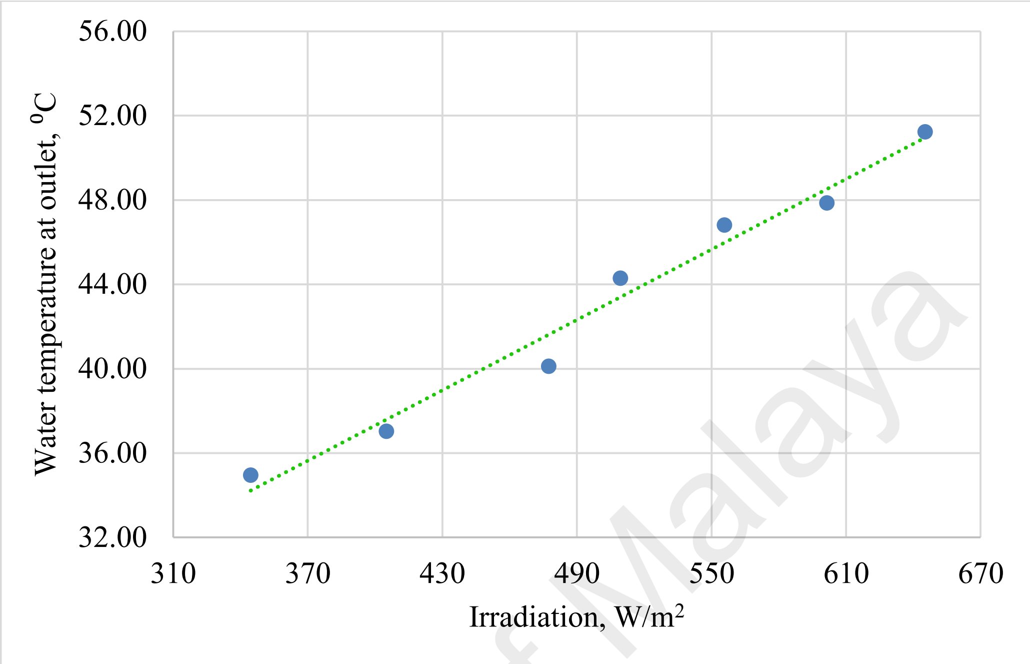

Figure 4.23: Water temperature at outlet for variable solar irradiation.

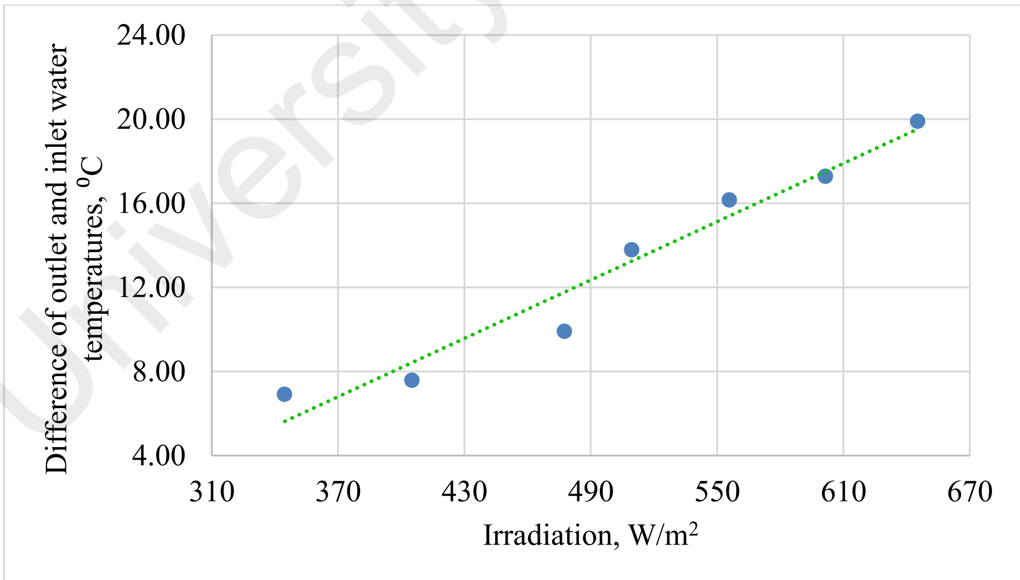

Figure 4.24: Water temperature difference at inlet and outlet for variable irradiation.

Figure. 4.25 exhibits the Influence of outlet water temperatures on heat gain and shows, heat gain follows linear relation to outlet water temperatures. Every 1^{o}C improvement of outlet water temperature causes increasing in heat gain by 0.02 kJ/s. Increase in heat gain causes thermal efficiency improvement. Thermal efficiency also follows almost linear relation to water temperature and that is presented in Figure. 4.26.

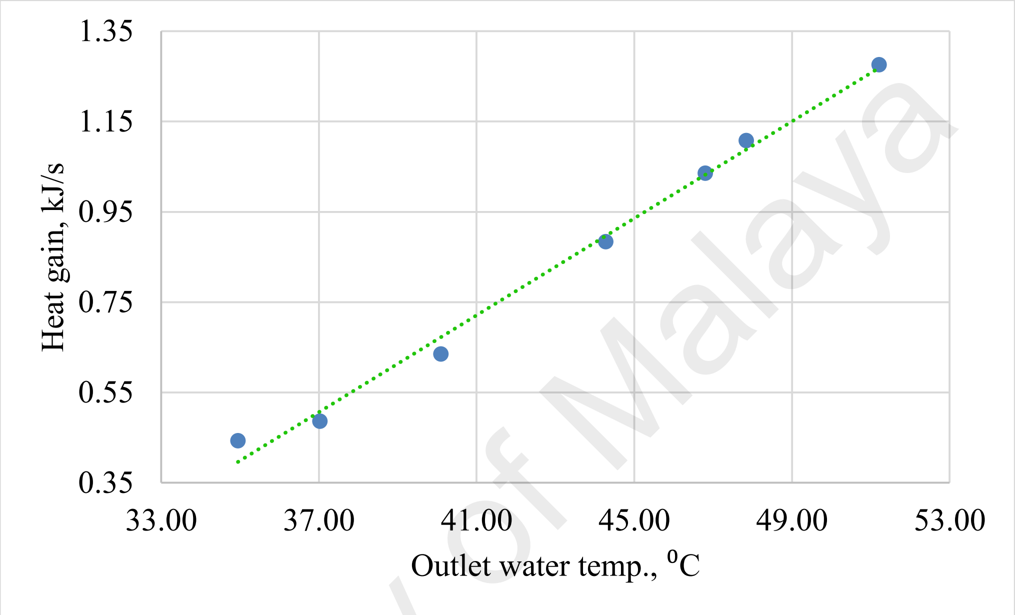

Figure 4.25: Effect of outlet water temperature on heat gain.

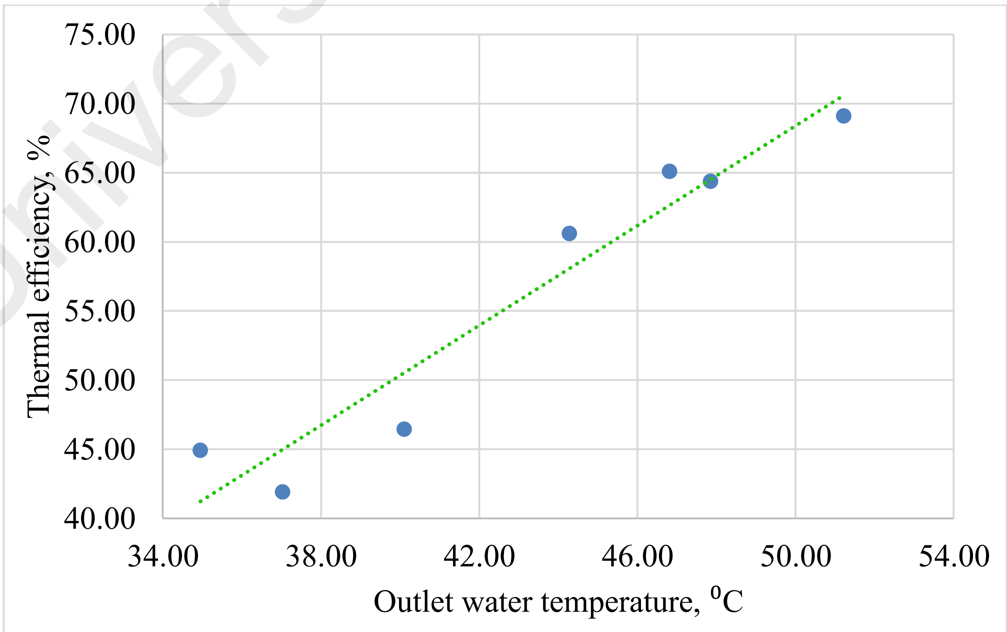

Figure 4.26: Effect of outlet water temperature on thermal efficiency.

Every increment of water temperature by 1°C leads to augmenting thermal efficiency by around 1.6%. Figure 4.27 and Figure 4.28 exhibit the effect of solar irradiation on heat gain and thermal efficiency respectively.

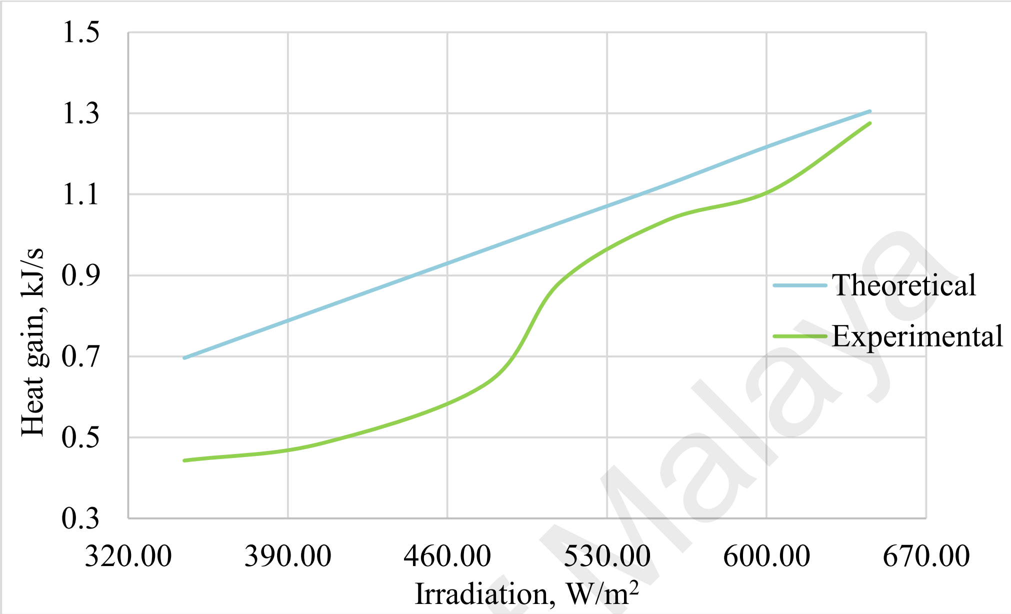

Figure 4.27: Effect of solar irradiation on heat gain.

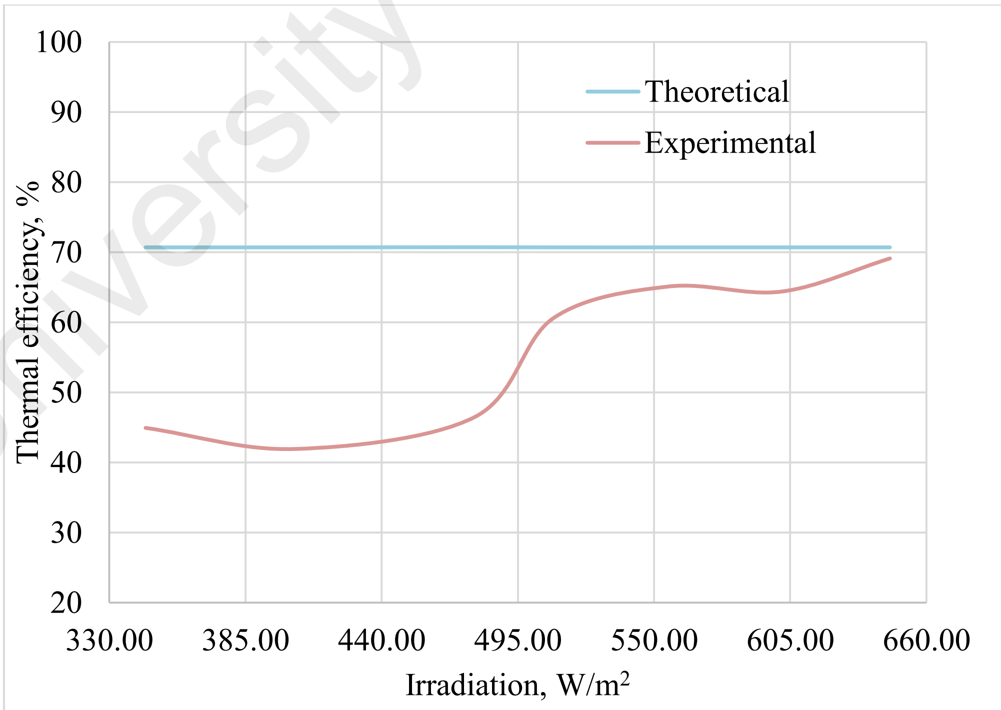

Figure 4.28: Effect of solar irradiation on thermal efficiency.

Solar irradiation acts as the main element for increasing heat gain and hence augmenting thermal efficiency. Increment of solar irradiation basically enhances heat transfer fluid temperature, and hence improves heat gain, and thermal efficiency. Heat gain improves by 9.69%, 30.60%, 39.19%, 17.19%, 19.38%, and 37.18% with augmenting irradiation (344 W/m^2, 405.17 W/m^2, 477.50 W/m^2, 509.47 W/m^2, 555.90 W/m^2, 601.49 W/m^2, and 645.29 W/m^2). But while augmenting irradiation from 344 W/m^2 to 405.17 W/m^2, thermal efficiency diminishes by 6.69%, because the increment of heat gain (0.44 kJ/s to 0.49 kJ/s) is very low and 405.17 W/m^2 is relatively higher. Thermal efficiency rises by 10.82%, 30.46%, 7.41%, 10.33% and 27.87% with increasing irradiation of 405.17 W/m^2, 477.50 W/m^2, 509.47 W/m^2, 555.90 W/m^2, 601.49 W/m^2, and 645.29 W/m^2.

4.4.2.2 Thermal performance of PTC at variable irradiation by using W-CNT nanofluid

Thermal performance of the PTC has been investigated for variable irradiation using W-CNT nanofluid. Investigation is done at 1.15 l/min and compared with theoretical values and also compared with performance done by water.

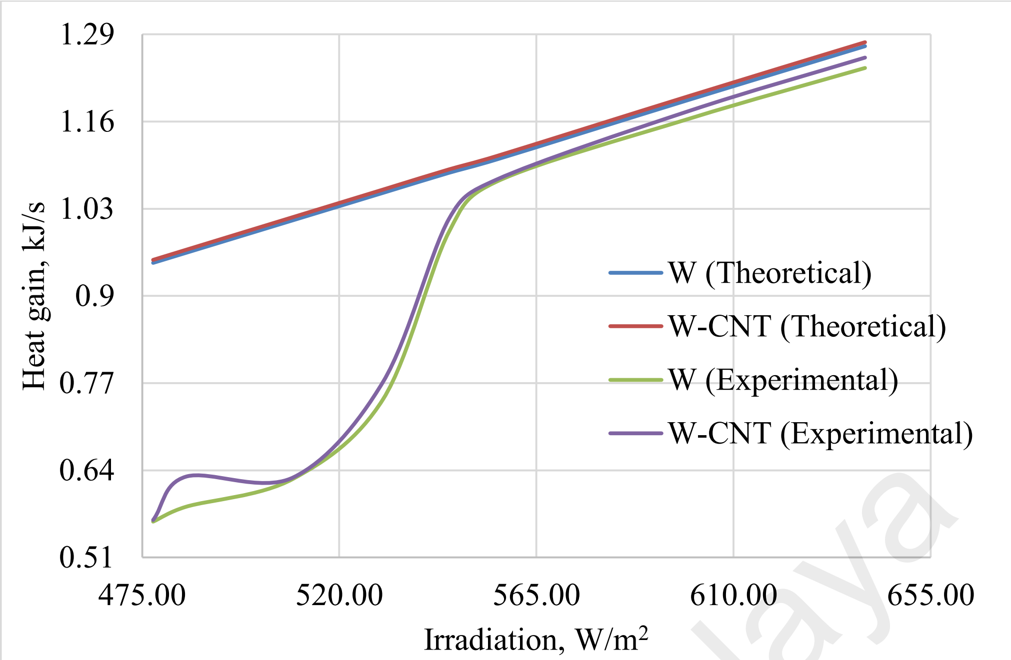

Figure 4.29: Effect of irradiation on heat gain at 1.15 l/min.

Figure 4.29 and Figure 4.30 exhibit the effect of irradiation on heat gain and thermal efficiency at 1.15 l/min. W-CNT nanofluid augments heat gain and ultimately thermal efficiency by 0.42%, 7.13%, 0.31%, 3.35%, 1.92%, 0.30%, 0.98%, 1.23% for the respective irradiation 477.50 W/m^2, 485.00 W/m^2, 509.47 W/m^2, 530.00 W/m^2, 545.00 W/m^2, 555.90 W/m^2, 600.00 W/m^2, 640.00 W/m^2. Every 1 W/m^2 increment of irradiation augments heat gain by around 2 J/s to 5 J/s which leads to increasing thermal efficiency by 9.70%, 4.98%, 17.92%, 27.79%, 3.74%, 1.50%, 0.06% for 477.50 W/m^2, 485.00 W/m^2, 509.47 W/m^2, 530.00 W/m^2, 545.00 W/m^2, 555.90 W/m^2, 600.00 W/m^2, 640.00 W/m^2 respectively. It is also shown that experimental investigation for water and W-CNT gives lower results than theoretical values by respectively 41.87%, 40.51%, 39.34%, 30.62%, 10.02%, 5.13%, 4.38%, 4.47% and 41.76%, 36.09%, 39.28%, 28.41%, 8.50%, 5.07%, 3.64%, 3.58% at 477.50 W/m^2, 485.00 W/m^2, 509.47 W/m^2, 530.00 W/m^2, 545.00 W/m^2, 555.90 W/m^2, 600.00 W/m^2, 640.00 W/m^2.

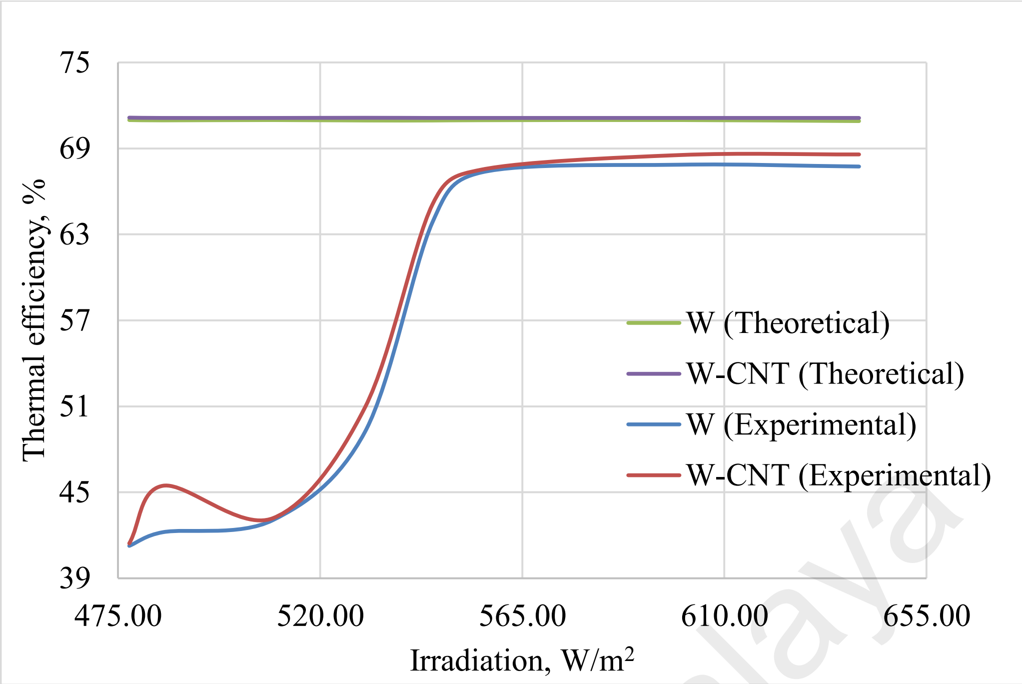

Figure 4.30: Effect of irradiation on thermal efficiency at 1.15 l/min.

Till 530 W/m^2 irradiation, experimental results of heat gain or thermal efficiency are very much lower compared to theoretical results. Above 530 W/m^2 irradiation experimental results are found nearer to theoretical results. So irradiation more than 530 W/m^2 is beneficial to heat fluid at 1.15 l/min flow rate. Experimental results show that maximum thermal efficiencies are 67% and 68% for water and W-CNT nanofluid respectively. Figure 4.31 and Figure 4.32 exhibit the effect of variable irradiation on heat gain and thermal efficiency at 1.25 l/min flow rate.

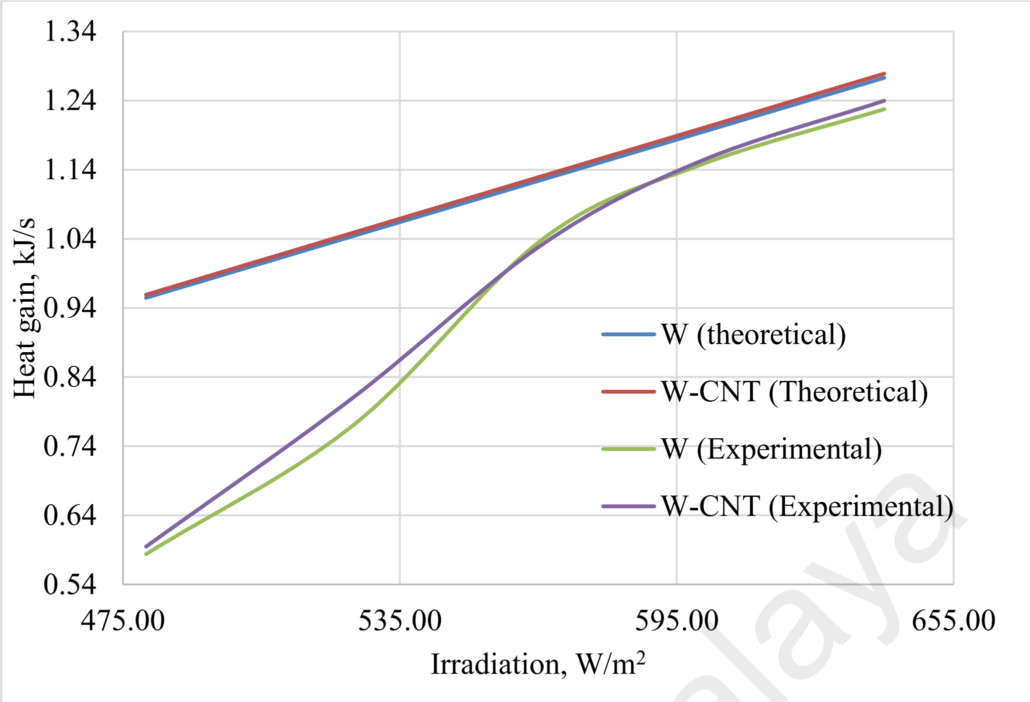

Figure 4.31: Effect of irradiation on heat gain at 1.25 l/min.

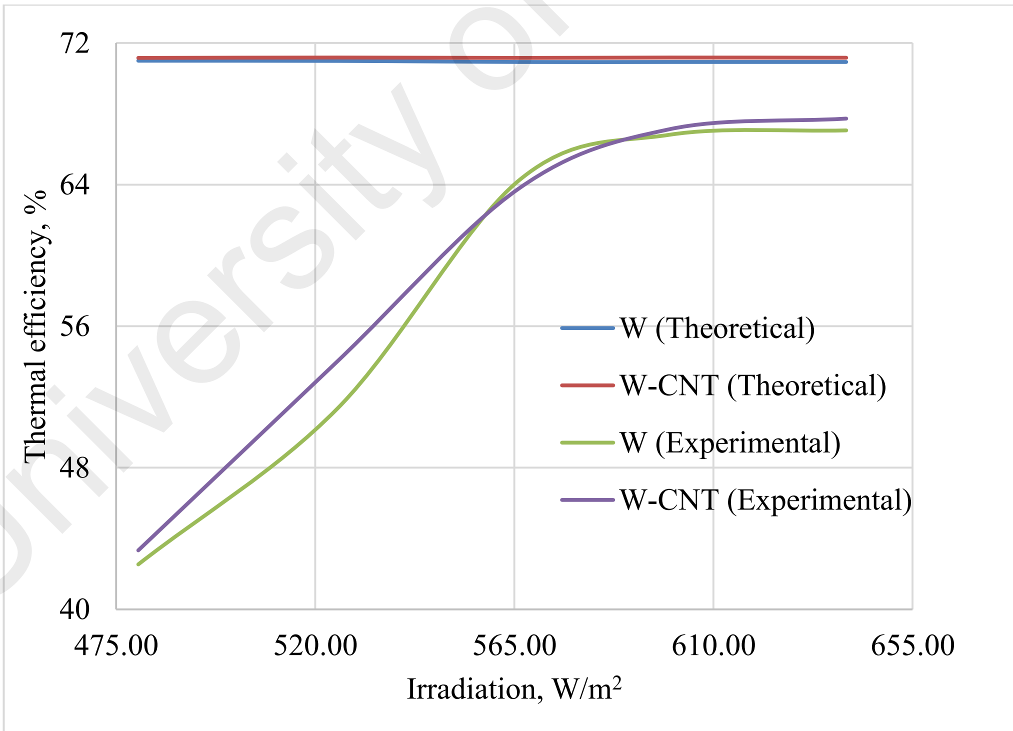

Figure 4.32: Effect of irradiation on thermal efficiency at 1.25 l/min.

According to Figure 4.31 and Figure 4.32, at 1.25 l/min W-CNT nanofluid augments heat gain or thermal efficiency by 1.86%, 5.20%, 0.70%, 0.46%, 0.99% at respective irradiation of 480 W/m^2, 525 W/m^2, 566 W/m^2, 600 W/m^2, 640 W/m^2. Every 1 W/m^2 increase in irradiation augments heat gain from around 2 J/sec to 5 J/sec which results 24.65%, 18.08%, 5.25%, 0.90% improvement in thermal efficiency for respective irradiation of 480 W/m^2, 525 W/m^2, 566 W/m^2, 600 W/m^2, 640 W/m^2. It is revealed that experimental results for water and W-CNT nanofluid are inferior by respectively 40.08%, 27.67%, 9.44%, 5.80%, 5.45% and 39.11%, 24.12%, 10.37%, 5.69%, 4.83% than theoretical values for 480 W/m^2, 525 W/m^2, 566 W/m^2, 600 W/m^2, 640 W/m^2 irradiation. Above 560 W/m^2 irradiation, thermal efficiency is closer to theoretical value. Maximum thermal efficiency is approximately 67% for W-CNT nanofluid. Figure 4.27 until Figure 4.32 shows deviation in experimental results in comparison to theoretical results. In this case, also the same factors ambient temperature and fluid inlet temperature affect the experimental results, because these factors could not be kept constant.

CHAPTER 5 : CONCLUSIONS AND FURTHER WORKS

5.1 Conclusions

A parabolic trough collector (PTC) has been modeled numerically and evaluated experimentally using various fluids and nanofluids. Influence of parameters like heat removal factor, collector efficiency factor, mass flow rate and collector aperture area on collector thermal efficiency are being observed. Three fluids such as CO_2, NH_2 and N_2 are used for the analysis. The optimum receiver size (diameter) which produces the maximum efficiency is detected to be 51.80 mm for the concentrator with an aperture of 1.50 m and a length of 2.0 m. The highest collector efficiencies at the same aperture area of 2.836 m^2 but at diverse flow rates of 0.049 kg/s, 0.019 kg/s and 0.036 kg/s, respectively for CO_2, NH_3 and N_2 are 67.22%, 67.05% and 66.81%. Water, Therminol VP1 and water/therminol VP1 based nanofluids are also used for investigating thermal performance of parabolic trough system. The influence of mass flow rate and solid volume fractions are counted for analyzing. Nanoparticles addition to water and therminol VP1 enhances heat transfer. At constant mass flow rate (0.8 kg/s), maximum heat transfer coefficient enhancements belong to W-Cu (4.08%) and VP1-SiC (4.17%) nanofluids and the lowest to W-TiO2 (1.31%) and VP1-ZnO (2.66%). With the exception of W-Cu and W-SiC, in other water based nanofluids, thermal conductivity of nanofluids is responsible for enhancing heat transfer coefficient. For the case of W-Cu, W-SiC, W-CNT and all Therminol VP1 based nanofluids, specific heat is responsible. While mass flow rates have been changed, maximum enhancement of heat transfer coefficients are found with W-CNT (9.19%) and VP1-SiC (9.21%) in laminar flow. In laminar flow thermal conductivity of nanofluids is the key for improvement in heat transfer. It is interesting that, during laminar flow or fully developed turbulent flow, heat transfer enhancement remains unchanged. The enhancement drops only during transition period: laminar to turbulent. During turbulent flow, the result is same as that of constant mass flow rate (0.8 kg/s). Addition of solid volume concentrations to base fluid below 0.05% has no noticeable effect on heat transfer coefficient. After that with increasing solid volume concentrations heat transfer coefficient has been enhanced. After theoretical analysis, experimental investigation has been done. Water and W-CNT are used depending on availability. Experimental investigation shows good results. The effect of flow rate and irradiation have been investigated. Investigation regarding the effect of flow rate is done at 640 W/m^2 irradiation. The augmentation of flow rate declines the outlet fluid temperature. In case of water, every 0.10 l/min increase of water flow rate, diminishes outlet water temperature by around 2.0^0C. Diminish in outlet water temperature causes dropping in heat gain or thermal efficiency by 0.46% and 0.97% respectively at 0.90 l/min to 1.10 l/min and 1.10 l/min to 1.22 l/min. Experimental results for heat gain and thermal efficiency are lower by 6.47%, 6.15%, 6.57% and 7.29% than that of theoretical values. On the other hand, W-CNT nanofluid augments heat gain or thermal efficiency by 1.23%, 0.98% at 1.15 l/min and 1.25 l/min compared to water. Heat gains are lower by 1.85%, 2.99% and thermal efficiency is lower by 3.63%, 4.74% for W-CNT nanofluid than theoretical values. Flow rate is kept fixed while variation is made in irradiation within the range of 470 W/m^2 to 640 W/m^2. Augmentation of irradiation rises fluid temperature which leads to improve heat gain or thermal efficiency. At 1.15 l/min, every 1^0C enhancement of outlet water temperature causes increasing in heat gain and thermal efficiency by around 0.02kJ/s and 1.6% respectively. In case of W-CNT nanofluid, at 1.15 l/min every 1 W/m^2 increase in irradiation improves heat gain by around 2 J/s to 5 J/s which leads to augmenting thermal efficiency by 9.70%, 4.98%, 17.92%, 27.79%, 3.74%, 1.50%, 0.06% for 477.50 W/m^2, 485.00 W/m^2, 509.47 W/m^2, 530.00 W/m^2, 545.00 W/m^2, 555.90 W/m^2, 600.00 W/m^2, 640.00 W/m^2 respectively. At 1.25 l/min, every 1 W/m^2 increase in irradiation augments heat gain by around 2 J/s to 5 J/s which consequences 24.65%, 18.08%, 5.25%, 0.90% improvement in thermal efficiency for respective irradiation of 480 W/m^2, 525 W/m^2, 566 W/m^2, 600 W/m^2, 640 W/m^2. Maximum thermal efficiency is approximately 67% and 68% for water and W-CNT nanofluid, respectively.

5.2 Further works

Future work should involve outdoor investigation using efficient and accurate tracking system. Followings could be recommended:

- Molten salt may be used as heat transfer fluid. Because molten salt can store thermal energy and at night or cloudy weather this stored enthalpy can be utilized in various applications.
- For better solar concentration, mirror should be banded at 90^o rim angle.
- Present analytical work using gas should be checked practically.

Also for a further work, exergy and exergoeconomic (which is a combination of exergy and economics) analysis have been recommended. In addition, the effect of varying dead state temperatures on the exergy efficiency of the system considered may be investigated.

REFERENCES

Ahmad, S., Kadir, M.Z.A.A., & Shafie, S. (2011). Current perspective of the renewable energy development in Malaysia. *Renewable and Sustainable Energy Reviews, 15*(2), 897–904.

Abdelrahman, M., Fumeaux, P., & Suter, P. (1979b). Study of solid–gas-suspensions used for direct absorption of concentrated solar-radiation. *Solar Energy, 22*(1), 45-48.

Abdin, Z., Alim, M.A., Saidur, R., Islam, M.R., Rashmi, W., Mekhiler, S., & Wadi, A. (2013). Solar energy harvesting with the application of nanotechnology. *Renewable and Sustainable Energy Reviews 26*, 837-852.

Abdullah, M.A., Agalgaonkar, A.P., & Muttaqi, K.M. (2014). Climate change mitigation with integration of renewable energy resources in the electricity grid of New South Wales, Australia. *Renewable Energy, 66*(0), 305-313.

Abu-Hamdeh, N.H., Alnefaie, K.A., & Almitani, K.H. (2013). Design and performance characteristics of solar adsorption refrigeration system using parabolic trough collector: Experimental and statistical optimization technique. *Energy conversion and management 74*, 162-170.

Arani, A.A.A., & Amani, J. (2012).Experimental study on the effect of TiO_2/water nanofluid on heat transfer and pressure drop, *Experimental Thermal and Fluid Science 42*, 107–115.

Ahmed, F., Al Amin, A. Q., Hasanuzzaman, M., & Saidur, R. (2013). Alternative energy resources in Bangladesh and future prospect. *Renewable and Sustainable Energy Reviews, 25*, 698-707.

Akbari, M. & Behzadmehr, A. (2006). Developing mixed convectionof a nanofluid in a horizontal tube with uniform heat flux. *Numer Methods Heat Fluid Flow, 17*(6), 566–586.

Akbarjadeh, A., & Wadowski, T. (1996). Heat pipe based cooling system for photovoltaic cells under concentrated solar radiation. *Applied Thermal Engineering, 16*(1), 81-87.

Amin, N., Lung, C.W., & Sopian, K. (2009). A practical field study of various solar cells on their performance in Malaysia. *Renewable Energy, 34*(8), 1939-1946.

Ambrosini, A, Lambert, TN., Bencomo, M, Hall, A, Every, K., & Siegel NP. (2011). Improved high temperature solar absorbers for use in concentrating solar power central receiver applications. *In: Proceedings of the ASME 2011energy sustainability and fuel cell conference, ESFuelCell2011-54241, Washington DC*.

Amsbeck L, Denk T., Ebert M, Gertig C, Heller P, & Herrmann P. (2010). Test of a solar-hybrid micro turbine system and evaluation of storage deployment *In: Proceedings of solar PACES 2010, Perpignan, France*.

Amsbeck, L, Buck, R., Heller, P, Jedamski, J, & Uhlig, R. (2008). Development of a tube receiver for a solar-hybrid microturbine system. *In: Proceedings of the 2008 Solar PACES Conference, Las Vegas, NV*.

Amrollahi, A, Rashidi, AM, Lotfi, R, Emami, MM, & Kashefi, K. (2010). Convection heattransfer of functionalized MWNT in aqueous fluids in laminar and turbulent flowat the entrance region, International Communication in Heat and Mass Transfer, 37 (6), 717–723.

Angellino, G. (1968). Carbondioxide condensation cycles for power production. *Journal of Engineering for Power, 90*(3), 287-296.

Angellino, G. (1969). Real gas effects in carbondioxide cycles. *In: ASME international gas turbine conference and products show GT-102, Cleveland, OH*.

Arasu, A. V., & Sornakumar, T. (2007). Design, manufacture and testing of fiberglass reinforced parabola trough for parabolic trough solar collectors. *Solar Energy, 81*(10), 1273-1279.

Argatov, I., Rautakorpi, P., & Silvennoinen, R. (2009). Estimation of the mechanical energy output of the kite wind generator *Renewable Energy, 34*(6), 1525-1532.

Arora, V., & Sheorey, T. (2012). Development and Performance Characteristics of a Low-Cost Parabolic Solar Collector. *International Conference on Power and Energy Systems (ICPES 2012), 56*.

Avila-Marin, AL (2011). Volumetric receivers in solar thermal power plants with central receiver system technology: a review. *Solar Energy, 85*(5), 891–910.

Azmi, W.H., Sharma, K.V., Sarma, P.K., Mamat, R., Anuar, S., & Rao, V.D. (2013). Experimental determination of turbulent forced convection heat transfer and friction factor with SiO_2 nanofluid, *Experimental Thermal and Fluid Science, 51*, 103–111.

Bergles, A. E. (1973). Recent development in convective heat transfer augmentation. *Applied Mechanics Reviews, 26*, 675–682.

Bertani, R. (2009). Geothermal energy: An overview on resources and potential.

Bienert, WB, Rind, H., & Wolf, AA. (1979). Conceptual design of an open cycle air Brayton Solar Receiver: Phase1 final report, DTM-79-1 prepared under contract no. 955135 for California Institute of Technology Jet Propulsion Laboratory. *Dynatherm Corporation,Cockeysville,*MD.

Billah, M. M., Rahman, M. M., Sharif, U. M., Rahim, N. A., Saidur, R., & Hasanuzzaman, M. (2011). Numerical analysis of fluid flow due to mixed convection in a lid-driven cavity having a heated circular hollow cylinder. *International Communications in Heat and Mass Transfer, 38*(8), 1093-1103.

Bohn MS, & Davis, SH. (1993). Thermocapillary breakdown of falling liquid films at high Reynolds numbers. *International Journal of Heat and Mass Transfer, 36*(7), 1875-1881.

Bohn, MS, & Green, HJ. (1989). Heat transfer in molten salt direct absorption receivers. *Solar Energy, 42*(1), 57-66.

Borhanazad, H, Mekhilef, S, Saidur, R, & Boroumandjazi, G. (2013). Potential application of renewable energy for rural electrification in Malaysia. *Renewable Energy 59*, 210-219.

Bradshaw, RW, & Meeker, DE. (1990). High-temperature stability of ternary nitrate molten salts for solar thermal energy systems. *Solar Energy Materials, 21*(1), 51-60.

Bridgwater, A.V. (2012). Review of fast pyrolysis of biomass and product upgrading *Biomass and Bioenergy, 38*, 68-94.

Brinkman, H.C. (1952). The Viscosity of Concentrated Suspensions and Solutions. *The J. of Chemical Physics, 20*, 571.

Cengel, Y. (2007). Heat and mass transfer-a practical approach.3rd ed. *Tata Mcgraw-Hill*.

Chen, W.N. (2012). Renewable Energy Status in Malaysia. *Sustainable Energy Development Authority Malaysia.*

Chavez, J.M., & Chaza, C. (1991). Testing of a porous ceramic absorber for a volumetric air receiver. *Solar Energy Materials, 24*(1-4), 172-181.

Chavez, J.M., Tyner, C.E., & Couch, WA. (1987). Direct absorption receiver flow testing and evaluation. *Albuquerque, NM: Sandia National Laboratories*.

Chen, H.J., Chen, Y.T., Hsieh, H.T., & Siegel N. (2007). Computational fluid dynamics modeling of gas-particle flow within a solid-particle solar receiver. *Journal of Solar Energy Engineering-Transactions of the ASME, 129*(2), 160-170.

Chen, H.J., Chen, Y.T., Hsieh, H.T., Kolb, G., & Siegel, N. (2007). Numerical investigation on optimal design of solid particle solar receiver. *In: Proceedings of the energy sustainability conference*, 971-979.

Cheng, Z.D., He, Y.L., Cui, F.Q., Xu, R.J., & Tao, Y.B. (2012). Numerical simulation of a parabolic trough solar collector with nonuniform solar flux conditions by coupling FVM and MCRT method. *Solar Energy, 86*(6), 1770-1784.

Churchill, S.W., & Chu, H.H.S. (1975). Correlating equations for laminar and turbulent free convection from a horizontal cylinder *Int J. Heat Mass Transfer 18*, 1049-1053.

Coyle, R.T., Thomas, T.M., & Schisse, I.P. (1986). The corrosion of selected alloys ineutectic lithium–sodium–potassium carbonate at 900 °C, SERI/PR-255-2561. *Solar Energy Research Institute, Golden, CO*.

CS, T. (2009). Supercritical CO2 for application in concentrating solar power systems. *In: SCCO2 power cycle symposium,Troy, NY*.

Das, S.K., Putra, N.P., & Roetzel, T.R. (2003). Temperature dependence of thermal conductivity enhancement for nanofluid. *Journal of Heat Transfer-Trans ASME, 125*, 567–574.

Barlev, D., Vidu, R., & Stroeve P. (2011). Innovation in concentrated solar power *Solar Energy Materials and Solar Cells, 95*(10), 2703–2725.

Delussu, G. (2012). A qualitative thermo-fluid-dynamic analysis of a CO_2 solar pipe receiver. *Solar Energy, 86*(3), 926-934.

Devabhaktuni, V.A., Depuru, M.S.S.R., Ii, S.G., Nims, R.C., & Craig, D.N. (2013). Solar energy: Trends and enabling technologies. *Renewable and Sustainable Energy Reviews, 19*, 555-564.

Dittus, F.W., & Boelter, L.M.K. (1930). *Univ. Calif (Berkeley) Pub. Eng., 2*, 443.

Dombi, M., Kuti, I., and Balogh, P. (2014). Sustainability assessment of renewable power and heat generation technologies. *Energy Policy*.

Dostal, V., Hejzlar, P., & Driscoll M.J. (2006). High-performance supercritical carbon dioxide cycle for next-generation nuclear reactors. *Nuclear Technology, 154*, 265-282.

Drotning, W.D. (1977a). Optical properties of a solar-absorbing molten salt heat transfer fluid. *Livermore, CA: Sandia National Laboratories*.

Drotning, W.D. (1977b). Solar absorption properties of a high temperature direct-absorbing heat transfer fluid. *In: Symposiumon thermophysical properties, Gaithersburg, MD*.

Drotning, W.D. (1978). Optical properties of solar-absorbing oxide particles suspended in a molten salt heat transfer fluid. *Solar Energy, 20*(4), 313-319.

Duangthongsuk, W., & Wongwises, S. (2009). Heat transfer enhancement and pressure drop characteristics of TiO_2–water nanofluid in a double-tube counter flow heat exchanger. *International Journal of Heat and Mass Transfer, 52*(7-8), 2059–2067.

Duangthongsuk, W., & Wongwises, S. (2008). Effect of thermophysical properties models onthe prediction of the convective heat transfer coefficient for low concentrationnanofluid, *Intenational Communication of Heat and Mass Transfer,35*, 1320–1326.

Duangthongsuk, W., & Wongwises, S. (2010). An experimental study on the heat transferperformanceand pressure drop of TiO_2–water nanofluids flowing under a turbulentflow regime, *InternationalJournal of Heat and Mass Transfer, 53* (15) 334–344.

Duffie J.A., & Beckman, W.A. (1991). Solar engineering of thermal processes.2nd edition. *New york: John Wiley & Sons, Inc.*

EC. (2012). National energy balance, Malaysia. *Energy commision, Malaysia*.

Eastman, J. A., Choi, S.U.S., Li, S., & Thompson, L.J. (1997). Enhanced thermal conductivity through the development of nanofluids. *Proc. Symp. on Nanophase Nanocomposite Materials II, 457*, 3–11.

EC. (2014). BP Statistical Review of World Energy 2014. *www.bp.com/.../bp/.../Energy.../statistical-review-2014/BP-statistical-review..., 01/08/2014*.

Epstein, M., Liebermann, D., Rosh, M., & Shor, A.J. (1991). Solar testing of 2MWth water/ steam receiver at the Weizmann Institute solartower. *Solar Energy Materials, 24*(1-4), 265-278.

ES, F. (1956). The kinetics of the thermal decomposition of sodium nitrate and of the reaction between sodium nitrite and oxygen. *Journal of Physical Chemistry, 60*(11), 1487-1493.

Esfe, M.H., Saedodin, S., & Mahmoodi, M. (2014). Experimental studies on the convectiveheat transfer performance and thermophysical properties of MgO–waternanofluid under turbulent flow, *Experimental Thermal and Fluid Science, 52*, 68–78.

Esfe, M.H., Saedodin, S., Mahian, O., & Wongwises, S. (2014). Thermophysical properties, heat transfer and pressure drop of COOH-functionalized multi walled carbon nanotubes/water nanofluids. *International communications in Heat and Mass Transfer, 58*, 176-183.

Etemoglu, A.B., & Can, M. (2007). Classification of geothermal resources in Turkey by exergy analysis. *Renewable and Sustainable Energy Reviews, 11*(7), 1596-1606.

Faghri, A, & Seban, R. (1985). Heat transfer in wavy liquid films. *International Journal of Heat and Mass Transfer, 28*(2), 506-508.

Faghri, A, & Seban, R. (1988). Heat and mass transfer to a turbulent liquid film. *International Journal of Heat and MassTransfer, 31*(4), 891-894.

Faghri, A., & Seban, R. (1989). Heatandmasstransfertoaturbulentfalling film—II. *International Journal of Heat and Mass Transfer, 32*(9), 1796-1798.

Falcone, P.K., Noring, J.E., & Hruby, J.M. (1985). Assessment of a solid particle receiver for a high temperature solar central receiver system. *Livermore, CA: Sandia National Laboratories*.

Fan, Z.L., Zhang, Y., Liu, D.Y., Wang, J., & Liu, W. (2007). Discussion of mechanical design for pressured cavity-air-receiver in solar power tower system. *In: Proceedings of Ises Solar World Congress 2007: Solar Energyand Human Settlement, I-V*, 1868–1872.

Farajollahi, B., Etemad, S.G., & Hojjat, M. (2010).Heat transfer of nanofluids in a shell and tubeheat exchanger, *International Journal Heat and Mass Transfer, 53* (1–3), 12–17.

Feldhoff, J.F., Benitez, D., Eck, M., & Riffelmann K.J. (2010). Economic potential of solar thermal power plants with direct steam generation compared with HTF plants. *Journal of Solar Energy Engineering, 132*, 041001–041009.

Feldhoff, J.F., Schmitzb, K., Eck, M., Schnatbaum-Laumann, L., Laing, D., Ortiz-Vives, F., & Schulte-Fischedick, J. (2012). Comparative system analysis of direct steam generation and synthetic oil parabolic trough power plants with integrated thermal storage. *Solar Energy, 86*(1), 520-530.

Fernández-García, A., Zarz, E., Valenzuel, L., & Pérez, M. (2010). Parabolic-trough solar collectors and their applications. *Renewable and Sustainable Energy Reviews, 14*(7), 1695–1721.

Forsberg, C.W., Peterson, P., & Zhao, H. (2007). High-temperature liquid-fluoride-salt closed-Brayton-cycle solar power towers. *Journal of Solar Energy Engineering, 129*, 141-146.

Fraidenraich, N., Tiba, C., Brandao, B.B., & Vilela, O.C. (2008). Analytic solutions for the geometric and optical properties of stationary compound parabolic concentrators with fully illuminated inverted V receiver *Solar Energy, 82*(2), 132-143.

Frey, G.W., & Linke, D.M. (2002). Hydropower as a renewable and sustainable energy resource meeting global energy challenges in a reasonable way. *Energy Policy, 30*(14), 1261-1265.

Godson, L., Raja, B., Lal, D.M., & Wongwises, S. (2012). Convective heat transfer characteristics of silver–water nanofluid under laminar and turbulent flow conditions. *Journal of Thermal Science and Engineering Applications, 4*(3), 031001.

Glatzmaier, G.C., & Turchi, C.S. (2009). Supercritical CO2 as a heat transfer and power cycle fluid for CSP systems. *in ASME Energy Sustainability, San Francisco, CA*.

Gnielinski, V. (1976). New equations for heat and mass transfer in turbulent pipe and channel flow. *In Chem. Eng., 16*, 359-368.

Güney, M.S., & Kaygusuz, K. (2010). Hydrokinetic energy conversion systems: A technology status review. *Renewable and Sustainable Energy Reviews, 14*(9), 2996-3004. doi: http://dx.doi.org/10.1016/j.rser.2010.06.016

Haris, A.H. (2008). MBIPV Project: catalyzing local PV market. *Finance & Investment Forum on PV Technology, : http://www.mbipv. net.my/dload/FIF-HH.pdf.*

Hall, A., Ambrosini, A., & Ho, C. (2012). Solar selective coatings for concentrating solar power central receivers. *Advanced Materials & Processes, 170*(1), 28-32.

Hammad, M., & Habali, S. (2000). Design and performance study of a solar energy powered vaccine cabinet. *Applied Thermal Engineering, 20*(18), 1785-1798.

Hasanuzzaman, M., Rahim, N.A., Hosenuzzaman, M., Saidur, R., Mahbubul, I.M., & Rashid, M.M. (2012). Energy savings in the combustion based process heating in industrial sector. *Renewable and Sustainable Energy Reviews, 16*(7), 4527-4536.

Heller, P., Jedamski, J., Amsbeck, L., Uhlig, R., Ebert, M., & Svensson, M. (2009). Development of a solar-hybrid micro turbine system for a mini-tower. *In: Proceedings of Solar PACES 2009, Berlin, Germany*.

Heller, P., Pfander, M., Denk T., Tellez, F., Valverde, A., Fernandez, J., & Ring, A. (2006). Test and evaluation of a solar powered gas turbine system. *Solar Energy, 80*(10), 1225–1230.

Hennecke, K., S. P., Alexopoulos, S., Gottsche, J., Hoffschmidt, B., & Beuter, M. (2008). Solar power tower Julich: the first test and demonstration plant for open volumetric receiver technology in Germany, in Solar PACES, LasVegas, NV.

Heris, S.Z, Esfahany, M.N., & Etemad S.G. (2007). Experimental investigation of convective heat transfer of Al2O3/water nanofluid in circular tube. *International Journal of Heat and Fluid Flow, 28*(2), 203–210.

Hischier, I., Hess, D., Lipinski, W., Modest, M., & Steinfeld, A. (2009). Heat transfer analysis of a novel pressurized air receiver for concentrated solar power via combined cycles *In: Ht 2009: Proceedings of the ASME summer heat transfer conference 1*, 105–112.

Ho, C.K., Roeger, M., Khalsa, S.S., Amsbeck, L., Buck, R., & Siegel N. (2009). Experimental validation of different modeling approaches for solid particle receivers, in Solar PACES 2009, SAND 2009-4140C, Berlin, Germany

Holman, J. P. (1997). Heat transfer, 2nd ed. *Macgraw-Hill, Inc*.

Hong, T.-K., & Yang, H.-S. (2005). Study of the enhanced thermal conductivity of Fe nanofluids. *Physics, 97*, 4-7.

Hosenuzzaman, M., Rahim, N. A., Selvaraj, J., Hasanuzzaman, M., Malek, A. B. M. A., & Nahar, A. (2015). Global prospects, progress, policies, and environmental impact of solar photovoltaic power generation. *Renewable and Sustainable Energy Reviews, 41*(0), 284-297.

Hunt A.J. & Brown C.T. (1983). Solar test results of an advanced direct absorption high-temperature gas receiver (SPHER). *In:Proceedings of the ISES Solar World Congress, Perth, Australia*.

Hunt, A.J. (1978). Small-particle heat exchangers, Lawrence Berkeley Laboratory report LBL-7841,Berkeley,CA.

IEA. (2012). Solar energy could meet one-sixth of global demand for heating and cooling in under 40 years. *http://www.iea.org/newsroomandevents/news/2012/july/name,28298,en.html accessed 12 December 2014*.

Inc, B. N. (1981). Preliminary heat pipe testing program: final technical report, contract no.DE-AC03-79SF10756, San Francisco, CA.

Islam, M. K., Hasanuzzaman M. & Rahim N. A. . (2015). Modelling and analysis of the effect of different parameters on a parabolic-trough concentrating solar system. *RSC Advances, 5*, 36540–36546.

Jaffar, A.J. (2009). Outlook of coal deand/supply &policy in malaysia,Cleaner coal:Moving towards Zero emmisions. *APEC*.

Jaramillo, O.A., Venegas-Reyes, E., Aguilar, J.O., Castrejon-Garcia, R., & Sosa-Montemayor, F. (2013). Parabolic trough concentrators for low enthalpy processes. *Renewable energy, 60*, 529-539.

Javadi, FS., Saidur, R., & Kamalisarvestani. (2013). Investigating performance improvement of solar collectors by using nanofluids. *Renewable and Sustainable Energy Reviews, 28*, 232-245.

JE, P. (2002a). Final test and evaluation results from the solar two project. *SAND 2002-0120. Albuquerque, NM: Sandia National Laboratories*.

Jorgensen, G., Schissel, P., & Burrows, R. (1986). Optical properties of high-temperature materials for direct absorption receivers. *Solar Energy Materials, 14*(3), 385-394.

Kalogirou, S.A. (2002). Parabolic trough collectors for industrial process heat in Cyprus. *Energy, 27*, 813-830.

Kalogirou, S.A. (2009). Solar energy engineering: Processes and Systems. *Elsevier's Science & Technology, UK*.

Kamyar, A., Saidur, R., & Hasanuzzaman, M. (2012). Application of Computational Fluid Dynamics (CFD) for nanofluids. *International Journal of Heat and Mass Transfer, 55*(15-16), 4104–4115.

Kasaeian, A., Sokhansefat, T., Abbaspour, M.J, & Sokhansefat, M. (2012). Numerical study of heat transfer enhancementby using Al_2O_3/synthetic oil nanofluid in aparabolic trough collector tube. *Rome: World Academy of Science, Engineering and Technology*, 1154–1159.

Kaushika, N.D., & Reddy, K.S. (2000). Performence of a low cost solar paraboloidal dish steam generating system. *Energy covers. Manage, 41*, 713-726.

Kaygusuz, K. (2011). Prospect of concentrating solar power in Turkey: The sustainable future. *Renewable and Sustainable Energy Reviews 15*(1), 808-814.

KH, S. (2001). High temperature properties and thermal decomposition of inorganic salts with oxyanions. BocaRaton, Fla: CRC Press.

Khalsa, S.S.S., Christian, J.M., Kolb, G.J., Roger, M., Amsbeck, L., Ho, C.K., …, Moya, A.C. (2011). CFD simulation and performance analysis of alternative designs for high-temperature solid particle receivers. *In: Proceedings of the ASME 2011 energy sustainability and fuel cell conference*.

Kolb, G.J., Diver, R.B., & Siegel, N. (2007). Central-station solar hydrogen power plant. *Journal of Solar Energy Engineering-Transactions of the ASME, 129*(2), 179-183.

Kolb, G.J. (2011). An evaluation of possible next-generation high-temperature molten-salt power towers. *Sandia National Laboratories, SAND 2011-9320, Albuquerque, NM*.

Kole, M., & Dey, T.K. (2012). Effect of prolonged ultrasonication on the thermal conductivity of ZnO–ethylene glycol nanofluids. *Thermochimica Acta, 535*, 58–65.

Kwak, H., Shin, D., & Banergee, D. (2010). Enhanced Sensible Heat Capacity of Molten Salt and Conventional Heat Transfer Fluid Based Nanofluid for Solar Thermal Energy Storage. *ASME 2010 4th International Conference on Energy Sustainability, 2*, 735-739.

Lee, M.T., Werhahn, M., Hwang, D.J., Hotz, N., Greif, R., Poulikakos, D., & Grigoropoulos, C.P. (2010). Hydrogen production with a solar steam methanol reformer and colloid nanocatalyst *International Journal of Hydrogen Energy, 35*, 118-126.

Lenert, A., & Wang, E.N. (2012). Optimization of nanofluid volumetric receivers for solar thermal energy conversion. *Solar energy, 86*(1), 253-265.

Leon, J., Sanchez, M., & Pacheco, J.E. (1999). Internal film receiver possibilities for the third generation of central receiver technology. *Journal De Physique IV*, 525-530.

Leong, K.C., Yang, C., & Murshed, S.M.S. (2006). A Model for the Thermal Conductivity of Nanofluids— The Effect of Interfacial Layer. *J. of Nanoparticle Res., 8*, 245–254.

LG, R. (1988). Final report on the power production phase of the 10MWe solar thermal central receiver pilot plant, SAND87-8022, Sandia National laboratories, Albuquerque, NM.

Li, X., Kong, W., Wang, Z., Chang, C., & Bai, F. (2010). Thermal model and thermodynamic performance of molten salt cavity receiver. *Renewable Energy, 35*(5), 981-988.

Lippke, F. (1996). Direct steam generation in parabolic trough solar power plants: numerical investigation of the transients and the control of a once through system. *Journal of Solar Energy Engineering, 118*, 9-14.

Liu, Q., Yang, M., Lei, J., Jin, H., Gao, Z., & Wang, Y. (2012). Modelling and optimizing parabolic trough solar collector systems using the least squares support vector machine method. *Solar Energy, 86*(7), 1973-1980.

Lu, L., Liu, Z.-H., & Xiao, H.-S. (2011). Thermal performance of an open thermosyphon using nanofluids for high-temperature evacuated tubular solar collectors: Part 1: Indoor experiment. *Sol Energy, 85*(2), 379–387.

Marcos, M.J., Romero, M., & Palero, S. (2004). Analysis of air return alternatives for CRS-type open volumetric reciever. *Energy, 29*(5-6), 677-686.

Menigault, T., Flamant, G., & Rivoire B. (1991). Advanced high-temperature 2-slab selective volumetric receiver. *SolarEnergyMaterials, 24*(1-4), 192-203.

Miller, F., & Koenigsdorff, R. (1991). Theoretical-analysis of a high-temperature small-particle solar receiver. *Solar Energy Materials, 24*(1-4), 210-221.

Miller, F.J., & Koenigsdorff, R. (2000). Thermal modeling of a small-particle solar central receiver. *Journal of Solar Energy Engineering-Transactions of the ASME, 122*(1), 23-29.

Moisseytsev, A., & Sienicki, J.J. (2010). Extension of supercritical carbon dioxide Brayton cycle for application to the very high temperature reactor. *In: International congress on the advances in nuclear powerplants, San Diego, CA*.

Montes, M.J., Rovira, A., Muñoz, M., & Martínez-Val J.M. (2011). Performance analysis of an Integrated Solar Combined Cycle using Direct Steam Generation in parabolic trough collectors. *Applied Energy, 88*(9), 3228–3238.

Bohn, M.S. (1987). Experimental investigation of the direct absorption receiver concept. *Energy, 12*(3), 227-233.

NE, B. (1986). Testing of the molten salt electric experiment solar central receiver in an external conFigureuration. *Livermore, CA: Sandia National Laboratories*.

NREL. (2014) China Direct Normal Solar Radiation. *http://www.nrel.gov/gis/pdfs/swera/china/china40kmdir.pdf, 10/12/2014*.

Oommen, R., & Jayaraman, S. (2001). Development and performance analysis of compound parabolic solar concentrators with reduced gap losses-oversized reflector. *Energy Conversion and Management, 42*(11), 1379-1399.

Pacheco, J.E, & Dunkin, S.R. (1996). Assessment of molten-salt solar central-receiver freeze-up and recoverevents. *In:ASME international solar energy conference, San Antonio, TX*.

Pacheco, J.E., Ralf, M., Chavez, J.M., Dunkin, S.R., Rush, E.E., & Ghanbari, C.M. (1994). Results of molten salt panel and component experiments for solar central receivers: cold fill, freeze/thaw, thermal cycling and shock, and instrumentation tests. *Albuquerque, NM: Sandia National Laboratories*.

Pacheco, J.E., Ralf, M.E., & Chavez, J.M. (1995). Investigation of cold filling receiver panels and pipinginmolten-nitrate-salt central-receiver solar power plants. *In: ASME international solar energy conference, Lahaina, Maui, HI*.

Pak, B., & Cho, Y.I. (1998). Hydrodynamic and Heat Transfer Study of Dispersed Fluids with Submicron Metallic Oxide Particles. *Experi. Heat Transfer, 11*, 151–170.

Palm, S.J., Roy, G., & Nguyen, C.T. (2004). Heat transfer enhancement in radial flow cooling system using nanofluid. *In: Proceeding of the ICHMT Inter. Symp. Advance Comp. Heat Transfer, Norway, CHT-04-121.*

Pepermans, G., Driesen, J., Haeseldonckx, D., Belmans, R., & D'haeseleer, W. (2005). Distributed generation: definition, benefits and issues. *Energy Policy, 33*(6), 787–798.

PitzPaal, R., Hoffschmidt, B., Bohmer M., & Becker M. (1997). Experimental and numerical evaluation of the performance and flow stability of different types of open volumetric absorbers under nonhomogeneous irradiation. *Solar Energy, 60*(3-4), 135-150.

PK, F. (1986a). A hand book for solar central receiver design, SAND 86-8009. *Livermore, CA: Sandia National Laboratories*.

PK, F. (1986b). A handbook for solar central receiver design, SAND 86-8009. Livermore, CA:Sandia National Laboratories.

Pramuang, S., & Exell, R.H.B. (2005). Transient test of a solar air heater with a compound parabolic concentrator. *Renewable Energy, 30*(5), 715-728.

Prasher, R., Bhattacharya, P., & Phelan, P.E. (2006). Brownian-motion-based convective-conductive model for the effective thermal conductivity of nanofluids. *Journal of Heat Transfer-Trans ASME, 128*, 588-595.

Prasher, R., Phelan, P.E., & Bhattacharya, P. (2006). Effect of aggregation kinetics on the thermal conductivity of nanoscale colloidal solutions (nanofluid). *Nano Letters*, 1529-1534.

Pye, J. SG4 500 m² paraboloidal dish solar concentrator at ANU. *solar-thermal.anu.edu.au/high-temperature/500-m2-dish/, (05/06/2013)*.

RE. (2013). Learning about renewable energy. NREL's vision is to develop technology. *National Renewable Energy Laboratory*.

RE. (2014). Renewable and non-renewable energy resources *www.bbc.co.uk › Home › Geography › Energy resources, 10/07/2014*.

Reddy, K.S., & Kumar, K.R. (2012). Solar collector field design and viability analysis of stand-alone parabolic trough power plants for Indian conditions. *Energy for Sustainable Development 16*(4), 456–470.

Reddy, V.S., Kaushik, S.C., & Panwar, N.L. (2013). Review on power generation scenario of India. *Renewable and Sustainable Energy Reviews, 18*, 43-48.

REGS (2014) Renewables 2014 Global Status Report *www.ren21.net/portals/0/.../2014/gsr2014_full%20report_low%20res.pdf, 01/08/2014*.

Roy, G., Nguyen, C.T., & Lajoie, P.R. (2004). Numerical investigation of laminar flow and heat transfer in a radial flow cooling system with the use of nanofluids. *Superlattices and Microstructures, 35*(3), 497–511.

Saidur, R., Meng, T.C., Said, Z., Hasanuzzaman, M., & Kamyar, A. (2012). Evaluation of the effect of nanofluid-based absorbers on direct solar collector. *International Journal of Heat and Mass Transfer, 55*(21–22), 5899-5907.

Sani, E, Mercatelli, L., Barison, S., Pagura, C., Agresti, Colla, F., & Sansoni P. (2011). Potential of carbon nanohorn-based suspensions for solar thermal collectors. *Solar Energy Materials and Solar Cells, 95*(11), 2994-3000.

Sani, E., Barison, S., Pagura, C., Mercatelli, L., Sansoni, P., & Fontani, D. (2010). Carbon nanohorns-based nanofluids as direct sunlight absrbers. *Optics Express, 18*, 5179-5187.

Sarkar, J. (2011). A critical review on convective heat transfer correlations of nanofluids. *Renew. Sustain. Energy Rev., 15*(6), 3271–3277.

Schiel, W.J.C, G. M. (1988). Testing an external sodium receiver upto heat fluxes of 2.5MW/m2: results and conclusions from the IEA-SSP Shigh flux experiment conducted at the central receiver system of the Plataforma Solarde Almeria (Spain). *SolarEnergy, 41*(3), 255-265.

Schmidt, G., Schmid, P., Zewen, H., & Moustafa, S. (1983). Development of a point focusing collector farm system. *Sol. Energy, 31*, 299-311.

Schroeder, M. (2009). Utilizing the clean development mechanism for the deployment of renewable energies in China. *Applied Energy, 86*(2), 237-242.

Seidel, W. (2010). Model developmenet and annual simulation of the supercritical carbon dioxide Brayton cycle for concentrating solar power applications. *In: Mechanical engineering.UniversityofWisconsin-Madison*.

Şen, Z. (2004). Solar energy in progress and future research trends. *Progress in Energy and Combustion Science, 30*(4), 367-416.

Shah, R.K., & London, A.L. (1978). Laminar flow: Forced convection in ducts. *New york: Academic Press*.

Shahrul, I.M., Mahbubul, I.M., Saidur, R., Khaleduzzaman, S.S., Sabri, M.F.M., & Rahman M.M. (2014). Effectiveness Study of a Shell and Tube Heat Exchanger Operated with Nanofluids at Different Mass Flow Rates. *Numerical Heat Transfer, Part A: Applications: An International Journal of Computation and Methodology, 65*(7), 699-713.

Sharma, P., Sarma, R., Chandra, L., Shekhar, R., & Ghoshdastidar, P.S. (2015). Solar tower based aluminum heat treatment system: Part I. Design and evaluation of an open volumetric air receiver. *Solar energy, 111*, 135-150.

Shiblee, N.H. (2011). Solar Energy in Urban Bangladesh: An Untapped Potential. *ChE Thoughts 2*(1), 8-12.

Suresh, S., Chandrasekar, M., & Sekhar, S.C. (2011). Experimental studies on heat transferand friction factor characteristics of CuO/water nanofluid under turbulent flow ina helically dimpled tube, *Experimental Thermal and Fluid Science, 35*, (2011) 542–549.

Suresh, S., Selvakumar, P., Chandrasekar, M., & Raman, V.S. (2012). Experimental studies onheat transfer and friction factor characteristics of Al2O3/water nanofluid under turbulentflow with spiraled rod inserts, *53*, 24–30.

SI (2014) Solar irradiation data of India. *www.eai.in/club/users/krupali/blogs/627, 20/08/2014*.

Siebers, D.L., & Kraabel, J.S. (1984). Estimating convective energy losses from solar central receivers. *Livermore,CA: Sandia National Laboratories*.

Siegel, N.P., Ho, C.K., Khalsa, S.S., & Kolb, G.J. (2010). Development and evaluation of a prototype solid particle receiver: on-sun testing and model validation. *Journal of Solar Energy Engineering-Transactions of the ASME, 132*(2).

Singer, C., Buck, R., Pitz-Paal, R., & Muller-Steinhagen, H. (2010). Assessment of solar power tower driven ultrasupercritical steam cycles applying tubular central receivers with varied heat transfer media. *Journal of Solar Energy Engineering, 132*(4), 1-12.

Smith, D.C., & Chavez, J. (1987). A final report on the phase I testing of a molten-salt cavity receiver, SAND87-2290, Sandia National Laboratories, Albuquerque, NM.

Smith, D.C. (1992). Design and optimization of tube-type receiver panels for molten salt application. *In: ASME international solar energy conference, Maui, HI, USA*.

Sokhansefat, T., Kasaeian, A.B., & Kowsary, F. (2014). Heat transfer enhancement in parabolic trough collector tube using Al2O3/synthetic oil nanofluid *Renewable and Sustainable Energy Reviews, 33*, 636-644.

Solar (2014). Solar energy and its potential in India. *www.borgenergy.com/solar-energy-potential-india/, 19/08/2014.Solar Energy Materials and Solar Cells 95*(10), 2703–2725.

SPS (2013). *www.nrel.gov/csp/solarpaces/project_detail.cfm/projectID=25, (05/06/2013)*.

Taylor, R.A., Phelan, P.E., Otanicar, T.P., Adrian, R., & Prasher R. (2011). Nanofluid optical property characterization: towards efficient direct absorption solar collectors. *Nanoscale Res. Lett., 6*(1), 1–11.

Timofeeva, E.V., Smith, D.S., Yu, W., France, D.M., Singh, D., & Routbo, J.L. (2010). Particle Size and Interfacial Ef- fects on Thermo-Physical and Heat Transfer Characteris- tics of Water-Based α-SiC Nanofluids. *Nanotechnology, 21*(21).

Tracey, T. (1992). Potential of modular internal film receivers in molten salt central receiver solar power systems. *In: ASME international solar energy conference*.

Tsai, C.Y., Chiena, H.T., Dingb, P.P., Chanc, B., Luhd, T.Y., & Chena, P.H. (2004). Effect of structural character of gold nanoparticles in nanofluid on heat pipe thermal performance. *Mater Lett, 58*(9), 1461–1465.

TVP. (13/03/2014). Therminol VP-1 Update.qxd. *www.therminol.com/pages/bulletins/therminol_vp1.pdf*.

UCS. (2014). Renewable energy technology. *http://www.ucsusa.org/clean_energy/our-energy-choices/renewable-energy accessed 12 November 2014*.

Uhlig, R. (2011a). Transient stresses at metallic solar tube receivers. *In: Proceedings of solar PACES 2011, Granada, Spain*.

Dostal, V. (2004). A super critical carbon dioxide cycle for next generation nuclear reactors. *In: Nuclear engineering. Massachusetts Institute of Technology*.

Variot, B., Menigault, T., & Flamant, G. (1994). Modeling and optimization of a 2-slab selective volumetric solar receiver. *Solar Energy, 53*(4), 359-368.

Veeraragavan, A., Lenert, A., Yilbas, B., Al-Dini, S., & Wang, E.N. (2012). Analytical model for the design of volumetric solar flow receivers. *International Journal of Heat and Mass Transfer, 55*(4), 556-564.

Waghole, D.R., Warkhedkar, R.M., kulkarni, V.S., & Shrivastva, R.K. (2014). Experimental Investigations on Heat Transfer and Friction Factor of Silver Nanofliud in Absorber/Receiver of Parabolic Trough Collector with wisted Tape Inserts *Energy Procedia, 45*, 558–567.

Webb, B.W., & Viskanta, R. (1985). Analysis of heat transfer and solar radiation absorption in an irradiated, thin, falling molten salt film. *Journal of Solar Energy Engineering, 107*(2), 113-119.

Wiki. Solar power in Japan. *http://en.wikipedia.org/wiki/Solar_power_in_Japan, 15/12/2014*.

Wu, S.F., & Narayama, T. (1988). Commercial direct absorption receiver design studies. *Albuquerque, NM: Sandia National Laboratories*.

Xi, F., Satyajayant, M., Guoliang, X., & Dejun, Y. (2012). Smart grid – the new and improved power grid: a survey. *IEEE Commun Surv Tutor, 14*(4), 944–980.

Xuan, Y., & Li, Q. (2000). Heat transfer enhancement of nanofluids. *Int. J. Heat Fluid Flow, 21*, 58–64.

Xuan, Y., & Li, Q. (2003). Investigation on convective heat transfer and flow features of nanofluids. *Journal of Heat Transfer-Trans ASME, 125*, 151–155.

Yih, S.M., & Seagrave, R.C. (1978). Hydrodynamic stability of thin liquid films flowing down an inclined plane with accompanying heat transfer and interfacial shear. *AIChE Journal, 24*(5), 803-810.

Yu, W., & Choi, S.U.S. (2003). The role of international layers in the enhanced thermal conductivity of nanofluids: A renovated Maxwell model. *Journal on Nanoparticle Research, 5*, 167–171.

Yu, W., France, D.M., Smith, D.S., Singh, D., Timofeeva, E.V., & Routbort, J.L. (2009). Heat transfer to a silicon carbide/water nanofluid, *International Journal of Heat and Mass Transfer, 52,* 3606-3612.

Zhang, S., Luo, Z., Wang, T., Shou, C., Ni, M., & Cen, K. (2010).Experimental study on the convectiveheat transfer of CuO–water nanofluid in a turbulent flow, *Journal of Enhanced Heat Transfer, 17* (2) 183–196.

Zunft, S., Hanel, M., Kruger, M., Dreissigacker, V., Gohring, F., & Wahl, E. (2011). Julich solar power tower-experimental evaluation of the storage subsystem and performance calculation. *Journal of Solar Energy Engineering-Transactions of the ASME, 133*, 3.

APPENDIX A: RELATED PUBLICATIONS

Journal

1. **M. K. Islam**, M. Hasanuzzaman and N. A. Rahim. Modelling and analysis of the effect of different parameters on a parabolic trough concentrating solar system, RSC Advances,2015 (5): 36540–36546 (Q1, IF: 3.840).

2. **M.K. Islam,** M. Hasanuzzaman, N.A. Rahim, Experimental Investigation of Thermal Performance of Parabolic Trough Collector, Energy Conversion and Management (Under Review) (ISI Q1, IF: 4.380).

3. **M.K. Islam,** M. Hasanuzzaman, N.A. Rahim, Effect of Nanofluid Properties and Mass-Flow Rate on Heat Transfer of Parabolic-Trough Concentrating Solar System (Under preparation).

Conference

1. **M.K. Islam**, M. Hosenuzzaman, M.M. Rahman, M. Hasanuzzaman, N.A. Rahim, Thermal Performance Improvement of Solar Thermal Power Generation, 2013 IEEE Conference on Clean Energy and Technology (CEAT).